Commission of the European Community

JOINT
RESEARCH
CENTRE

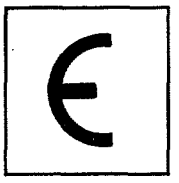

NEANDC (E) 262 "U" Vol. III Euratom
INDC (EUR) 019/G

ANNUAL PROGRESS REPORT ON NUCLEAR DATA

1984

CENTRAL BUREAU FOR NUCLEAR MEASUREMENTS

GEEL (BELGIUM)

January 1986

Commission of the European Community

JOINT
RESEARCH
CENTRE

NEANDC (E) 262 "U" Vol. III Euratom
INDC (EUR) 019/G

ANNUAL PROGRESS REPORT ON NUCLEAR DATA
1984

CENTRAL BUREAU FOR NUCLEAR MEASUREMENTS

GEEL (BELGIUM)

January 1986

TABLE OF CONTENTS

1. NUCLEAR DATA

1.1. NUCLEAR DATA FOR STANDARDS

A.J. Deruytter

From 12 to 16 November an Advisory Group Meeting was organized at CBNM-Geel by INDC(IAEA) and NEANDC(OECD) Standard Sub-Committees with world-wide participation. For this meeting an invited paper [1] was presented on the requirements for nuclear standard reference data from the users' point of view with the following abstract:

> "The requirements from the users' point of view for nuclear standards reference data with respect to accuracy of the data, traceability (documentation), representation (i.e. numerical values with uncertainties and correlation matrices, parametrization), availability of materials in suitable form (well-defined layers, gases) and applicability in real life detectors (Q-values of reactions, type of particles or photons produced, smoothness and magnitude of cross-section) will be discussed.
> From these primary requirements additional requirements follow for internal consistency (via ratio measurements), for verification of physical constraints (total cross-section, inverse reaction), for additional basic information (angular distributions of reaction products, fragment energy distributions, description and understanding of the basic processes).
> The user is seen as the measurer who determines values of partial cross-sections or other quantities relative to one or more of the selected standard reference data."

A Summary Report of this IAEA Advisory Group Meeting was presented at the UK Nuclear Data Forum held on December 18, 1984 at AEE Winfrith (UK) [2].

1.1.1. Neutron Data for Standards

Intercomparison of neutron flux detectors

C. Bastian, K.H. Böckhoff, A. Brusegan, F. Corvi, H.-H. Knitter, J.A. Wartena, H. Bax, C. Bürkholz, R. Pijpstra, R. Vogt

Neutron flux detectors play a crucial role in partial neutron cross section determination. The uncertainty of the neutron flux data obtained with them has a large impact on the quality of the partial cross section data, in particular when high accuracies are requested.

---

(1) To be published "Proceedings IAEA Advisory Group Meeting on Nuclear Standard data".

(2) Ibidem.

Two papers were presented at the IAEA AGM on Standard Reference Data at Geel dealing with CBNM detector intercomparisons, of respectively low and high efficiency detectors. The abstracts read:

"Part 1: Low efficiency detectors.
Four detectors, currently in use at GELINA for the determination of the neutron flux spectra were intercompared. All the detectors combine low count rate and high transparency for the neutron flux. The four detectors (3 ionization chambers and one parallel plate proportional counter) and their advantages and disadvantages are briefly described. Two different methods of background determination are described, criticized and results are compared."

"Part 2: High efficiency detectors.
An intercomparison of highly efficient neutron flux detectors is under way. The neutron spectrum investigated is that emitted from the moderator surrounding the neutron producing target of the Geel electron Linac and the energy of interest ranges from thermal to about 1 MeV. The results of two intercomparisons are reported here: one deals with a thin ^{6}Li-glass scintillator and a ^{10}B ionization chamber. The second is concerned with the same ^{6}Li-glass and a multiplate ^{235}U fission chamber. Good agreement is obtained in the first case for the range 4 eV to 2 keV and in the second case from 8 eV to 100 keV."

Measurement of $^{6}Li/^{10}B(n,\alpha)$ cross section ratio

C. Bastian, H. Riemenschneider

There is a never ending quest for improving the accuracy of the ^{6}Li(n,α) and ^{10}B(n,α) cross sections since these are as standard reference cross sections basic for the determination of almost all partial cross sections in the eV and keV neutron energy range. For a consistency control of both cross sections, but also for an improvement of the standard data base as a whole, the accurate determination of the (n,α) cross section ratio of ^{6}Li and ^{10}B is important.
The results of our measurement of this cross-section ratio were presented at the IAEA AGM on Standard Reference Data. The abstract reads:

"The charged particle emission of ^{6}LiF and ^{10}B sample layers placed alternatively in the neutron beam of GELINA was detected by scintillation in Xenon gas. In order to compensate for the anisotropy of the emission each sample is deposited on the inside of a hollow cylindrical quartz support. Recording of a dummy sample support was also included in the measurement sequence. The ratio of ^{6}Li to ^{10}B(n,α) cross sections, thus measured under the same conditions, agrees up to 400 keV with point data deduced from ENDF/BV, within the measurement uncertainty."

Fission cross-section of ^{235}U between 0.025 eV and 30 keV

C. Wagemans*, A. Deruytter, R. Barthélémy, J. Van Gils*

The fission integrals $I_1 = \int_{7.8\ eV}^{11\ eV} \sigma_f(E)dE$ and $I_2 = \int_{0.1\ keV}^{1.0\ keV} \sigma_f(E)dE$ are important as secondary standard for the normalization of fission cross-sections. An interim report of these integrals has been presented at the IAEA Advisory Group Meeting on Nuclear Standard Reference Data (Geel, November 1984), with the following abstract:

> "New measurements of the $^{235}U(n,f)$ cross-section relative to $^{10}B(n,\alpha)^7Li$ have been performed in the neutron energy region from 0.02 eV up to 30 keV under various experimental conditions. From these data, the fission integrals $I_1 = \int_{7.8\ eV}^{11eV} \sigma_f(E)dE$ and $I_2 = \int_{0.1\ keV}^{1.0\ keV} \sigma_f(E)dE$ have been calculated. These results are compared with the literature, and the present status of the integrals I_1 and I_2 is reviewed."

To verify the influence on these integrals of the neutron flux monitor and of the permanent neutron filter used, an additional measurement has been performed.

Evaluation of the thermal neutron constants of ^{233}U, ^{235}U, ^{239}Pu and ^{241}Pu and the fission neutron yield of ^{252}Cf

E.J. Axton*

The importance of these data stems from the role they play in the prediction of the neutron economy in nuclear power reactors. The continued appearance of new data has prompted a continuous re-evaluation of the data over the years. The Maxwellian data have been introduced in the previously published evaluation [1] which only used monoenergetic data. This updated evaluation has been presented at the IAEA AGM on Nuclear Standards Reference Data. The abstract reads:

---

* SCK-CEN Mol, Belgium.

** Visiting Scientist from NPL, Teddington (UK).

(1) E.J. Axton, "Evaluation of thermal neutron constants of ^{233}U, ^{235}U, ^{239}Pu and ^{241}Pu and the fission yield of ^{252}Cf" European Applied Research Reports - Nucl. Sci. Technol. Vol 5, No.4 (1984) pp 609-676.

"In 1982 a simultaneous least-squares evaluation of the thermal neutron constants of ^{233}U, ^{235}U, ^{239}Pu, and ^{241}Pu together with the fission neutron yield from the spontaneous fission of ^{252}Cf was performed with, for the first time, a full covariance matrix for the input data. The input data set was limited in that measurements in Maxwellian reactor spectra were excluded. (A) Concurrently, a similar evaluation was performed at Brookhaven which included the Maxwellian data set but which did not have an input covariance matrix, although the more important correlations were handled by other methods. (B) In the present work the Maxwellian data from B has been added to A, and the differences between the input and output data for the various evaluations are discussed."

It was stressed at the IAEA AGM that whenever the fitted values are propagated in reactor calculations they should always be accompanied by the associated correlation matrix.

Fission fragment mass, kinetic energy and angular distribution for $^{235}U(n,f)$ in the neutron energy range from thermal to 6 MeV

Chr. Straede, C. Budtz-Jørgensen, H.-H. Knitter

The complete knowledge of mass-, energy-, and angular distributions of fission fragments provides a basis for the theoretical understanding of the process. The knowledge of angular distribution is moreover important in the evaluation of experimental fission cross section measurements in which fission fragments are detected in a small range of angles.
A paper was presented at the IAEA Advisory Group Meeting on Nuclear Standard Reference Data, 12-16 November 1984 at CBNM. The abstract is as follows:

"A double Frisch gridded ionization chamber has been used for the measurements. For both fission fragments the mass, kinetic energy and emission angle is found. Data have been measured at different neutron energies, E_n, ranging from thermal to 6.0 MeV in steps of 0.5 MeV. The measured angular anisotropies will be shown. A fit, based on statistical theory, to earlier measurements of negative anisotropies for $E_n \leq 0.2$ MeV will be discussed.
The measured total kinetic energy averaged over all fragment masses, $\overline{TKE}(E_n)$, shows a sudden decrease at $E_n \approx 4.5$ MeV in agreement with earlier measurements. This sudden decrease can not be explained by the measured change in the mass distribution. The present data of $\overline{TKE}(E_n)$ as function of mass-split reveal that $\overline{TKE}(E_n)$ decreases with E_n for mass splits around the 104/132 split as predicted by calculations of B.D. Wilkins et al.. It is also seen that $\overline{TKE}(E_n)$ increases with E_n for the symmetric and the extreme asymmetric fissions. The very structured mass distribution from approximately cold fragmentation will be presented."

Because of the nature of this IAEA meeting the content of the paper is concentrated on the angular distribution data, and the fragment mass and kinetic energy distributions are only presented briefly. These data will mainly be discussed and interpreted in the frame of the scission point model of B.D. Wilkins et al. (1). This model seems to be able to explain many of the structures found in the measured mass and kinetic energy data. Contacts have been made with B.D. Wilkins for further discussion of the model and related data.

Finally the cold fragmentation data for thermal induced fission can be compared with several other measurements, e.g. with data measured by U. Quade et al. (2). In Fig. 1.1. the data from (2) and the present data are compared for the total excitation energy of the fragments with high kinetic energy at a yield level, such that each mass only occurs for 1 out of 10^5 fissions in total. The total kinetic energy for the fragments at this yield level is subtracted from Q-values for the splits. The Q-values are taken from Möller and Nix (3) and weighted with the yield of the different isotopes for each mass. The agreement between the data of (2) and the present data is rather good.

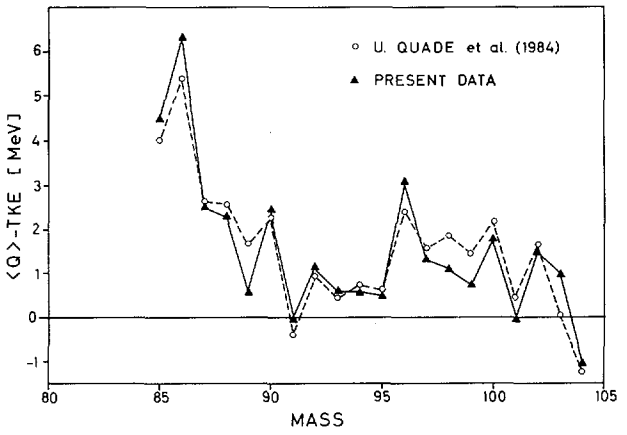

Fig. 1.1. Total excitation energy as function of the light fission fragment mass for thermal neutron induced fission of ^{235}U at such high kinetic energies that for each mass only 1 out of 10^5 total fissions is concerned

(1) B.D. Wilkins, E.P. Steinberg and R.R. Chasman, Phys. Rev. C14, 1832 (1976).

(2) U. Quade et al., Cold Fragmentation of ^{234}U and ^{236}U. The International Symposium on Nuclear Fission and Related Collective Phenomena and Properties of Heavy Nuclei, Bad Honnef, October 1981.

(3) P. Möller and J.R. Nix, Atomic Data and Nuclear Data Tables 26, 165 (1981).

The present measurement contains further information on the cold fragmentations induced by neutrons with energy E_n between 0.5 and 6 MeV. These data are at present being interpreted.
A thesis on the discussed subjects is being prepared by Chr. Straede.

Neutron emission from the spontaneous fission of ^{252}Cf

C. Budtz-Jørgensen, H.-H. Knitter, R. Vogt, H. Bax

The spontaneous fission neutron spectrum of ^{252}Cf is used as a standard spectrum in instrument calibrations. Several attemps have recently been made to give a theoretical description of this spectrum. However, these theoretical approaches suffer from a lack of knowledge about the mechanism of the fission emission i.e. the fraction of scission neutrons, emission during fragment acceleration, etc. There is therefore a strong need not only for precise neutron spectrum data, $N(E_n)$, but also for double- or multiple-differential measurements, $(N(E_n,\theta_n,A,TKE))$ which can help to clarify the nature of the fission neutrons.
The results of a measurement of the angular distributions for ^{252}Cf fission neutrons with respect to the related fission fragments were presented at the IAEA Advisory Group Meeting on Nuclear Standard Reference Data, Geel, 12-16 November 1984. The abstract of the paper reads:

> "The gridded ion chambers developed at CBNM provide a powerful tool for measurements of fission fragment angle, kinetic energy and mass distributions simultaneously with an angular efficiency close to 4π. They can also serve in measurements where fission neutron spectra are studied as function of these physical quantities. Preliminary tests have been made with a fission chamber loaded with a ^{252}Cf source of $\sim 4 \times 10^3$ fissions s^{-1}. The fission neutrons were detected with a 4" x 1" plastic scintillator and conventional time-of-flight electronics. The coincidence resolution between the neutron detector and the fission chamber was < 2 ns. The neutron detector was placed 2.05 m from the ^{252}Cf source with a direction normal to the chamber electrodes. The cosines of the angles ϑ, between this direction and the path of the light fission fragments were determined using the chamber anode and cathode pulses. At higher neutron energies it can be seen, that the neutrons are emitted mainly in the direction of either the light or the heavy fragments, confirming that most of the neutrons are emitted from the fully accelerated fragments."

A ^{252}Cf source on a thin backing has been received, and the investigations are continued with a multiple-differential measurement, $(N(E_n,\theta_n,A,TKE))$, of the ^{252}Cf prompt fission neutrons.

Feasibility study for nuclear charge determination of fission fragments

F.-J. Hambsch, H.-H. Knitter, C. Budtz-Jørgensen, Chr. Straede

Frisch gridded ionization chambers are used at CBNM in measurements of fission fragment parameters such as fragment energy, mass and fragment emission angle with respect to the incident neutron beam or with respect to emitted neutrons in case of spontaneous fission. However, up to now information on the nuclear charge was not obtained although it would complete the information. The ionization density along the fragment track is also a function of the fragment charge and it is hoped that the nuclear charge can be determined from the measurement of the ionization density. The ionization density distribution was experimentally obtained from the differentiated anode signals in addition to the two energy and angle informations of a twin ionization chamber [1]. These parameters were measured for thermal neutron induced fission fragments of ^{235}U. The evaluation with respect to fragment charge is being made.

Assaying of targets for nuclear measurements with a gridded ionization chamber

C. Budtz-Jørgensen, H.-H. Knitter, G. Bortels, H. Bax, R. Vogt

Two papers "Assaying of Targets for Nuclear Measurements with a Gridded Ionization Chamber" and "Assaying of ^{235}U Fission Layers for Nuclear Measurements with a Gridded Ionization Chamber" were presented at the 12th World Conference of the International Nuclear Target Development Society, Antwerp, September 1984 and at the IAEA Advisory Group Meeting on Nuclear Standard Reference Data, Geel, November 1984, respectively. The abstract of the former paper reads:

> "An ionization chamber with a Frisch grid is used to determine both the energy (E) of the charged particles emitted from the sample positioned coplanar with the cathode, and the cosine of the emission angle (ϑ) with respect to the normal of the cathode. Using the combined information on cos ϑ and E, problems in particle counting due to sample absorption and scattering effects can be circumvented and sample source strengths are readily determined to an accuracy of 0.3 %. However, it is emphasized that the source strength can be determined from the particles emitted in a large solid angle close

(1) Chr. Straede, C. Budtz-Jørgensen, H.-H. Knitter, Fission Fragment Mass, Kinetic Energy and Angular Distribution for $^{235}U(n,f)$ in the Neutron Energy Range from Thermal to 6 MeV. IAEA Advisory Group Meeting on Nuclear Standard Reference Data, 12-16 November 1984, Geel.

to 2π steradian, which means a considerable higher efficiency than for the conventional low geometry counting techniques. Moreover, the present method, within reasonable limits, is insensitive to source shape and thickness homogeneity.
The technique will be illustrated by measurements of alpha particles and fission fragments emitted from a set of four vacuum evaporated UF_4 . three electrodeposited and one suspension-sprayed $^{235}U_3O_8$ layers. The energy and angular distributions of alpha particles and of the heavy alpha recoils emitted from a self transferred ^{224}Ra source will be discussed. The low energetic alpha recoils might be useful as probes for the investigation of ultra thin (< 400 A) layers."

During the investigations it was demonstrated that the heavy recoil nuclei from alpha decay of the ^{228}Th decay chain can be detected with an ionization chamber. Their measured pulse height spectra yielded also information on the location of the decaying nuclei with respect to the source surface. The recoils can, because of their short ranges < 400 Å, be used as sensitive probes for the characterization of ultra thin sources and layers.

1.1.2. Non-Neutron Data for Standards

This sub-project contains both measurements and evaluation of radionuclide decay data.

Data measurements and standardization of ^{47}Sc

D. Reher, E. Celen, B.M. Coursey★, B. Denecke, H.H. Hansen, D. Mouchel, R. Vaninbroukx, W. Zehner

At the occasion of an international comparison on activity-concentration measurements of a ^{47}Sc solution (1), some decay data which were not very accurately known, have been measured. The nuclide ^{47}Sc is of importance for efficiency calibration of γ-ray detectors for energies of about 160 keV. An internal report (2) on these data measurements has been written having the following abstract:

---

(1) D. Reher, E. Celen, B.M. Coursey, R. Vaninbroukx and W. Zehner, Standardization of a ^{47}Sc solution, CBNM Internal Report GE/R/RN/26/83, 1983.

(2) D. Reher, H.H. Hansen and R. Vaninbroukx, The decay of ^{47}Sc, CBNM Internal Report GE/R/RN/12/84, 1984.

★ Visiting Scientist from NBS, Washington, USA.

"Decay data of ^{47}Sc have been re-measured applying various methods. The following results were obtained: The half life, $T_{1/2}$ = (3.3501 ± 0.0005)d, the γ-ray emission probability, P_γ = 0.677 ± 0.004, the transition probabilities for the two β^- branches, P_{β_1} = 0.326 ± 0.014 and P_{β_2} = 0.674 ± 0.014, the endpoint energies of the two β^- spectra, E_{β_1} = (600.5 ± 1.9) keV and E_{β_2} = (439.0 ± 1.6) keV, and the K-shell internal conversion coefficient, a_K = 0.00409 ± 0.00021. These data have been compared with results obtained from previous measurements."

The data will be combined with those measured at NPL and LMRI and be published in a joint paper in 1983.

Decay of ^{133}Ba

H.H. Hansen, D. Mouchel, R. Vaninbroukx, W. Zehner

The nuclide ^{133}Ba is widely used as radioactivity standard for detector calibration. The exact knowledge of the half life is most important. JRC-Geel is following the decay of this nuclide for several years. New sets of γ-ray spectra for the determination of the half life of ^{133}Ba have been recorded with the HPGe detector and with the NaI(Tl) spectrometer. The measurements will be continued.

Decay of ^{234}U

G. Bortels, B. Denecke, W. Oldenhof, R. Vaninbroukx

An accurate assay of a suitable sample for actinides can be performed by α-particle or γ-ray spectrometry provided that the α-particle and photon-emission probabilities are well known.
For the nuclide ^{234}U, which is the major contributor to the disintegration rate of most enriched uranium samples, detailed α-emission-probability data are lacking, the estimated accuracy being only about 4 % [1]. Also the accuracies of the photon-emission probabilities are only about 10 % and hence accurate new measurements are required. Such measurements increase confidence in the completeness and consistency of the decay scheme [1]. The required accuracies are 1 % and 2 % for the α-particle and photon-emission probabilities, respectively [2].

---

(1) A.L. Nichols, in Transactinium Isotope Nuclear Data - 1979, IAEA-TECDOC-232, IAEA, Vienna 1980, p. 67.

(2) A. Lorenz, Fifth Research Coordination Meeting on the Measurement and Evaluation of Transactinium Isotope Nuclear Data, INDC(NDS)-138/GE (1982).

Alpha-particle emission probabilities

The probabilities per decay P_{a0}, P_{a53} and P_{a174} for emission of a particles to the ground level and the 53- and 174 keV levels in ^{230}Th, respectively, were measured. The corresponding a-particle energies are about 4776, 4724 and 4605 keV. Figure 1.2 shows the corresponding peaks in the a-particle pulse-height distribution. All other a-emission probabilities, the sum of which is less than 10^{-6}, can be neglected. The P_{ai} values were obtained by measurements of $I_{ai} = N_i/\Sigma N_i$ in various solid angles Ω and by extrapolation to Ω equals zero. N_i is the number of events recorded in the a_i peak. A small permanent magnet was used to reduce the number of conversion electrons reaching the detector.

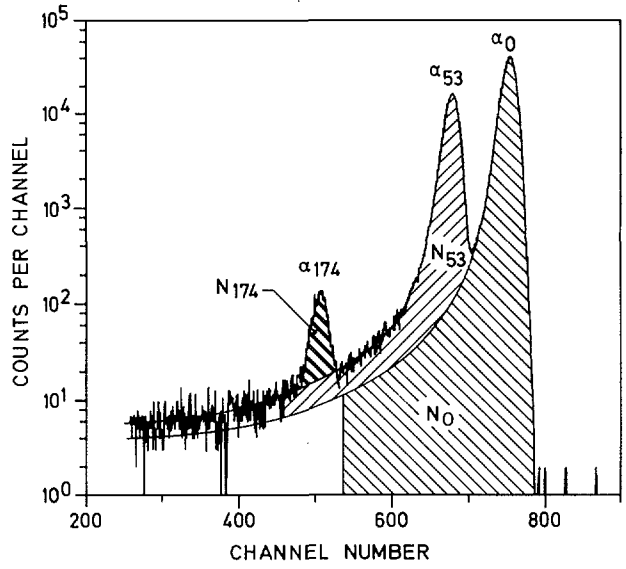

Fig. 1.2. Typical a-particle spectrum of ^{234}U

The results for P_{ai} are presented in Table 1.1. The quoted random uncertainties (68 % confidence interval, n = 16) are obtained from linear regression analyses.

Table 1.1. Alpha-particle-emission probabilities in the decay of ^{234}U

Levels in ^{230}Th	Corresponding a-particle energy (keV)	Emission probability (P_{ai})	Typical Uncertainty components		
			Random	^{230}Th influence	Tail correction
174 keV	4605	0.00206 ± 0.00004	0.00002	0.00001	0.00003
53 keV	4724	0.2842 ± 0.0005	0.0003	0.0001	0.0003
0	4776	0.7138 ± 0.0005	0.0003	0.0001	0.0003

The systematic uncertainties are mainly due to the ^{230}Th grown into the ^{234}U samples and to the peak-tailing corrections. The uncertainties due to interferences by the other uranium isotopes and by background pulses were found to be negligible. These results, for which a substantial effort has been devoted to reach a high accuracy, are about 30 times more accurate than the values given by various evaluators [1,2].

Photon-emission probabilities

The disintegration rates, N_o, of the sources used were measured by α-particle counting in well-defined low solid angles, and the photon-emission rates, N_{ph}, for the most important γ and X rays were measured using an efficiency calibrated high-purity-Ge detector. The uncertainties on the detection efficiencies were estimated to vary between 0.5 and 2 % depending on the energy region concerned. The photon-emission probabilities P_{ph} were obtained from the ratios N_{ph}/N_o after applying several corrections such as those for photon self-absorption, summing effects and differences in the source diameters with those of the calibration sources. The results are listed in Table 1.2.

Table 1.2. Photon-emission probabilities in the decay of ^{234}U

Nuclide	Photon energy (keV)	Photon-emission probability, P_{ph}		
		This work	Nuclear Data Sheets	Recent measurements (not included in NDS)
^{234}U	11.1 ThL_ℓ	0.0022 ± 0.0001		0.0022 ± 0.0001
	13.0(Ē) ThL_α	0.0360 ± 0.0007		0.0366 ± 0.0008
	16.2(Ē) ThL_β	0.0530 ± 0.0012		0.0487 ± 0.0010
	19.0(Ē) ThL_γ	0.0123 ± 0.0003		0.0105 ± 0.0004
	Total ThLX	0.1035 ± 0.0014		0.0981 ± 0.0013
	53.20	$(1.24 \pm 0.02)10^{-3}$	$(1.19 \pm 0.10)10^{-3}$	
	89.95 Th$K_{\alpha 2}$	$(2.53 \pm 0.07)10^{-5}$		
	93.35 Th$K_{\alpha 1}$	$(4.15 \pm 0.10)10^{-5}$		
	120.88	$(3.41 \pm 0.04)10^{-4}$	$(4.10 \pm 0.40)10^{-4}$	

(1) Y.A. Ellis, Nuclear Data Sheets 21, 493 (1977).

(2) C.M. Lederer and V.A. Shirley, Table of Isotopes, 7th Edition, John Wiley and Sons, New York (1978).

The quoted uncertainties, corresponding to a 68 % confidence level, take into account random uncertainties, estimated from the various individual results obtained from the different sources, and the uncertainties in the disintegration rates N_o and the photon-emission rates N_{ph}. For comparison, Table 1.2 gives also the values recommended by the Nuclear Data Sheets (NDS) [1] and the results of recent measurements [2] not included in NDS.

Consistency of the P_α and P_{ph} results

The total transition probability, P_{tr}, for de-excitation of a given level by γ rays and conversion electrons is equal to the sum of all transitions populating that level. Since for the 121-keV and the weak higher levels no cross-over γ rays are observed, the probabilities for depopulating the 121-keV and 53-keV levels are equal to the sum of all α-particle transitions to the respective level and to all higher levels. The quantities P_{tr} and P_{ph} are related by the equation $\alpha = P_{tr}/P_{ph} - 1$, where α is the total internal-conversion coefficient for the γ transition considered.

The results for the total conversion coefficients deduced from our measurements are given in Table 1.3 together with theoretical values obtained from Rösel et al. [3]. The excellent agreement between the experimental and theoretical values supports the reliability of our results and improves appreciably the confidence in the completeness and consistency of the ^{234}U decay scheme.

Table 1.3. Internal-conversion coefficients in the decay of ^{234}U

Level in ^{230}Th	Corresponding photon energy (keV)	Transition and photon-emission probabilities		Total internal conversion coefficients α	
		P_{tr}	$P_{ph} \times 10^3$	Experimental	Theoretical
174 keV	120.88	0.00206 ± 0.00004	0.341 ± 0.004	5.04 ± 0.11	5
53 keV	53.20	0.2862 ± 0.0005	1.24 ± 0.02	231 ± 4	233

(1) Y.A. Ellis, Nuclear Data Sheets 21, 493 (1977).

(2) C.E. Bemis, Jr. and L. Tubbs, Absolute L-Series X-Ray and Low-Energy Gamma-Ray Yield for Most Transuranium Nuclides, U.S. ERDA, Report ORNL-5927 (1977) p. 93.

(3) F. Rösel, H.M. Fries, K. Alder and H.C. Pauli, Atom. Data and Nucl. Data Tables 21, Nrs. 4,5 (1978).

The investigation is finished and the results have been published [1].

^{238}Pu alpha-activity fraction in the NBS plutonium SRM 946 and 947

G. Bortels, A. Verbruggen

At the 1981 and 1983 seminars on alpha-particle spectrometry, which were sponsored by the International Committee for Radionuclide Metrology (ICRM), several authors have shown that for radionuclides of high specific activity, measured in a low geometry, peak-area ratios can be determined with an accuracy of better than 0.5 % and even 0.1 % [2,3]. In order to provide a sound basis for the evaluation of accuracies at this level, the need for multinuclide reference materials, standardized for α-activity ratios, and for reference α spectra was expressed at the 1983 Harwell Seminar [3].
Mixed plutonium sources are very well suited in this respect since the α-particle spectra contain a simple group of two singles (^{238}Pu) which is well separated from a complex $^{239+240}$Pu group.
Moreover, the accurate mass-spectrometric measurements of abundances and the rather well known half lives of the plutonium isotopes provide important additional information to the α spectrometrist.
The NBS SRM's are still the only plutonium reference materials available today. Although the ^{238}Pu abundance in the SRM's 946 and 947 is low, these are well suited for improving α-peak-analysis codes. The authors have therefore undertaken accurate measurements of the ^{238}Pu/$^{239+240}$Pu α-activity ratios in these materials. The results of the measurements are shown in Table 1.4.
A paper has been presented at the 6th ESARDA Symposium, Venice (Italy), May 1984 [4].

---

(1) R. Vaninbroukx, G. Bortels and B. Denecke, Int. J. Appl. Radiat. Isot., 35, 1081 (1984).

(2) Alpha-Particle Spectrometry Techniques and Applications, Proceedings of a Seminar of the ICRM, Geel, Belgium, 1981 (Eds. G. Bortels, G.A. Brinkman and W.B. Mann), Int. J. Appl. Radiat. Isot. 35, No. 4 (1984).

(3) Proceedings of the Second Seminar on Alpha-Particle Spectrometry and Low-Level Measurements, Harwell, England, May 10-13, 1983 (Eds. K.M. Glover, M. Ivanovich and A.E. Lally), Nucl. Instr. and Meth. 223, 617-618 (1984).

(4) G. Bortels and A. Verbruggen, Accurate measurement of the ^{238}Pu Alpha-Activity Fraction in the NBS Plutonium SRM 946 and 947, 6th ESARDA Symposium on Safeguards and Nuclear Material Management, Venice, Italy, 14-18 April 1984, edited by L. Stanchi (ESARDA Symposium Secretariat, JRC-Ispra, 1984), p. 431.

Table 1.4. Results of the $^{238}Pu/^{239+240}Pu$ a-activity ratio measurements as of 1 April 1984

	SRM 946	SRM 947
Mean	0.4873	0.5187
Overall uncertainty for the mean		
standard deviation	± 0.0004	± 0.0005
95 % confidence level	± 0.0008	± 0.0010
Number of measurements	20	21
Uncertainty components		
random (st.dev. for the mean)	± 0.0003	± 0.0004
minor peaks	± 0.00005	± 0.00005
tailing correction	± 0.0001	± 0.00005
impurities and background	--	--
^{241}Am separation	± 0.0002	± 0.0002
Overall uncertainty for the mean (st.dev.)	± 0.0004	± 0.0005

Half life of ^{241}Pu

R. Vaninbroukx

This half-life value is requested [1] to 0.5 % accuracy for mass-determination and non-destructive assay. In an attempt to solve the apparent discrepancies in the results of ^{241}Pu half-life determinations, direct decay measurements using a high-purity Ge detector were started about 1.6 years ago.

---

(1) A. Lorenz (ed.), Third IAEA Advisory Group Meeting on Transactinium Isotope Nuclear Data, Uppsala, 21-25 May 1984, INDC(NDS)-158 (1984).

Four sources sealed into small Al boxes were used. For two of them the Am-Pu separation was performed about nine years ago, while for the two others the separation was done just before the present measurements. The changes in the count rates in the peaks of the UK_{a_2} X-ray and the gamma rays at 148.6, 164.6 and 208.0 keV were observed. The first two peaks are completely due to ^{241}Pu. For the 164.6 and 208.0 keV peaks small corrections for the contribution by the ^{241}Am grown into the samples had to be applied. These corrections, which can be calculated accurately from the ^{241}Am content determined by evaluating the count rates in the 60 keV peak, amount to about 2.6 % for the nine years old sources and 0.35 % for the two others. Over the period of observation, only 8 % of the ^{241}Pu atoms decayed and the uncertainty on the least squares fit is still of the order of 2 %. The preliminary result obtained is (14.26 $\pm$ 0.25)a. This value is in good agreement with the results of (14.33 $\pm$ 0.02)a, obtained by a recent mass-spectrometric measurement [1].

Decay of ^{242}Pu

R. Vaninbroukx, G. Bortels, B. Denecke

For non-destructive assay of Pu samples and environmental studies α-particle and γ-ray emission probabilities of ^{242}Pu are required with accuracies of about 5 % [2]. Since only very few experimental data are available and because of the limited information on these data [3], new measurements were performed at CBNM.

The ^{242}Pu sample used contained 99.85 atom % ^{242}Pu. For the materials used in the γ-ray-emission-probability measurements the ^{241}Am grown into the sample was separated before starting the measurements. The ratio of the ^{242}Pu activity to the total Pu activity was 0.8637 $\pm$ 0.0003. This value was calculated from the isotopic analysis of the sample by mass spectrometry and from alpha-particle and gamma-ray spectrometry. Small corrections for the ^{241}Am ingrowth after the separation were applied. The disintegration rates

---

(1) P. De Bièvre, M. Gallet, R. Werz, Int. J. Mass Spectr. Ion Phys., 51, 111 (1983).

(2) A. Lorenz (ed.), Third IAEA Advisory Group Meeting on Transactinium Isotope Nuclear Data, Uppsala, 21-25 May 1984, INDC(NDS)-158 (1984).

(3) Y.A. Ellis, R.L. Haese, Nuclear Data Sheets for A = 242, Nucl. Data Sheets 21, 615 (1977).

of the sources used were measured by alpha-particle counting at well defined solid angles. The overall uncertainty on the disintegration rates was estimated to be ± 0.1 %. The source used for the alpha-particle spectrometric measurements has been prepared without Am/Pu separation by sublimation in vacuum at the CBNM Sample-Preparation Group. An amount of ^{242}Pu with an activity of about 2660 Bq was deposited in a spot of 12 mm in diameter on a stainless steel disc. Other nuclides present in the source were ^{238,239,240,241}Pu and ^{241}Am. The total alpha activity of the source was about 6100 Bq.

The alpha-spectrometric measurements were done using a surface-barrier detector of 100 mm^2 active area in connection with a small magnet which eliminated most of the conversion electrons [1]. The relative solid angle $\Omega/4\pi$ used in the measurements was about 1 %. A series of 18 measurements, runs of 3 hours each, was made. These spectra have been added together, after correcting them for instrumental drift, to obtain 3 spectra for analysis. In the spectrum analysis, corrections have been made for peak tailing. The results have been corrected for extrapolation of the solid angle $\Omega \to 0$ [2,3] and for interferences mainly due to the ^{241}Pu impurities present in the source. A typical alpha-particle spectrum is shown in Fig. 1.3.

The gamma-ray emission rates were measured with calibrated high-purity Ge detectors. The uncertainty on the detection efficiencies was estimated as ± 1.5 % for the γ rays at 44.9 and 103.5 keV and ± 0.5 % for the γ rays at 158.8 keV. Small corrections for self-absorption of the γ rays and for summing effects were applied. The main uncertainty for the three peaks were due to the contributions by other Pu isotopes. A typical γ ray spectrum is shown in Fig. 1.4.

The results are summarized in Table 1.5. The quoted uncertainties, corresponding to a 68 % confidence level, take into account random and systematic uncertainties.

---

(1) G. Bortels, W. Oldenhof, in: Annual Progress Report on Nuclear Data 1983, NEANDC(E)252"U" Vol. III, Euratom/INDC(EUR)-018/G (CBNM, Geel, 1984) p. 80-81.

(2) G. Bortels, B. Denecke, R. Vaninbroukx, Nucl. Instr. and Meth. 223, 329 (1984).

(3) R. Vaninbroukx, G. Bortels, B. Denecke, Int. J. Appl. Radiat. Isot., 35, 1081 (1984).

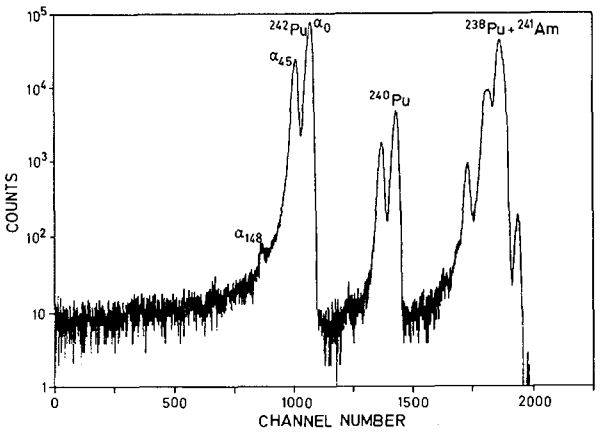

Fig. 1.3. Alpha-particle spectrum of ^{242}Pu sample

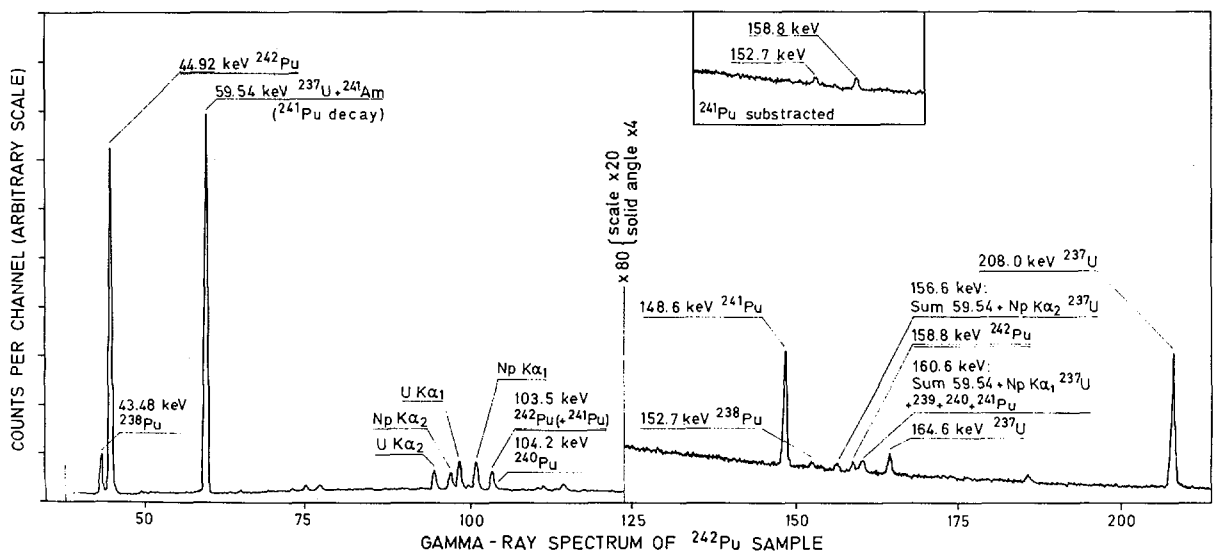

Fig. 1.4. Photon spectrum of ^{242}Pu sample

Table 1.5. Alpha-particle and gamma-ray emission probabilities in the decay of ^{242}Pu

Levels in ^{238}U (keV)	Corresponding energies (a)		α_{theor} (b)	Emission probabilities					
				P_α			P_γ		
	E_α (keV)	E_γ (keV)		Measured	Calculated (c)	Adopted	Measured	Calculated (d)	Adopted
307	4598	158.8	1.86		$(8.6 \pm 0.7)10^{-6}$	$(8.6 \pm 0.7)10^{-6}$	$(3.0 \pm 0.2)10^{-6}$		$(3.0 \pm 0.2)10^{-6}$
148	4755	103.5	11.6	$(2.90 \pm 0.14)10^{-4}$	$(3.22 \pm 0.13)10^{-4}$	$(3.07 \pm 0.14)10^{-4}$	$(2.63 \pm 0.09)10^{-5}$	$(2.37 \pm 0.12)10^{-5}$	$(2.55 \pm 0.10)10^{-5}$
45	4856	44.92	626	0.2352±0.0017	0.2329±0.0060	0.2350±0.0017	$(3.72 \pm 0.07)10^{-4}$	$(3.75 \pm 0.08)10^{-4}$	$(3.73 \pm 0.07)10^{-4}$
0	4901			0.7645±0.0017		0.7647±0.0017(e)			

(a) From Ellis and Haese, Nucl. Data Sheets 21, 615 (1977).

(b) *Total internal-conversion coefficients of the γ transitions, from Rösel et al., Atom. Data and Nucl. Data Tables 21, 293 (1978) (estimated uncertainty ± 2 %)*

(c) Calculated from P_γ measured and conversion coefficient α: $P_\alpha = (1+\alpha)P_\gamma$ - Sum P_α to higher levels

(d) Calculated from P_α measured and conversion coefficient α: P_γ = Sum P_α (to considered level and higher levels):$(1+\alpha)$

(e) 1-Sum P_α to higher levels

The measured alpha-particle and gamma-ray emission probabilities, combined with theoretical values for the total internal-conversion coefficients, yield finally a consistent set of data. The uncertainties of the deduced values are considerably smaller than those previously adopted [1]. The investigation is finished and the results will be published.

Decay of ^{243}Am-^{239}Np

R. Vaninbroukx, G. Bortels, B. Denecke, W. Zehner

Photon-emission probabilities for ^{239}Np are often needed for decay heat calculations [2] and for the determination of the ^{239}Pu accumulation in reactors [3]. The most practical way to determine the photon-emission

---

(1) Y.A. Ellis, R.L. Haese, Nuclear Data Sheets for A=242, Nucl. Data Sheets 21, 615 (1977).

(2) A. Lorenz, Second IAEA Advisory Group Meeting on Transactinium Isotope Nuclear Data, Cadarache 1979, Summary Report, IAEA, Vienna (1979).

(3) V.K. Mozhaev, V.A. Dulin and Yu.A. Kazanskii, Sov. A. Energy 47, 566 (1979).

probabilities is to perform measurements on the radioactive pair ^{243}Am-^{239}Np. The nuclide ^{243}Am is long-lived and can be accurately standardized by α-particle counting. Generally, the 2.4-day ^{239}Np is in secular equilibrium with ^{243}Am. This pair could also be used as a long-lived reference material for efficiency calibration of photon detectors [1,2] in the energy range 40 to 340 keV, if the photon-emission probabilities were accurately known. It should be noted that, for the same solid angles of the detection systems, the corrections for summing effects between coincident photons are much lower for ^{243}Am-^{239}Np than for ^{133}Ba, a nuclide which is frequently used for the calibration of photon detectors in the same energy range.

For the measurements on ^{243}Am-^{239}Np, a material obtained in 1979 from ORNL, Oak Ridge, was used. The radionuclidic purity of the sample was determined by α-particle and γ-ray spectrometry. The only impurity which could be detected was ^{241}Am. The activity ratio ^{241}Am/^{243}Am was found to be 0.0027 $\pm$ 0.0001. From these measurements it could also be estimated that any contribution to the disintegration rate by other impurities was smaller than 0.1 % of the ^{243}Am activity. Seven sources were prepared by drop deposition on stainless-steel backings. The diameter of the active spot varied between 6 and 12 mm and, the amount of ^{243}Am between 1 and 6 μg, corresponding to ^{243}Am activities from 7 to 43 kBq.

The photon emission probabilities $P_{ph} = N_{ph}/N_o$ were obtained from the ratio of the photon-emission rates, N_{ph}, measured with a calibrated HP-Ge detector and the disintegration rates, N_o, measured by α-particle counting. Similar corrections had to be applied as for the measurement of ^{234}U.

A typical photon spectrum is shown in Fig. 1.5.

The results are given in Table 1.6. For comparison, Table 1.6 gives also the values recommended by the Nuclear Data Sheets (NDS) [3,4] and the results

---

(1) V.K. Mozhaev, V.A. Dulin and Yu.A. Kazanskii, Sov. At. Energy 47, 566 (1979).

(2) I. Ahmad and M. Wahlgren, Nucl. Instrum. Methods 99, 333 (1972).

(3) M.R. Schmorak, Nuclear Data Sheets 21, 91 (1977).

(4) Y.A. Ellis-Akovali, Nuclear Data Sheets 33, 79 (1981).

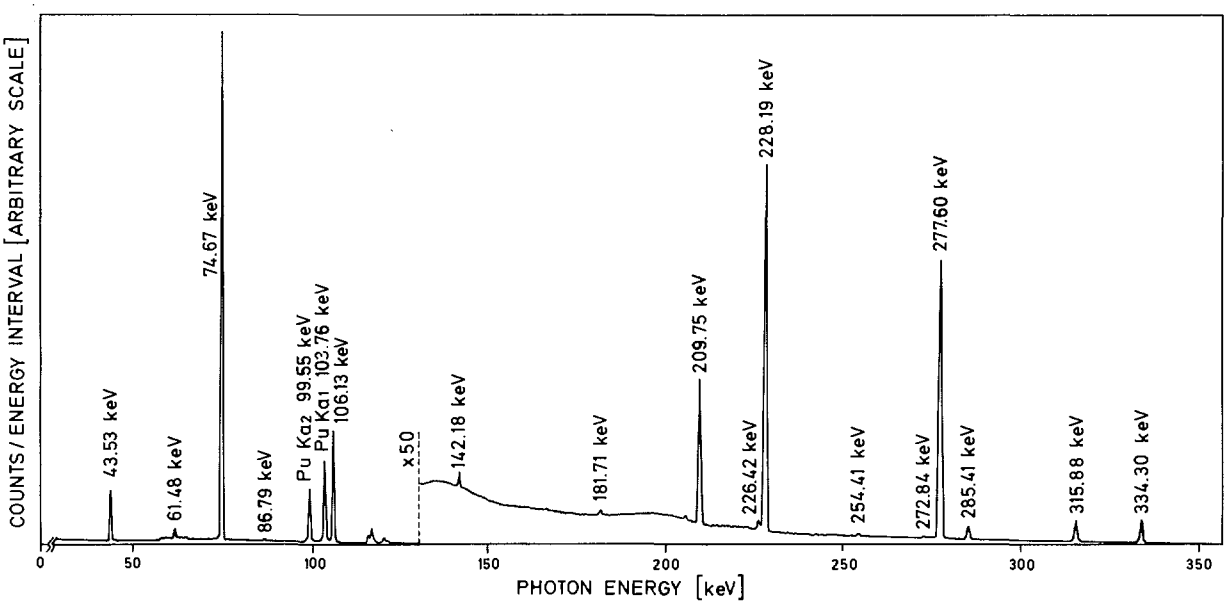

Fig. 1.5. Photon spectrum of ^{243}Am - ^{239}Np

of recent measurements [1-3] not included in NDS. The results obtained by Ahmad and Wahlgren [4] for ^{239}Np and ^{243}Am, although included in the NDS, are also given. They are quoted with considerably lower uncertainties than the NDS values and have perhaps been somewhat underweighted in the evaluations. The present measurements improve the accuracy status of the photon-emission probabilities. The measurements are finished and the results are published [5].

---

(1) D.I. Starozhukov, Yu.S. Popov and P.A. Privalova, Sov. At. Energy 42, 355 (1977).

(2) V.K. Mozhaev, V.A. Dulin and Yu.A. Kazanskii, Sov. At. Energy 47, 566 (1979).

(3) S.P. Holloway, J.B. Olomo and T.D. Mac Mahon in K.H. Böckhoff (ed.), Nuclear Data for Science and Technology, D. Reidel publishing Co., Dordrecht (1983) p. 287.

(4) I. Ahmad and M. Wahlgren, Nucl. Instrum. Methods 99, 333 (1972).

(5) R. Vaninbroukx, G. Bortels and B. Denecke, Int. J. Appl. Radiat. Isot. 35, 1081 (1984).

Table 1.6. Photon-emission probabilities in the decay of ^{239}Np and ^{243}Am

Nuclide	Photon energy (keV)	Photon-emission probability, P_{ph}			
		This work	Nuclear Data Sheets	Recent measurements (not included in NDS)	Ahmad and Wahlgren Ref. 6 (1972)
^{239}Np	61.48	0.0129 ± 0.0002	0.0096 ± 0.0013		
	99.55 $PuK_{\alpha 2}$	0.1360 ± 0.0030			0.1450 ± 0.0060
	103.76 $PuK_{\alpha 1}$	0.2220 ± 0.0050		0.1970 ± 0.0080	0.2220 ± 0.0080
	106.13	0.2750 ± 0.0040	0.2270 ± 0.0130	0.2660 ± 0.0100	0.2780 ± 0.0090
	181.71	0.0007 ± 0.0001	0.0011 ± 0.0001		0.00075± 0.00008
	209.75	0.0346 ± 0.0005	0.0324 ± 0.0024	0.0336 ± 0.0014 Ref.(3)	0.0342 ± 0.0010
	226.42	0.0028 ± 0.0002	0.0034 ± 0.0004 Ref.(1)	0.0024 ± 0.0003 (1977)	
	228.19	0.1121 ± 0.0018	0.1072 ± 0.0064 (1977)	0.1178 ± 0.0044	0.1140 ± 0.0030
	254.41	0.0012 ± 0.0001	0.0010 ± 0.0002		0.0011 ± 0.0001
	272.84	0.0008 ± 0.0001	0.0008 ± 0.0001		0.0008 ± 0.0001
	277.60	0.1438 ± 0.0021	0.1410 ± 0.0040	0.1500 ± 0.0050	0.1450 ± 0.0040
	277.60			0.1430 ± 0.0024 Ref.(4) (1979)	
	285.41	0.0077 ± 0.0002	0.0078 ± 0.0007	0.0093 ± 0.0006	0.0076 ± 0.0002
	315.81	0.0160 ± 0.0003	0.0159 ± 0.0011	0.0163 ± 0.0007 Ref.(3)	0.0152 ± 0.0005
	334.30	0.0208 ± 0.0003	0.0203 ± 0.0018	0.0210 ± 0.0010	0.0195 ± 0.0007
^{243}Am	43.53	0.0604 ± 0.0013	0.0504 ± 0.0060	0.0610 ± 0.0016	0.0550 ± 0.0030
	74.67	0.6850 ± 0.0150	0.6000 ± 0.0600 Ref.(2)	0.6700 ± 0.0100 Ref.(5)	0.6600 ± 0.0300
	86.79	0.0035 ± 0.0001	0.0031 ± 0.0004 (1981)	0.0033 ± 0.0001 (1983)	
	142.18	0.0013 ± 0.0001	0.0011 ± 0.0002	0.0012 ± 0.0001	

(1) M.R. Schmorak, Nuclear Data Sheets 21, 91 (1977).

(2) Y.A. Ellis-Akovali, Nuclear Data Sheets 33, 79 (1981).

(3) D.I. Starozhukov, Yu.S. Popov and P.A. Privalova, Sov. At. Energy 42, 355 (1977).

(4) V.K. Mozhaev, V.A. Dulin and Yu.A. Kazanskii, Sov. At. Energy 47, 566 (1979).

(5) S.P. Holloway, J.B. Olomo and T.D. Mac Mahon in K.H. Böckhoff (ed.), Nuclear Data for Science and Technology, D. Reidel publishing Co., Dordrecht (1983) p. 287.

(6) I. Ahmad and M. Wahlgren, Nucl. Instrum. Methods 99, 333 (1972).

Current status of nuclear decay data of transactinium nuclides

C.W. Reich★, R. Vaninbroukx

A paper has been presented at the third IAEA Advisory Group Meeting on Transactinium Isotope Nuclear Data, Uppsala, 1984 (1). It has the following abstract:

> "In 1977, the IAEA organized a Coordinated Research Programme to address the needs for highly accurate actinide-nuclide decay data identified at the first Advisory Group Meeting on Transactinium Isotope Nuclear Data, held in Karlsruhe in 1975.
> During the years of its existence, this CRP has made significant strides towards achieving the goals outlined at Karlsruhe and subsequently refined at a second Advisory Group Meeting, held in Cadarache in 1979. In this paper, the make-up of the CRP and its work in the areas of decay-data measurement and evaluation are presented and its significant accomplishments summarized.
> We also discuss the contents and philosophy of the final report, containing the results of the measurements and evaluations carried out by the CRP participants, to be published following the planned termination of this Programme in November, 1984."

Evaluation of selected decay data for some actinides

R. Vaninbroukx, W. Bambynek

As a part of the CBNM contribution to the IAEA Coordinated Research Programme on the Measurement and Evaluation of Transactinium Isotope Decay Data, the published values for some selected data have been critically reviewed and recommended values are proposed for the following decay parameters (2):

^{231}Th : gamma-ray-emission probabilities
^{232}U-^{208}Pb decay chain : gamma-ray-emission probabilities
^{235}U : gamma-ray-emission probabilities
^{239}Np : gamma-ray-emission probabilities
^{240}Pu : half life

---

(1) C.W. Reich and R. Vaninbroukx, Current Status of Nuclear Decay Data and Report on the IAEA Coordinated Research Programme on the Measurement and Evaluation of Transactinium-Isotope Nuclear Decay Data, Transactinium Isotope Nuclear Data - 1984, IAEA-TECDOC-3361 (International Atomic Energy Agency, Vienna, 1985) p. 275.

(2) R. Vaninbroukx and W. Bambynek, Evaluation of Selected Decay Data for some Actinides, CBNM Internal Report GE/R/RN/15/84, 1984.

★ Idaho National Engineering Laboratory, Idaho Falls, USA.

^{241}Am : half life and gamma-ray-emission probabilities
^{243}Am : half life and gamma-ray-emission probabilities

The data will be published together with the contributions of other collaborators of the Coordinated Research Programme in the IAEA Technical Report Series.

Emission probabilities of selected gamma rays for radionuclides used as detector-calibration standards

R. Vaninbroukx

For the reliability of the results of gamma-ray measurements with efficiency-calibrated detectors and for the intercomparison of these results, it is essential that the available most accurate data for the calibration radionuclides are used by all investigators.
The evaluation proposes a set of values which is estimated to consist of the current "best" available data. For the detector calibration, the gamma-ray energies are considered to be known to the required accuracy and have been adopted from the Nuclear Data Sheets. Here only the emission probabilities are evaluated.
The nuclides for which emission-probability data are given are subdivided into two categories:

1. Primary calibration gamma rays.

In this category only nuclides are considered which:
- can be accurately standardized,
- have an appropriate half life,
- are available with high radionuclidic purity,
- have a simple and well known decay scheme, so that corrections for summation effects between coincident photons are small or can be calculated accurately.

2. Secondary calibration gamma rays.

In this category nuclides which may be helpful for detector calibrations, but which do not fulfil all the above mentioned criteria, are considered. A paper on this subject has been presented at the IAEA Advisory Group Meeting on Nuclear Standard Reference Data, Geel, 12-16 November 1984.
Tables 1.7 and 1.8 list recommended values for primary and secondary calibration γ rays, respectively.

Table 1.7. Primary calibration gamma rays

Nuclide	E_γ (keV)	Emission probability (P_γ) Recommende value
^{22}Na	1274.5	0.99935 ± 0.00020
^{24}Na	1368.6	0.99994 ± 0.00002
	2754.0	0.99878 ± 0.00008
^{46}Sc	889.28	0.99984 ± 0.00001
	1120.5	0.99987 ± 0.00001
^{51}Cr	320.08	0.0985 ± 0.0009
^{54}Mn	834.84	0.99975 ± 0.00001
^{57}Co	14.41	0.093 ± 0.002
	122.06	0.8563 ± 0.0015
	136.47	0.1062 ± 0.0010
^{58}Co	810.78	0.9944 ± 0.0002
^{60}Co	1173.24	0.9989 ± 0.0002
	1332.51	0.99983 ± 0.00001
^{65}Zn	1115.55	0.5065 ± 0.0020
^{85}Sr	514.00	0.988 ± 0.005
^{88}Y	898.02	0.942 ± 0.004
	1836.0	0.9930 ± 0.0005
^{94}Nb	702.63	0.9982 ± 0.0001
	871.10	0.9989 ± 0.0001
^{95}Nb	765.80	0.9980 ± 0.0002
^{109}Cd	88.03	0.0368 ± 0.0005
$^{113}In^m$	391.69	0.649 ± 0.002
$^{115}In^m$	336.23	0.459 ± 0.002
^{125}I	35.49	0.0660 ± 0.0010
^{134}Cs	604.70	0.9763 ± 0.0004
	795.84	0.8552 ± 0.0004
^{137}Cs	661.66	0.852 ± 0.001
^{139}Ce	165.85	0.799 ± 0.001
^{141}Ce	145.44	0.486 ± 0.004
^{198}Au	411.80	0.9556 ± 0.0007
^{203}Hg	279.20	0.8150 ± 0.0008
^{241}Am	26.35	0.0241 ± 0.0005
	59.54	0.359 ± 0.003

Table 1.8. Secondary calibration gamma rays

Nuclide	E_γ (keV)	Emission probability (P_γ) Recommended value	Nuclide	E_γ (keV)	Emission probability (P_γ) Recommended value
^{7}Be	477.60	0.1045 ± 0.0010	^{152}Eu	121.78	0.2840 ± 0.0023
^{56}Mn	846.75	0.9887 ± 0.0003		244.70	0.0751 ± 0.0007
	1810.72	0.272 ± 0.008		344.28	0.2658 ± 0.0019
	2113.05	0.143 ± 0.004		411.12	0.0223 ± 0.0002
^{56}Co	846.76	0.99925 ± 0.00006		443.98	0.0312 ± 0.0003
	1037.84	0.1411 ± 0.0005		778.90	0.1296 ± 0.0007
	1238.29	0.663 ± 0.005		964.1	0.1462 ± 0.0006
	1360.21	0.0426 ± 0.0002		1085.9	0.1014 ± 0.0006
	1771.35	0.1548 ± 0.0004		1112.1	0.1354 ± 0.0006
	2034.76	0.0776 ± 0.0004		1408.0	0.2085 ± 0.0008
	2598.46	0.1696 ± 0.0004	^{182}Ta	100.11	0.1423 ± 0.0025
	3253.42	0.0770 ± 0.0012		152.43	0.0702 ± 0.0008
^{95}Zr	724.20	0.4415 ± 0.0020		222.10	0.0757 ± 0.0008
	756.73	0.5450 ± 0.0025		1121.3	0.3530 ± 0.0020
$^{99}Tc^{m}$	140.51	0.890 ± 0.002		1189.0	0.1642 ± 0.0010
$^{110}Ag^{m}$	446.81	0.0372 ± 0.0003		1121.4	0.2720 ± 0.0022
	657.76	0.9440 ± 0.0010		1221.0	0.1157 ± 0.0008
	677.62	0.1040 ± 0.0008	^{192}Ir	295.96	0.287 ± 0.001
	687.02	0.0644 ± 0.0003		308.46	0.298 ± 0.001
	706.68	0.1660 ± 0.0010		316.51	0.830 ± 0.003
	744.28	0.0470 ± 0.0004		468.07	0.477 ± 0.002
	763.94	0.2239 ± 0.0008		588.59	0.0449 ± 0.0002
	818.03	0.0732 ± 0.0004		604.41	0.0811 ± 0.0004
	884.68	0.727 ± 0.003		612.47	0.0528 ± 0.0003
	937.49	0.3431 ± 0.0012	^{207}Bi	569.70	0.979 ± 0.001
	1384.30	0.2425 ± 0.0008		1063.66	0.741 ± 0.003
	1475.79	0.0399 ± 0.0002		1770.2	0.0687 ± 0.0004
	1505.04	0.1304 ± 0.0004	^{232}U	238.63	0.435 ± 0.002
^{111}In	171.28	0.902 ± 0.003	and	241.00	0.0404 ± 0.0005
	245.35	0.940 ± 0.002	^{228}Th	510.80	0.0825 ± 0.0014
^{124}Sb	602.73	0.9800 ± 0.0010	decay	583.14	0.3060 ± 0.0017
	645.86	0.0730 ± 0.0010	chains	727.18	0.0662 ± 0.0006
	722.79	0.1130 ± 0.0020	at equi-	860.37	0.0450 ± 0.0005
	1690.98	0.0566 ± 0.0009	librium	2614.6	0.3586 ± 0.0006
	2090.94	0.0566 ± 0.0009	^{243}Am	43.5	0.0605 ± 0.0013
^{133}Ba	53.16	0.0219 ± 0.0003	and	74.7	0.686 ± 0.015
	79.62	0.0262 ± 0.0007	^{239}Np	106.13	0.272 ± 0.002
	81.00	0.341 ± 0.005	at equi-	228.19	0.1127 ± 0.0018
	276.40	0.0716 ± 0.0004	librium	277.60	0.1438 ± 0.0021
	302.85	0.1831 ± 0.0007			
	356.02	0.6200 ± 0.0014			
	383.85	0.0892 ± 0.0005			

Emission probabilities of selected X rays for radionuclides used as detector-calibration standards

W. Bambynek

The availability of high-resolution solid-state detectors has extended the field of X-ray spectrometry towards lower energies. Usually, Si(Li) detectors are used for energies between 5 and 25 keV and planar high-purity germanium detectors for 25 to about 100 or 150 keV. Accurate efficiency calibration of these detectors requires reliable standard data.
The current status of the X-ray emission probabilities of radionuclides useful for detector calibration was reviewed. Experimental, compiled and/or evaluated data were considered. The literature between 1965 and 1984 has been scanned.
In the present work transition energies are considered to be known with sufficient accuracy. They were not evaluated. Half lives were given only as indicative values. Data for both quantities were taken from C.M. Lederer [1] and D.C. Kocher [2]. A list of recommended emission probabilities is given in Tables 1.9.a, 1.9.b and 1.9.c, including information on the availability of the radionuclides [3].
A paper has been presented at the IAEA Advisory Group Meeting on Nuclear Standard Reference Data, Geel, 12-16 November 1984.

---

(1) C.M. Lederer and V.S. Shirley (eds.), Table of Isotopes, 7th Edition (J. Wiley & Sons, New York, 1978) (1978).

(2) D.C. Kocher, Radioactive Decay Data Tables (Technical Information Center, US-Department of Energy, 1981), DOE/TIC-11026 (1981).

(3) G. Grosse and W. Bambynek, International Directory of Certified Radioactive Sources, Physics Data 27-1 (1983).

Table 1.9.a. Primary calibration nuclides and their recommended KX-ray emission probabilities

Nuclide	$T_{1/2}$ (a)	Z	Element	$E_{K\alpha}$ (b) (keV)	$P_{K\alpha}$ (c) (%)	$E_{K\beta}$ (b) (keV)	$P_{K\beta}$ (c) (%)	P_{KX} (c) (%)	Availability (d)
^{49}V	330 d	22	Ti	4.51	17.9 (11)	4.93	2.4 (2)	20.3 (10)	1
^{51}Cr	27.7 d	23	V	4.95	20.1 (6)	5.43	2.7 (1)	22.8 (3)	13
^{54}Mn	312.7 d	24	Cr	5.41	22.6 (4)	5.95	3.0 (1)	25.6 (8)	14
^{55}Fe	2.7 a	25	Mn	5.89	24.9 (5)	6.49	3.4 (2)	28.3 (10)	12
^{57}Co	207 d	26	Fe	6.40	51.0 (2)	7.06	6.9 (3)	57.9 (34)	12
^{58}Co	70.8 d	26	Fe	6.40	23.5 (4)	7.06	3.2 (1)	26.7 (10)	11
^{65}Zn	244.4 d	29	Cu	8.04	34.1 (6)	8.91	4.6 (1)	38.7 (9)	12
^{85}Sr	64.8 d	37	Rb	13.38	50.0 (8)	14.98	8.7 (8)	58.7 (8)	10
^{88}Y	160.6 d	38	Sr	14.14	51.3 (8)	15.86	9.2 (2)	60.5 (8)	11
^{109}Cd	464 d	47	Ag	22.10	82.1 (18)	25.01	17.3 (7)	99.4 (20)	12
^{111}In	2.8 d	48	Cd	23.11	68.4 (20)	26.18	14.5 (6)	83.0 (2)	5
^{113}Sn	115.1 d	49	In	24.14	79.6 (18)	27.36	17.2 (6)	96.8 (6)	7
^{125}I	60.1 d	52	Te	27.38	113.4 (30)	31.12	25.0 (8)	139.0 (30)	14
^{131}Cs	9.9 d	54	Xe	27.75	60.1 (15)	36.20	14.0 (5)	74.1 (10)	2
^{139}Ce	137.7 d	57	La	33.30	63.9 (17)	37.98	15.3 (5)	79.2 (22	11

Table 1.9.b. Secondary calibration nuclides and their recommended KX-ray emission probabilities

Nuclide	$T_{1/2}$ (a)	Z	element	$E_{K\alpha}$ (keV) (b)	$P_{K\alpha}$ (keV) (c)	$E_{K\beta}$ (keV) (b)	$P_{K\beta}$ (%) (c)	P_{KX} (%) (c)	Availa-(d) bility
^{67}Ga	3.3 d	30	Zn	8.63	49.5 (12)	9.57	6.9 (6)	56.4 (13)	8
^{75}Se	49.8 d	33	As	10.53	48.9 (30)	11.72	7.6 (6)	56.5 (40)	10
$^{93}Nb^{m}$	16.1 a	41	Nb	16.58	9.27 (20)	18.66	1.79 (10)	11.06 (14)	
^{99}Mo	66.0 h	43	Tc	18.33	9.3 (4)	20.66	1.9 (2)	11.2 (5)	10
^{103}Ru	39.4 d	45	Rh	20.17	7.29 (28)	22.78	1.51 (6)	8.80 (30)	6
^{123}I	13.1 h	52	Te	27.38	70.5 (20)	31.12	15.9 (6)	86.4 (20)	3
^{133}Ba	10.5 a	55	Cs	30.85	98.0 (16)	34.9 - 35.9	23.0 (5)	121.0 (16)	13
^{137}Cs	30.2 a	56	Ba	32.06	5.66 (18)	36.3 - 37.4	1.34 (4)	7.0 (2)	14
^{141}Ce	32.5 d	59	Pr	35.85	13.2 (4)	40.6 - 42.0	3.2 (2)	16.4 (5)	8
^{152}Eu	13.6 a	62	Sm	39.91	59.1 (12)	45.3 - 46.6	14.9 (3)	74.8 (12)	10
		64	Gd	42.75	0.648 (22)	48.5 - 50.0	0.176 (18)		

				$E_{K\alpha 2}$ (keV)	$P_{K\alpha 2}$ (%)	$E_{K\alpha 1}$ (keV)	$P_{K\alpha 1}$ (%)	$E_{K\beta '1}$ (keV)	$P_{K\beta '1}$ (%)	$E_{K\beta '2}$ (keV)	$P_{K\beta '2}$ (%)		
^{201}Tl	73.1 h	80	Hg	68.96	27.6(10)	70.12	46.9(18)	80.2	16.2(40)	82.5	4.5 (2)	95.2 (16)	2
^{203}Hg	46.6 d	81	Tl	70.83	3.8(2)	72.87	6.4(2)	82.5	2.2(1)	84.9	0.63 (3)	13.0 (4)	12
^{207}Bi	33.4 a	82	Pb	72.80	22.6(12)	74.97	38.2(20)	84.9	13.0(10)	87.3	3.9 (3)	77.7 (40)	3

Table 1.9.c. Secondary calibration nuclides and their recommended LX-ray emission probabilities

Nuclide	$T_{1/2}$ [a]	Z	Element	$E_{L\ell}$ [b] (keV)	$P_{L\ell}$ [c] (%)	$E_{L\alpha}$ [b] (keV)	$P_{L\alpha}$ [c] (%)	$E_{L\eta\beta}$ [b] (keV)	$P_{L\eta\beta}$ [c] (%)	$E_{L\gamma}$ [b] (%)	$P_{L\gamma}$ [c] (%)	P_{LX} [c] (%)	Availability [d]
^{207}Bi	33.4 a	82	Pb	9.18	0.51 (6)	10.45	9.58(15)	11.3-15.4	19.6 (22)	11.6-15.8	4.5(6)	34.2(10)	3
^{238}Pu	38.8 a	92	U	11.62	0.26 (3)	13.60	4.1 (2)	17.0	6.24(30)	20.4	1.2(1)	11.8(4)	3
^{241}Am	432.2 a	93	Np	11.9	0.86 (3)	13.9	13.3 (4)	17.8	19.4 (6)	20.8	4.9(2)	38.5(8)	12

(a) Half lives are taken from D.C. Kocher

(b) Energies are taken from C.M. Lederer

(c) Uncertainties in units of the last digit(s) are given in parentheses

(d) The figures indicate the number of producers offering reference solutions with certified activity concentration, G. Grosse and W. Bambynek [3]

Fluorescence yields

W. Bambynek

A re-evaluation of the K-shell fluorescence yield, ω_K, has been performed. There are about 100 new results since the last evaluation in 1972 [4]. In addition to the various techniques to measure ω_K directly, there are methods which yield the product of the relative K-capture probability P_K and the fluorescence yield ω_K. About 90 of those measurements have been evaluated and included in the file.

For the calculation of the P_K values electron-wave functions have been used according to Mann and Waber. Exchange and overlap corrections of Bahcall and of Vatai were employed, as recalculated by Chen, for $Z \leqslant 58$, and the

(1) D.C. Kocher (1981), Radioactive Decay Data Tables (Technical Information Center, US-Department of Energy, 1981), DOE/TIC-11026

(2) C.M. Lederer and V.S. Shirley (eds.)(1978), Tables of Isotopes, 7th Edition (J. Wiley & Sons, New York, 1978)

(3) G. Grosse, W. Bambynek, Physics Data 27-1, (1983).

(4) W. Bambynek, R.W. Fink, H.-U. Freund, Hans Mark, C.D. Swift, R.E. Price and P. Venugopala Rao, X-Ray Fluorescence Yields, Auger and Coster-Kronig Transition Probabilitites, Rev. Mod. Phys. 44 (1972) 716.

ones of Suslov and of Martin and Bichert-Toft for $Z > 58$. The method of calculation is described elsewhere [1].

Following a thorough evaluation of all experimentally determined values a set of 118 results was selected which were judged to be most reliable. These results were obtained from measurements using carefully prepared sources and after making all necessary corrections. Unfortunately, in the majority of publications the information is incomplete. It is therefore probable that some "good" results were omitted from the list of selected ω_K. Furthermore, the uncertainties quoted by various authors are not strictly comparable because they were determined on the basis of different principles. We have re-estimated the uncertainties and used their squared reciprocals as weights in the calculation of mean values.

The values of the selected data were fitted to the relation

$$\left(\frac{\omega_K}{1 - \omega_K}\right)^{1/4} = \sum_{i=0}^{p} B_i Z^i$$

and a detailed polynomial regression analysis was performed. Starting from a linear relation powers of the independent variable Z were generated to calculate polynomials of successively increasing degrees. For each polynomial of degree p some statistical quantities were calculated: The regression coefficients B_i ($i = 0, \ldots, p$), their standard deviations $s(B_i)$, the t values t_i which were used to test the null hypothesis for the regression coefficients, the confidence coefficients S_i which indicate the statistical confidence with which B_i is different from zero, the multiple correlation coefficient r and the residual standard deviation of the fit S_{res}. The term with the lowest t value was discarded. A new set of regression coefficients and the other quantities mentioned above were calculated and the null hypothesis for the new regression coefficients was tested. Again the term with the lowest t value was eliminated from the polynomial. This procedure was continued until only one term remained. We have analysed polynomials up to the seventh degree in ascendant and descendant order.

---

(1) W. Bambynek, H. Behrens, M.H. Chen, B. Crasemann, M.L. Fitzpatrick, K.W.D. Ledingham, H. Genz, M. Mutterer and R.L. Inteman, Orbital Electron Capture by the Nucleus, Rev. Mod. Phys. 49, 77 (1977).

A detailed study of the results indicated that the polynomial up to the third order yields a statistically very reliable approximation to the experimental points with $r = 0.99940$, $S_{res} = 1.36\ \%$, $(S_i)_{min} = 99.99\ \%$, $B_0 = (3.70 \pm 0.52) \cdot 10^{-2}$, $B_1 = (3.112 \pm 0.044) \cdot 10^{-2}$, $B_2 = (5.44 \pm 0.11) \cdot 10^{-5}$, $B_3 = -(1.250 \pm 0.070) \cdot 10^{-6}$.
In Fig. 1.6 these fitted ω_K values are compared with the theoretical results from relativistic Dirac-Hartree-Slater (DHS) calculations of Chen et al. [1] and with the experimental data of the present evaluation. The DHS results are in excellent agreement with the selected experimental data and the fitted data.

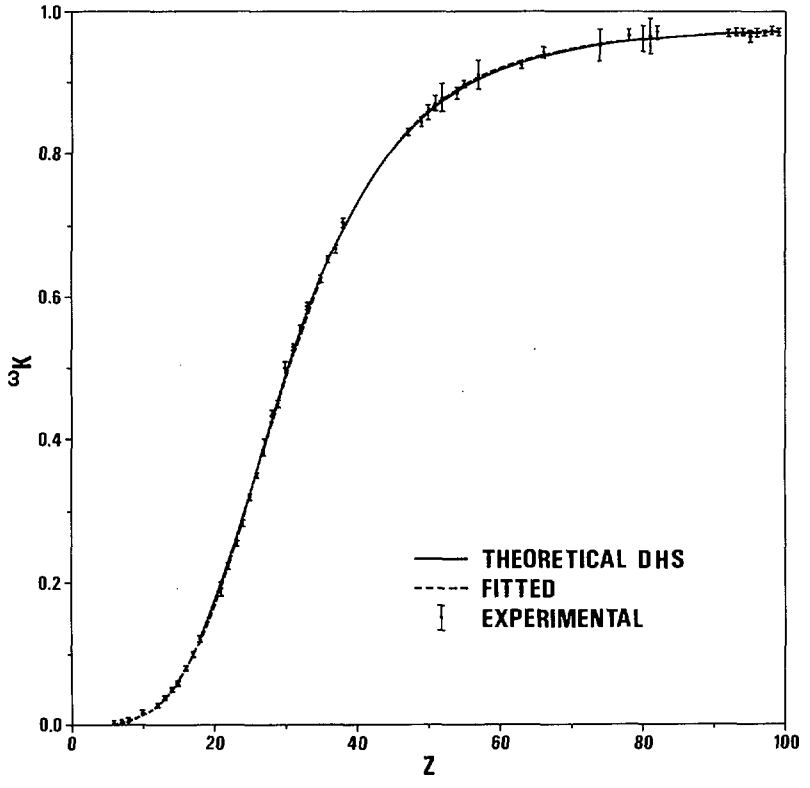

Fig. 1.6. K-shell fluorescence yield as function of atomic number

The results of the evaluation will be published.

---

(1) M.H. Chen, B. Crasemann, Hans Mark, Relativistic K-shell Auger Rates, Level width, and Fluorescence Yields, Phys. Rev. A 21, 436 (1980).

1.2. NUCLEAR DATA FOR FISSION TECHNOLOGY

1.2.1. Cross Sections of the Actinides

The measurements of the fission cross-section and eta of ^{235}U in the sub-thermal region are part of a campaign to improve the accuracy of the temperature coefficient of thermal reactors, which relates to reactor safety. The measurements are initiated by french and british requests to CBNM.

Fission cross-section measurements of ^{235}U at low energies

C. Wagemans*, A. Deruytter, R. Barthélémy, J. Van Gils*

The experimental set-up has been optimalized for measurements at very low neutron energies (down to 1 meV). The measurements are scheduled to start in January 1985. Preliminary measurements were reported at the IAEA Advisory Group Meeting on Nuclear Standards Reference Data. The paper has the following abstract:

> "Accurate new neutron induced cross-section data in the sub-thermal energy region were requested recently by reactor physicists. To fulfill these requests, a liquid nitrogen cooled methane moderator was installed at GELINA, resulting in a five times increased neutron flux below 20 meV.
> Preliminary measurements of the $^{235}U(n,f)$ cross-section in the meV-region and the influence of the cross-section shape on the Westcott g_f-factor are discussed."

Eta of ^{235}U in sub-thermal region

J.A. Wartena, H. Weigmann, C. Bürkholz, R. Pijpstra

An experiment has been set up to measure the energy dependence of eta, the number of neutrons produced per neutron absorbed, in ^{235}U, in the thermal and sub-thermal neutron energy regions. A thick ^{235}U sample (93 % enrichment) is placed in the neutron beam at a 7 m flight path station of GELINA. The thickness of the sample is such that it is essentially black for the neutron energies of interest. Neutrons emitted from the sample are detected by four NE-213 liquid scintillation detectors foreseen with pulse shape discrimination for neutron identification. The relative neutron flux is measured by two

---

* SCK-CEN, Mol, Belgium.

parallel plate proportional counters loaded with ^{6}Li and ^{235}U, which are positioned upstream from the liquid scintillator detector. The actual measurements on eta will use neutrons from the "cold" (liquid methane) moderator of GELINA when it will be available.
Up to now, a number of tests have been performed with the usual polyethylene moderator which were intended to investigate backgrounds and dead-time effects. It turned out that the rate of events accepted by the pulse shape discriminator circuits is sufficiently high to cause important dead-time effects in the liquid scintillator detectors for neutron energies above about 100 meV. The first measurement campaign with the "cold" moderator is foreseen for early 1985.

Neutron capture measurements on ^{241}Am

G. Vanpraet*, E. Cornelis*, G. Rohr, T. van der Veen

A series of neutron absorption measurements have been performed for the first time with a pure metallic ^{241}Am sample in the neutron energy range from thermal to 600 keV. The absorption cross section which is predominantly capture is technologically important for assessing the effect of this non fuel actinide on reactor core neutronics and also waste management due to its long term (~ 500 y.) decay activity.
An improved shielding facility housing the two C_6D_6 liquid scintillator capture detectors, was used to carry out the time-of-flight measurements at a distance of 8.577 m from the neutron source. The electronic signals are sorted out in 16 pulse height groups of 8k time-of-flight channels. This two-parameter information is required for the Maier-Leibnitz weighting method in which the detector response is proportional to the total energy released in the capture process.
The metallic sample was prepared for the joint ORNL-EURATOM experiment by the Isotope Research Materials Laboratory, ORNL, from a batch of highly pure americium oxide by vacuum reduction-distillation techniques. The thickness of the 2 cm x 2 cm disk was 1.063×10^{-3} atoms per barn. A 0.6 mm thick $^{10}B_4C$ disk was used as a capture sample to measure the shape of the neutron flux according to the reaction $^{10}B(n,a\gamma)^{7}Li$. The thickness corresponds to 4.6×10^{-3} atoms per barn.

---

* University of Antwerpen, RUCA, Belgium.

A critical background evaluation of the time dependent background was made by the black resonance technique using S, Na, Co, W and Ag filters as they deplete all primary neutrons at their characteristic resonance energies. This allows to evaluate the remaining background at these energies. For the flux measurements the same technique was applied. A Cd filter was kept permanently in the beam to prevent time-overlap from accelerator burst-to-burst neutrons.

The data taken at a repetition rate of 800 Hz have been analyzed between 600 eV and 200 keV and normalized to well resolved and saturated resonances in ^{241}Am at 0.576 and 1.270 eV respectively. Values of the differential cross section have been averaged over decade intervals and represented in Table 1.10. They have a statistical uncertainty of 0.5 %. An accuracy of 5 % is obtained by assuming a 15 % uncertainty on the background. For normalization and flux procedures an additional systematic error of 0.5 % is estimated.

Table 1.10. Neutron capture cross sections of ^{241}Am

ΔE_n(keV)	$< \sigma_A >$	ΔE_n(keV)	$< \sigma_A >$
0.6-0.7	17.064	9- 10	3.512
0.7-0.8	13.678	10- 15	3.299
0.8-0.9	13.618	15- 20	2.897
0.9-1.0	11.604	20- 30	2.453
1.0-1.5	11.963	30- 40	2.199
1.5-2.0	8.947	40- 50	1.934
2.0-3.0	7.690	50- 60	1.770
3.0-4.0	6.111	60- 70	1.635
4.0-5.0	5.007	70- 80	1.513
5.0-6.0	4.608	80- 90	1.457
6.0-7.0	4.280	90-100	1.387
7.0-8.0	3.992	100-150	1.159
8.0-9.0	3.670	150-200	1.054

The final results are compared in Fig. 1.7 with experimental results obtained by other investigators. Our data agree very well with those of ORNL and confirm the earlier observed discrepancy with those of Harwell and KfK, ranging from 10 to 20 % above 15 keV.

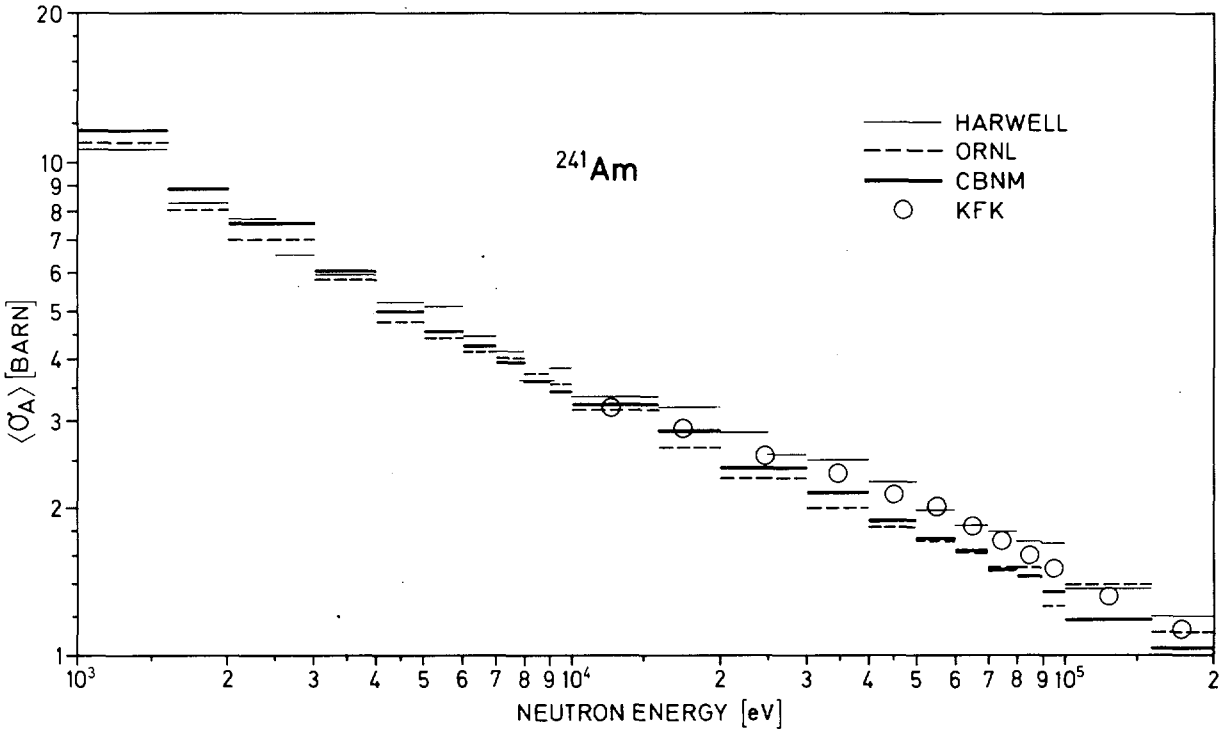

Fig. 1.7. Neutron absorption cross section of ^{241}Am compared with the data of ORNL, AERE Harwell and KfK in the energy range 1 keV to 200 keV

^{243}Am fission cross section measurements

H.-H. Knitter, C. Budtz-Jørgensen, R. Vogt, H. Bax

This cross section is needed and requested to estimate the production of higher actinides in fuel elements.
The data taking of this experiment at an eight meter flight path station of GELINA was ended in the very beginning of this reporting period. The data cover a neutron energy range from 0.8 eV to some 100 keV. The list data evaluation has started and a complete time-of-flight spectrum for ^{243}Am(n,f) is shown in Fig. 1.8.

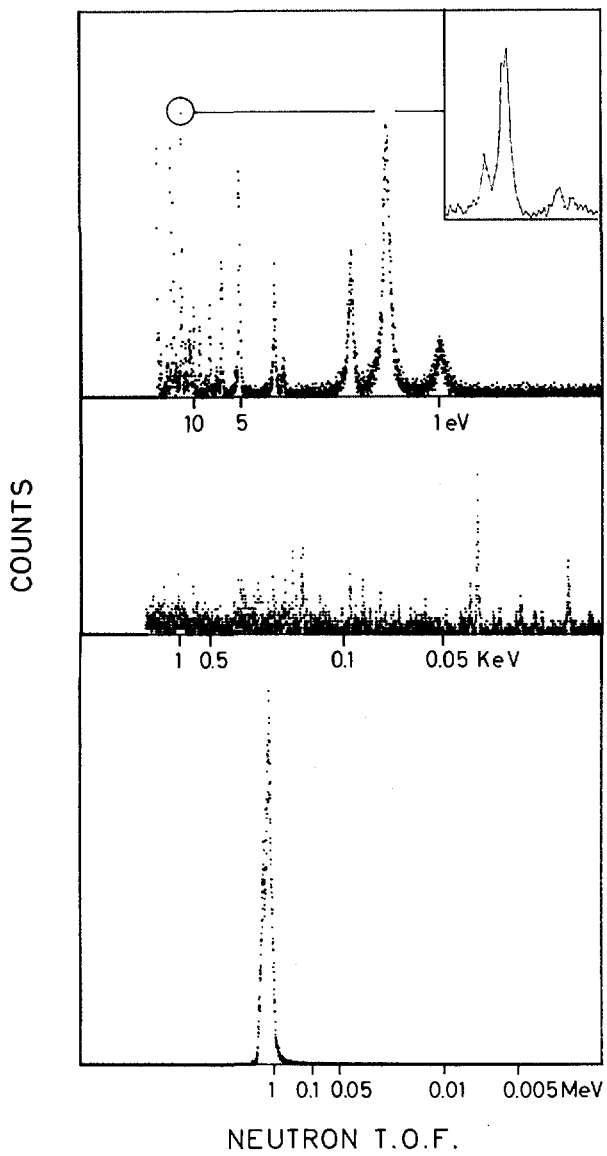

Fig. 1.8. Time-of-flight spectrum for $^{243}Am(n,f)$

For further evaluation of the data also the GELINA neutron spectrum shape at the position of the ^{243}Am-sample must be known. For this purpose the ^{243}Am ionization chamber was replaced by a ^{6}LiF ionization chamber with two back-to-back positioned ^{6}LiF-layers. The ^{6}LiF layers had a thickness of 75 $\mu g/cm^2$ and a diameter of 28 mm, the same as the diameter of the ^{243}Am-sample.

With this detector the GELINA neutron spectrum shape was measured. The evaluated neutron spectrum was fitted in the neutron energy range between 1.6 eV and 10 keV with the function

$$\Phi(E) \cong E^{\alpha+\beta\sqrt{E}}$$

where E was taken in MeV. The parameters were determined by the method of least squares to α = (-0.8721 $\pm$ 0.0013) and β = (-0.497 $\pm$ 0.033) $MeV^{-1/2}$. The errors are only of statistical nature as obtained from the least squares fit.

Fission fragment mass- and energy distribution for the spontaneous fission of ^{238}Pu

C. Wagemans*, P. Schillebeeckx*, A. Deruytter, R. Barthélémy

The analysis of the ^{238}Pu(s.f.) measurements has been completed. The fission fragment mass-distribution is given in Fig. 1.9, which clearly shows fine structures due a.o. to the neutron shells with 82 and 88 neutrons.

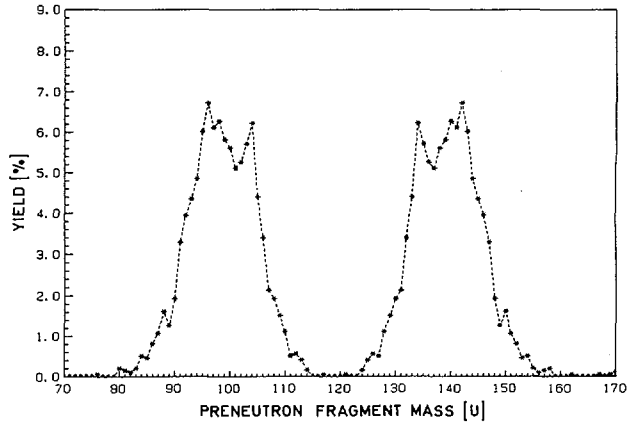

Fig. 1.9. Pre-neutron emission fission fragment mass-distribution for ^{238}Pu(s.f.)

* SCK/CEN Mol, Belgium.

In Fig. 1.10 the average (single) fission fragment kinetic energy is plotted as a function of the fragment mass. This curve shows the well-known constant behaviour of the light fragments' energy, the dip in the symmetric fission region and the energy decrease for the heavy fragments. These results have been presented at the Neutron Interlab Seminar at Braunschweig (June 1984). They will be further interpreted after comparison with other spontaneously fissioning Pu-isotopes.

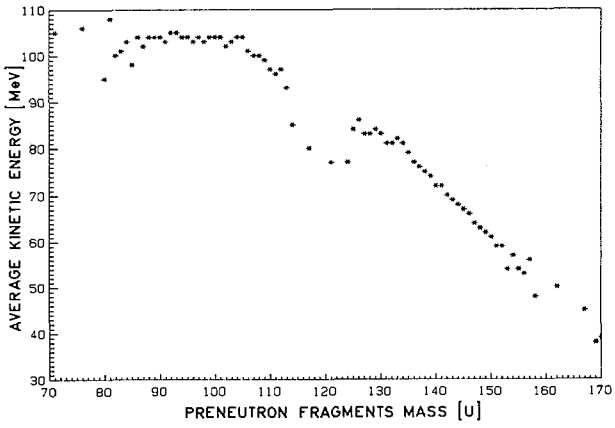

Fig. 1.10. Average fission fragment kinetic energy as a function of the fragment mass for the spontaneous fission of ^{238}Pu

Fission fragment mass- and energy distribution for the spontaneous fission of ^{242}Pu

P. Schillebeeckx★, C. Wagemans★, A. Deruytter, R. Barthélémy

The measurements are part of a systematic study of the fission characteristics of the plutonium isotopes.
Previously, the spontaneous fission of ^{238}Pu and ^{240}Pu has been studied relative to the thermal neutron induced fission of ^{239}Pu as calibration reaction. The same experimental set-up was used for the study of the ^{242}Pu(s.f.) characteristics. In the present experiments, a high quality combined ^{239}Pu-^{242}Pu target was used. A 1.5 $\mu g/cm^2$ ^{239}Pu and a 5.8 $\mu g/cm^2$ ^{242}Pu layer were each evaporated on a 16 $\mu g/cm^2$ polyimide backing and then put together.
The experiments are finished and the analysis is being done. The fission fragment mass-distribution is given in Fig. 1.11, which clearly shows fine structures due to neutron shells with 82 and 88 neutrons.

★ SCK/CEN Mol, Belgium.

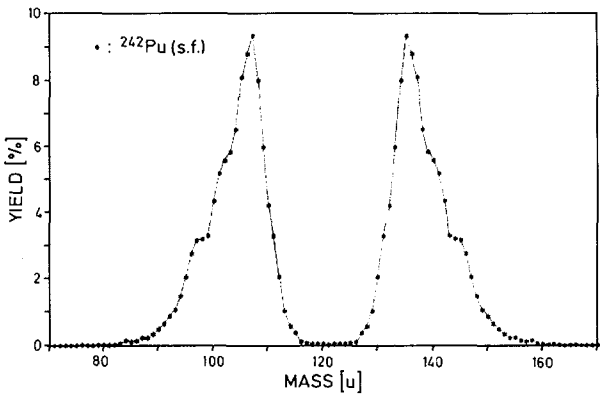

Fig. 1.11. Pre-neutron emission fission fragment mass-distribution for $^{242}Pu(s.f.)$

The average pre-neutron emission kinetic energy of the fragments $\bar{E}_K^{\star}$ is equal to 180.5 MeV, which is about 1 MeV lower than the corresponding value obtained after calibration relative to $^{241}Pu(n_{th},f)$.

Ion chamber test in unshielded direct linac beam

F.-J. Hambsch, C. Budtz-Jørgensen, H.-H. Knitter

For measurements of neutron induced reactions in the 1 to 2 MeV neutron energy range, the most intense neutron source available at CBNM is the bare uranium Linac target. For measurements of fission fragment parameters in this neutron energy range a gridded ion chamber was tested with respect to its response on the γ-flash from the linac target. The response to the γ-flash corresponded to a fission fragment energy of ~ 45 MeV. Since we want to perform fission fragment energy measurements at the time of appearance of the γ-flash, an electronic subtraction technique using a dummy and a $^{235}UF_4$ loaded ionization chamber was tried. A test measurement was run for a period of 4 weeks to determine the countrate in certain energy bins above 1 MeV and to measure the energy resolution of the compensated ionization chamber response as function of neutron fligth time (what is the energy jitter due to the compensated γ-flash). The data evaluation is going on and should answer the question whether the planned measurements can be made with sufficient accuracy.

1.2.2. Cross Sections of Structural Materials and Fission Products

A large fast power reactor contains about 25 (volume) per cent of stainless steel, half of which is iron, one quarter nickel and the rest mainly chromium. The neutron capture data of these primary structural materials influence the critical enrichment, the breeding gain and in particular the Doppler coefficient which is most important for safety considerations. The steel contributes to more than 60 % to the Doppler effect, whereby 70-80 % of this share is due to the 1.15 keV resonance in ^{56}Fe. These data demonstrate the importance of the neutron cross sections of these structural materials. They have been and are subject of extensive investigations at the Linac, for which separated isotopes for each of the three elements have been made available by the US Department of Energy.
Discrepancies in the resonance parameters of the 1.15 keV resonance of ^{56}Fe have caused the Nuclear Energy Agency Nuclear Data Committee to form an ad-hoc international task force to solve the problem in a concerted action.
^{149}Sm is an important fission product. Capture data for this isotope are required with priority for nuclear fuel burn-up calculations.

^{50}Cr neutron capture

F. Corvi, R. Buyl, A. Brusegan, G. Rohr, T. van der Veen

High resolution neutron capture measurements were carried out at the Geel linac on a 43 g sample of Cr_2O_3 enriched to 95.9 % of ^{50}Cr. The linac was operated with 4 ns burst widths and the flight path was 58 m long. The data were normalized to the capture area of the 1.63 keV resonance whose parameters were determined in a separate transmission experiment. A total of about 140 resonances in the range 1 to 300 keV were analysed with the shape code FANAC: neutron widths from high resolution transmission experiments of Poortmans et al. were introduced as fixed input in the code. For each resonance, a value of the capture area and of $g\Gamma_\gamma$ is given. The distribution of $g\Gamma_\gamma$ values is inspected in order to derive information on the resonance spin under the assumption of an approximate constancy of Γ_γ. The data are compared with the ORNL results which cover the region up to 200 keV.

Neutron resonance parameters for ^{50}Cr from high resolution transmission experiments

I. Van Marcke*, F. Poortmans**, L. Mewissen**

The two data sets from the 200 meter (moderated neutrons) and 400 meter (unmoderated neutrons) measurements have been analysed with the multi-level shape fitting code MULTI. The analysis is completed. Neutron widths are obtained for 300 resonances between 28 keV and 800 keV. For an important fraction of the resonances, the spin and parity was deduced from the peak total cross section, resonance-potential or resonance-resonance interference.

Resonance parameters of ^{52}Cr

G. Rohr, R. Shelley, A. Brusegan, F. Corvi, L. Mewissen**, F. Poortmans**, T. van der Veen

High resolution neutron transmission and capture measurements have been performed at the 150 MeV Geel linac with a pulse width of 4.5 ns and with a repetition rate of 800 Hz. Enriched ^{52}Cr-oxide samples have been employed at 200 m as well as at 400 m and 60 m covering energy ranges up to 1 MeV and 600 keV for transmission and capture respectively. The 400 m transmission measurement was performed with unmoderated neutrons. The capture cross section data were obtained with C_6D_6-detectors applying the weighting technique and for the transmission data NE-110 plastic scintillators have been used.
The relative flux has been measured with a boron-slab detector of 3 mm thickness using C_6D_6-detectors to view the 478 keV photons. The absolute calibration of the capture data has been done with the transmission value of the almost pure capture resonance at 1.63 keV in ^{52}Cr. The data sets have been analysed by means of MULTI, FANAC and TACASI computer programmes.
The resonance parameters of about 80 resonances have been determined in the energy range below 400 keV.

---

* Visiting Scientist.
** SCK-CEN Mol, Belgium.

Resonance parameters of ^{53}Cr

A. Brusegan, F. Corvi, L. Mewissen*, F. Poortmans*, G. Rohr, R. Shelley, T. van der Veen, C. Van der Vorst

One capture and three transmission measurements of ^{53}Cr were performed at CBNM at flight distances of 60, 50, 200 and 400 m resp. with GELINA operated at 4.5 ns burst width and 800 Hz repetition frequency. The 400 m transmission measurement was carried out in an unmoderated neutron beam.
In the capture measurement two C_6D_6 detectors viewed the Cr sample (96.4 % enriched in ^{53}Cr) and the capture events were weighted following the Maier-Leibnitz method.
The Cr sample was replaced by a 0.3 cm thick boron-slab during the flux measurement and the capture yields were normalized to the $g\Gamma_n \cdot \Gamma_\gamma/\Gamma$ value of the 1.63 keV resonance of ^{52}Cr, present as an impurity (3.44 %) in the sample.
The transmission measurements were carried out with two different detector systems:

1) a 0.5 cm thick boron-slab viewed by two 4x3" NaI(Tl) detectors, placed at 50 m distance from the neutron source.
2) a 2.5 cm thick NE-110 scintillator and 4 RCA-4516 PM's for the 200 and 400 m measurements.

Resonance parameters were deduced from the complete set of measurements by means of FANAC, TACASI and FANAL computer programmes up to 200 keV. For s-wave resonances it is intended to extend the analysis of the high resolution transmission spectra up to 350 keV.

Neutron resonance parameters for ^{54}Fe from high resolution transmission experiments

E. Cornelis**, L. Mewissen*, F. Poortmans*, I. Van Marcke***

Two data sets are available for analysis; a first one covering the energy range between 30 keV and 500 keV from transmission experiments on a 200 meter flight path with moderated neutrons and a second one covering the energy

---

* SCK/CEN Mol, Belgium.
** University of Antwerpen, RUCA, Belgium.
*** Research fellow.

range from 250 keV up to 19 MeV from a 400 meter flight path length experiment with unmoderated neutrons.
The first data set had been analysed previously only for the s-wave resonance structure using the multi-level R-matrix code FANAL. This analysis is repeated now using the code MULTI also for the resonances of higher angular momentum. The resonance parameters are available up to 400 keV and the analysis for the region 400 keV - 1 MeV is in progress.

Transmission measurements of the 1.15 keV resonance in ^{56}Fe

(NEANDC Task Force)

A. Brusegan, C. Van der Vorst

Two independent high resolution transmission measurements of the 1.15 keV resonance in ^{56}Fe have been completed at 99.4 m flight distance.
The two Fe samples, respectively 1 mm and 6 mm thick, were cooled down to the liquid nitrogen temperature to reduce the Doppler effect.
GELINA was running at 800 repetition rate and with a burst width of 1 ns.
The background in the 'vicinity' of the resonance was determined with the black resonance technique (Bi and Na filters permanently in the beam) and is of the order of 4 %.
The data analysis of the transmission will be carried out with the area code Atta-Harvey and with the shape code Siob.

Neutron capture in the 1.15 keV resonance of ^{56}Fe using Moxon-Rae detectors

(NEANDC Task Force)

F. Corvi, C. Bastian, H. Riemenschneider, T. van der Veen, K. Wisshak*

The capture measurements of the 1.15 keV resonance performed in Geel and Oak Ridge yield values of the kernel A_γ which are about 20 % larger than the values derived from transmission. Since the capture measurements were performed in both laboratories with the same type of detectors, i.e. liquid scintillators (either C_6D_6 or C_6F_6) and the weighting method, it is interesting to try other detectors: for this reason we have set up at GELINA a measurement which makes use of Moxon-Rae type detectors with converters of bismuth,

---

* Kernforschungszentrum Karlsruhe.

bismuth + graphite and graphite. These detectors have been currently employed at the KfK Van de Graaff mainly in the measurement of large s-wave resonances. The experiment was performed at a flight distance of 28.4 m. A top view of the experimental set up used is shown in Fig. 1.12.

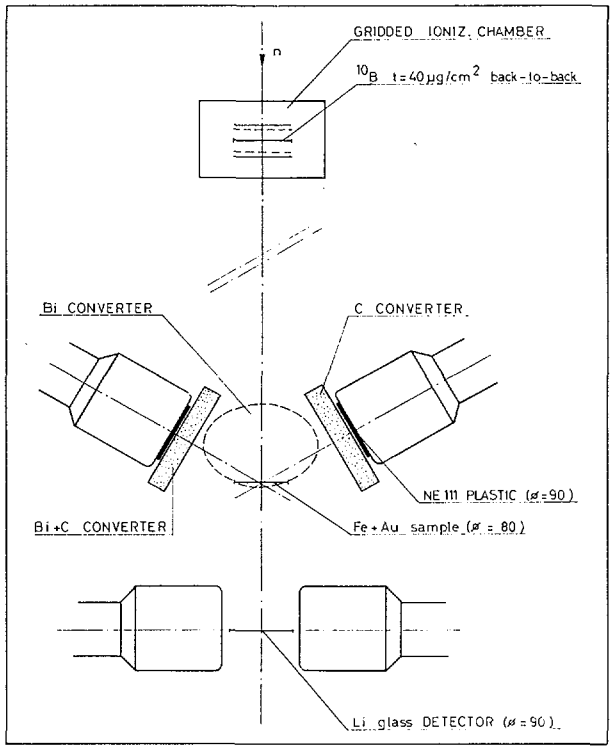

Fig. 1.12. Top view of the experimental set up

The three capture detectors are placed with their axis at 120° with respect to the neutron beam direction. The sample of 8 cm diameter consists of 0.5 mm thick metallic iron enriched to 99.87 % ^{56}Fe, "sandwiched" between two gold foils of thickness 20 and 30 micron respectively. The reason for using such a composite sample is to cancel the effect of detector instabilities, due mainly to variations of PM gain, and also to be independent of any normalization of the integrated neutron flux. The neutron flux shape was measured at the same time as capture by a double gridded ionization chamber placed in front of the capture sample and having at its centre a cathode with back-to-back deposits of ^{10}B of thickness 40 μg/cm^2.

Besides the measurement in the geometry of Fig. 1.12, a second run with higher statistics was performed, in which the detectors were placed with their axis at 90° with respect to the neutron beam axis. In this way their efficiency could be increased by almost a factor two. In between the two

runs the capture sample was removed and a 0.5 mm thick ^{6}Li-glass scintillator was introduced in the beam in order to have an independent measurement of the relative neutron flux. The analysis was carried out with the area programme TACASI and the data were normalized on the top of the 4.9 eV saturated gold resonance.

The results are summarized in Table 1.11. For each of the two runs, corresponding to the two detector configurations at 120° and 90°, and for each of the three detector types, values of Γ_n and of the kernel $g\Gamma_n\Gamma_\gamma/\Gamma$ are given. The errors are those directly obtained from TACASI: they are statistical only and correspond to 1σ. Besides that, a maximum systematic uncertainty of 3.8 % is estimated as a sum of several independent components.

Table 1.11. Summary of the results of the capture measurements relative to the 1152 eV resonance in ^{56}Fe

Run	Converter Material	Uncorrected Results		Correction Factor	Final Results
		Γ_n [(1)] (meV)	$A'_\gamma = g\Gamma_n\Gamma_\gamma/\Gamma$ (meV)	k_{eff}	$A_\gamma = k_{eff} \cdot A'_\gamma$ (meV)
I 120°	Bi	80.5 ± 2.2	70.6 ± 2.0	0.883	62.3 ± 1.8
I 120°	Bi + C	80.5 ± 2.2	70.6 ± 2.0	0.964	68.1 ± 1.9
I 120°	C	66.6 ± 1.6	59.7 ± 1.4	1.076	64.2 ± 1.5
II 90°	Bi	77.8 ± 1.5	68.5 ± 1.3	0.883	60.5 ± 1.2
II 90°	Bi + C	79.3 ± 1.5	69.7 ± 1.3	0.964	67.2 ± 1.3
II 90°	C	65.0 ± 1.1	58.4 ± 0.9	1.076	62.8 ± 1.0

(1) Uncorrected neutron widths obtained by fixing Γ_γ = 574 meV.

The kernel values A_γ are then multiplied by correction factors to obtain the final values A'_γ. These factors correct for deviations of the detection efficiency from a linear dependence with γ-ray energy: a discussion on how to calculate them can be found in [(1)].

---

(1) K. Wisshak, F. Käppeler, G. Reffo and F. Fabbri, Nucl. Sci. Eng. 86, 168 (1984).

From the data listed in Table 1.11 the following conclusions can be drawn:

- For each detector type, the results of the two runs with the 120° and 90° configurations agree well within the (statistical) errors. This indicates that there is no appreciable anisotropy of the gross capture γ-ray spectrum in the 1.15 keV resonance in agreement with the assignment p-1/2.
- The corrected kernel values averaged over the three detectors are A'_γ = 64.9 meV for the 120° configuration and A'_γ = 63.5 meV for the 90° configuration. If we take as a reference the value A_γ = 55.7 meV from the ORNL transmission data, we notice that the present results exhibit the same trend as with the total energy detectors, i.e. the kernels are larger than in transmission though here the effect is less pronounced: 13 to 14 % as compared to 17 to 23 % for C_6D_6 and C_6F_6.
- The uncorrected results for the graphite converter closely approach the transmission value. This fact is interesting because, if corrections are negligible, it is possible to use such a detector also in cases where the capture γ-ray spectra are unknown, e.g. in all ^{56}Fe resonances. However, to prove that such an agreement is not a mere coincidence due to the special shape of the 1.15 keV capture spectrum but is more general, one should extend the present exercise to other resonances (e.g. in ^{57}Fe, ^{52}Cr and ^{60}Ni) where capture and transmission can be directly compared.

High resolution neutron transmission measurements on the nickel isotopes ^{58,60,61}Ni

L. Mewissen★, F. Poortmans★

A first series of transmission experiments has been started on a 200 meter flightpath, covering the energy range from 30 keV up to 450 keV. A second series of measurements on a 400 meter flightpath and unmoderated neutron beam, covering the energy range from 250 keV up to 20 MeV is planned.

★ SCK/CEN Mol, Belgium.

$^{149}Sm(n,\gamma)$ average capture

F. Corvi, A. Brusegan, T. van der Veen

Sizeable discrepancies exist between recent differential experimental data, integral data and evaluations based on resolved resonance parameters for the important fission product nucleus ^{149}Sm. For this reason the average capture cross section of ^{149}Sm was measured at the Geel linac in the energy range from 1 keV to 1 MeV. Two different ways of data normalization were used, one based on comparison with a gold standard, the other based on the saturated resonance method applied to the 14.9 eV resonance. Relative neutron flux was measured with a Li-glass scintillator up to 100 keV and with a ^{235}U fission chamber above.

High resolution transmission measurements of thick iron filters

A. Brusegan, C. Van der Vorst

The transmission through a composite "filter", consisting of Fe, Al, S, Ti (respectively 35 cm, 23 cm, 7.5 cm and 0.5 cm thick), has been measured at GELINA.

The experiment has been performed on demand of Dr. H.G. Priesmeyer (IKK - Kiel University and GKSS Forschungszentrum, Germany), who also supplied the filter.

The linac was running at 800 Hz repetition rate and 1 ns burst width. The transmitted neutrons were detected at 98.2 m flight distance by a 0.5 cm thick ^{10}B slab + 4 [(4" x 3") NaI(Tl)] detectors shielded by a "castle" of lead and Li_2CO_3.

The neutron energy range under investigation extended from 1.6 keV up to 1.06 MeV.

In the first part of the experiment ("run 1") the transmission spectra through Fe, Al, S and through Fe, Al, S, Ti have been measured together with the flux and the background (black resonance method).

The second part of the experiment ("run 2") was devoted to an accurate study of the background and, in particular of its "slope".

In "run 2", the ^{10}B slab was replaced by a 0.62 cm thick carbon scatterer and measurements were performed for the same 4 cases of "run 1".

The gain of the PMs has been stabilized during the whole experiment:

γ-rays from a ^{133}Ba source ($E_\gamma < 382$ keV) were detected simultaneously with the 478 keV γ-rays present in the reaction $^{10}B(n,a\gamma)^{7}Li$. A special device stabilized the H.T. of the PMs, by monitoring the amplitude of the signals from the ^{133}Ba γ-rays.

In Fig. 1.13, the "24.3 keV Fe window" is shown for the two cases: a) no Ti in the beam; b) Ti in the beam. The plotted spectra have no background subtraction and are normalized simply to equal "monitor counts".

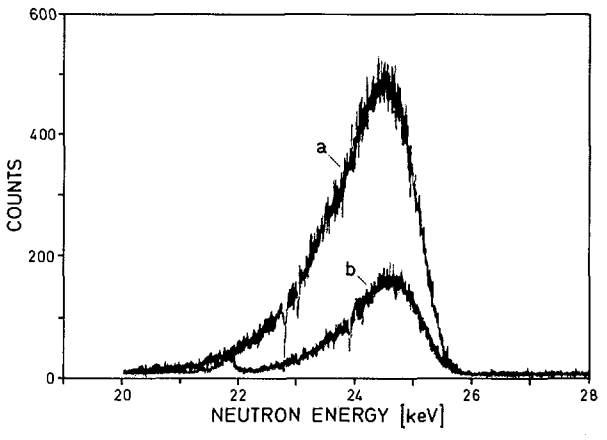

Fig. 1.13. "The 24.3 keV Fe window":
a) Al+Fe+S composite filter;
b) Al+Fe+S+Ti composite filter

In Fig. 1.14, the "windows" in the energy range from 225 keV to 375 keV are plotted. Above 30 keV, spectra measured with the Ti sample in the beam show "little differences" with those spectra obtained with no Ti in the beam.

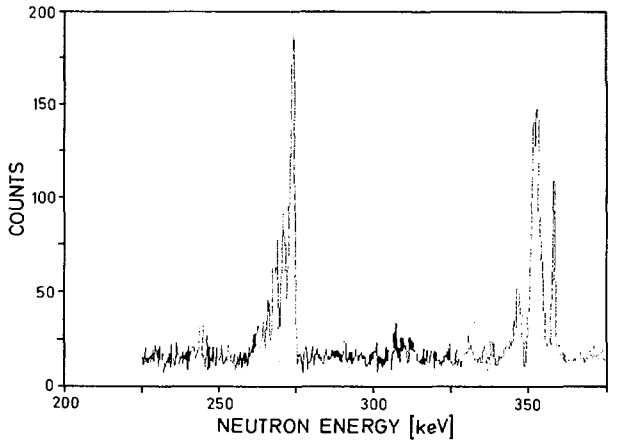

Fig. 1.14. Neutron spectrum transmitted through the composite filter "Al+Fe+S+Ti" vs neutron energy

High resolution total cross section measurements on ^{207}Pb

R. Köhler, L. Mewissen*, F. Poortmans*, J. Theobald**, H. Weigmann

The measurements on ^{207}Pb are part of a thesis work of a research fellow. They take profit of the ultra-high resolution power of the linear accelerator neutron time-of-flight spectrometer, and contribute to a better understanding of the basic neutron interactions.

A transmission measurement was performed at a 400 m flightpath using a 1 ns time-coder. The linac burst width was controlled with a monitor detector with 200 ps time-resolution which records the width of the gamma-flash from the linac target. The burst width was less than 1 ns during the complete run. Figure 1.15 compares the resolution available with these parameters to the expected average spacing of resonances in $^{207}Pb+n$ with J = 0-3.

The measurement covered the neutron energy range from 200 keV to 20 MeV. Resonance structure is observed up to about 2.5 MeV neutron energy, with most of the individual resonances being resolved up to 1.5 MeV.

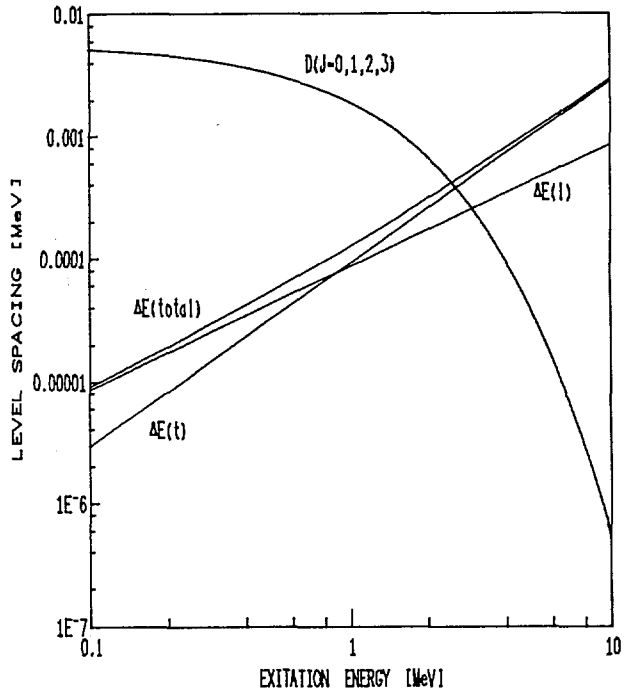

Fig. 1.15. Level spacing ^{208}Pb compared to experimental resolution

---

* SCK/CEN Mol, Belgium.

** Technisch Hochschule Darmstadt.

Figure 1.16 shows as an example the measured cross section around 1.9 MeV neutron energy: The energy resolution of the time-of-flight measurement is seen from the indicated width of the peak at 1.944 MeV.
The data are being analysed with the multi-level R-matrix routine MULTI (1). The routine has been modified to allow different channel radii for each spin-parity component.

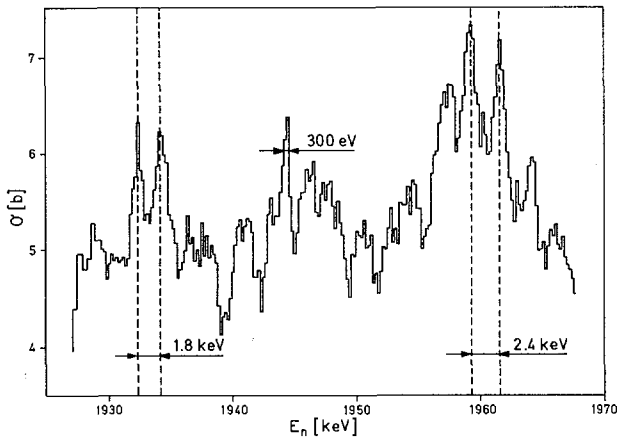

Fig. 1.16. Total cross section of ^{207}Pb between 1.93 and 1.97 MeV

The analysis will be possible in an essentially complete way up to about 800 keV neutron energy. It will primarily yield the neutron widths of resonances, and for most of the resonances with a neutron width larger than the experimental resolution, it will give the spin of the resonance. For many spin 1 resonances the parity cannot be determined unambiguously, mainly because a superposition of s- and d-wave contributions may produce a resonance shape very similar to a p-wave resonance.

Neutron capture gamma-rays from ^{28}Si

P.W. Martin★, J.A. Wartena, H. Weigmann

This work is intended to contribute to a better understanding of the neutron resonance capture. It uses the high resolution capability of GELINA.

---

(1) G.F. Auchampaugh, LANL report LA-5473-MS (1974).

★ University of British Columbia, Vancouver, Canada.

The resonances of ^{28}Si have previously been studied by high resolution transmission measurements (see PPR January-June, 1983). In order to further investigate the structure of the observed resonances, a measurement of the high energy capture gamma-rays is being performed. Of interest are E1 transitions to the ground state of ^{29}Si in connection with theoretical work [1] in a single particle model, as well as M1 transitions which are expected to be comparatively strong in Si due to the possible $d^{-5/2}$ to $d^{-3/2}$ spin flip transitions across the P = 14 and N = 14 subshells.
The experimental set-up is the same as in the measurements on ^{207}Pb capture gamma-rays, again utilizing the 130 m flight path station of GELINA. Two runs on Si samples of different thickness have been performed, and data reduction is presently in progress.

The $^{33}S(n,\alpha)^{30}Si$ and $^{41}Ca(n,\alpha)^{38}Ar$ reactions in the resonance region

C. Wagemans★, H. Weigmann

The $^{33}S(n,\alpha)^{30}Si$ and $^{41}Ca(n,\alpha)^{38}Ar$ reactions are of importance for astro-physical calculations.
The study of the $^{33}S(n,\alpha)$ reaction has been finalized, and the results are being combined with total cross section measurements performed at ORNL in order to yield a complete set of resonance parameters.
The study of the $^{41}Ca(n,\alpha)$ reaction has been continued and extended up to 1 MeV neutron energy. About 40 resonances have been observed so far. These measurements will be continued.

---

(1) M. Micklinghoff and B. Castel, Proc. Int. Conf. on Neutron Capture Gamma-Ray Spectroscopy, BNL 1978; Plenum Press, NY 1979.

★ SCK-CEN Mol, Belgium.

New perspectives on the level density of compound resonances

G. Rohr

A paper with this title has been published [1]. The abstract reads as follows:

"The level density of compound resonances observed at neutron separation energy is subject of closer investigation and interpretation. The structures in the level density parameter as a function of the mass number allow the determination of the hierarchy of the compound states and the definition of a base line which represents the level density parameter of spherical nuclei with no residual interaction and no shell effects. Using the base line a method becomes available enabling the separation of the residual interaction from properties of the average potential defined in the framework of the shell model. The following examples in different mass regions are discussed: the change of the pairing energy due to the blocking effect at $A \approx 70$; the breakdown of the pairing correlation at $A \approx 105$ is interpreted as neutron-proton interaction; similar effects in the mass region $150 < A < 170$ are discussed with neutron-proton interaction and the backbending phenomen. Finally it will be shown that there is no enhancement of states due to collective properties of nuclei at high excitation energy."

---

(1) G. Rohr, New Perspectives on the Level Density of Compound Resonances, Zeitschrift für Physik A, Atoms and Nuclei X 318, 299 (1984).

1.3. NUCLEAR DATA FOR FUSION TECHNOLOGY

Determination of double-differential neutron emission cross section for ^{7}Li

E. Dekempeneer*, H. Liskien, L. Mewissen*, F. Poortmans*

This cross section will be determined in view of its importance for the neutron spectrum in blankets of fusion reactors.
Measurements of the response functions for the NE-213 scintillators were performed on a 100 meter flight path but suffered from pile-up effects in the energy range between 1 MeV and 3 MeV. For this reason a second series of measurements were done, using the 400 meter flight path. A first run of double-differential neutron emission experiments on ^{7}Li has been completed. The experiments were done with a thin metallic sample (0.0325 at/b) for emission angles ϑ = 24, 60, 90, 120, 150, 160 degree and for incident neutron energies between 1.6 and 16 MeV. The data are normalized to the shape of the incident neutron flux as determined with a ^{235}U fission chamber. The absolute values of the cross sections will be based on the differential elastic cross section of ^{12}C below 2 MeV.
The analysis of the data has been started.

Neutron angular distribution for $^{7}Li(n,n')^{7}Li^{*}$ (478) from Doppler-broadened γ-lines

H. Liskien

Blankets of future fusion reactors have to contain lithium as tritium breeding material and natural lithium contains 92.5 atom % ^{7}Li. Therefore neutron transport calculations need double-differential ^{7}Li cross sections as input data. However, scattering experiments at higher neutron energy cannot separate by time-of-flight the transition to the first excited state (478 keV, 73 fs, $1/2^{-}$) from the ground state transition. Our knowledge on the angle-integrated inelastic (Q = -478 keV) cross section stems from experiments observing the C.M.-isotropic 478 keV γ-line. It is demonstrated that the missing neutron angular distributions can be deduced from the Doppler broadened shape of this γ-line.

---

* SCK-CEN Mol, Belgium.

A test measurement was conducted at a neutron energy of about 8 MeV using a metallic lithium sample (3.7 cm Ø x 3.0 cm) enriched to 99.98 % in ^{7}Li. The 70 cm^{3} pure germanium detector used for the detection of the 478 keV γ-rays was mounted in a collimator made out of paraffine, lithium carbonate and lead to shield it against primary neutrons and γ-radiation not originating from the sample. The neutron source was pulsed ($\approx$ 2 ns) and conventional electronics applied for n/γ event discrimination by time-of-flight. In contrast to earlier experiments the observation angle was not kept constant, but varied (between $\approx$ 45° to $\approx$ 135°). As may be seen from Fig. 1.17 the observed γ-line changes its position and shape depending on the observation angle α. Its width is about ten times the resolution of the Ge-detector, which was determined to be 1.7 keV FWHM under realistic background conditions with a ^{7}Be-source.

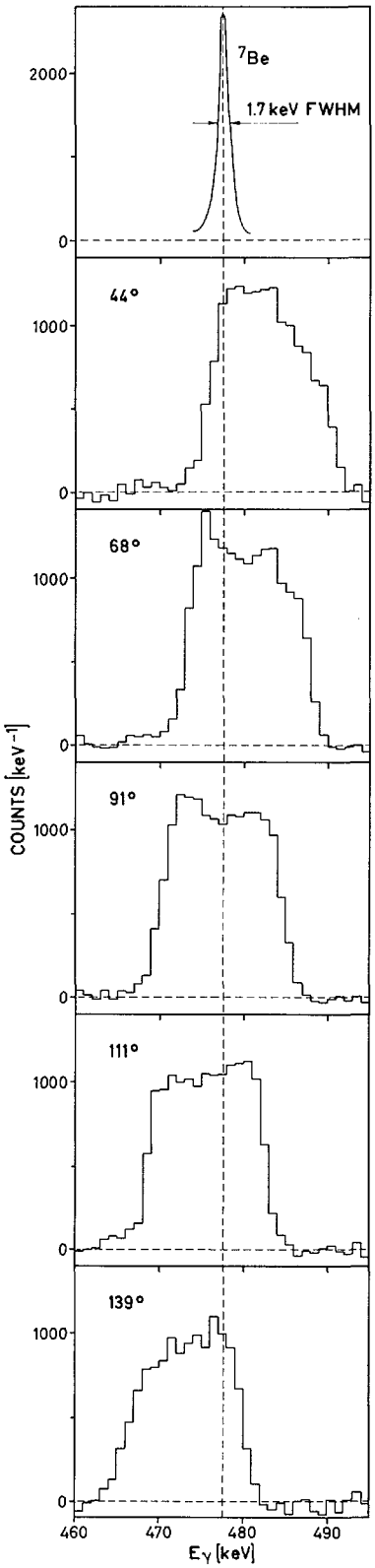

Fig. 1.17. The changing position and shape of the Doppler-broadened 477.6 keV γ-line from $^{7}Li^{\star}$ compared to the calibration line from ^{7}Be-decay

The analysis of these spectra is based on the following relation for the Doppler-shift energy ΔE_γ:

$$\Delta E_\gamma = \frac{E_\gamma}{c} v_{LAB} (\cos \vartheta_{LAB} \cos a + \sin \vartheta_{LAB} \sin \varphi \sin a)$$

where both v_{LAB} and ϑ_{LAB} are determined by ϑ_{CM}, and averaging over the azimuthal angle φ has to be performed. A Monte Carlo programme to simulate such Doppler-broadened γ-lines has been written which takes into account

(1) energy- and angle-distribution of the primary neutrons,
(2) elastic neutron scattering in the sample,
(3) the combined effect of stopping power and half life,
(4) γ-detector resolution.

As may be seen from Fig. 1.18 all these corrections lead only to minor changes in the line shape. Point (2) is responsible for the low energy tail, point (3) leads to a shift towards the original γ-energy, while points (1) and (4) smear out the spectrum. Analysis to use the Monte-Carlo results in a least-squares fit procedure is underway.

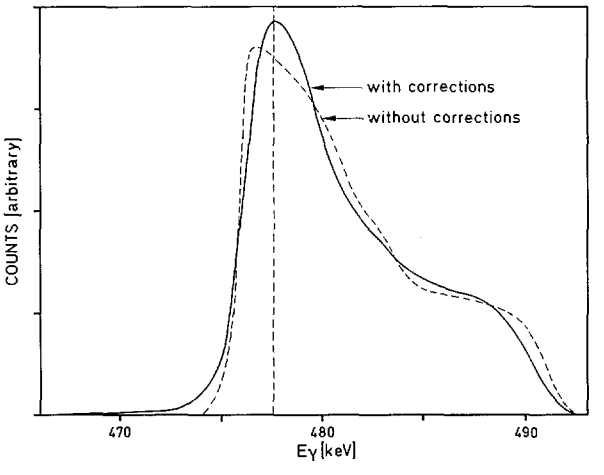

Fig. 1.18. The effect of energy distribution of the primary neutrons, the sample size, stopping power and half life, and detector resolution on a certain Doppler-broadened γ-line

Be(n,t) cross sections

H. Liskien, S. Qaim★, R. Widera, R. Wölfle★

In view of the importance of beryllium as a potential neutron multiplier material in fusion reactors it is intended to extend the Be(n,t)/Al(n,α) ratio measurements.
Results in the compact source-sample geometry have confirmed the relatively large (~ 20 mb) Be(n,t) cross section. The project is delayed due to an error of the sample supplying firm: instead of the ordered metallic samples we received beryllium oxide ceramic samples.

(n,t)-cross sections of Be, V and In

S. Qaim★, R. Wölfle★, H. Liskien, R. Widera

In continuation of earlier work on systematics of tritium production cross sections [1] we have irradiated beryllium, vanadium, indium and tantalum samples by neutrons of 16 to 20 MeV produced by the $T(d,n)^4He$ reaction. The expected low cross sections necessitated a very compact source-sample assembly so that all the neutrons emitted in the forward hemisphere are used. Nevertheless, irradiations of more than two days per element were necessary. In the case of Be the neutron fluence determination relies on the $^{27}Al(n,\alpha)^{24}Na$ cross section: Aluminium foils were inserted at regular distances between the beryllium pieces forming the sample. The neutron fluences for the vanadium, indium and tantalum irradiations stem from the internal standards $^{51}V(n,\alpha)^{48}Sc$, $^{115}In(n,2n)^{114}In^m$, and $^{181}Ta(n,2n)^{180}Ta^m$. Activity counting of the end products was performed in a calibrated Ge(Li)-detector.
As in the earlier work the (n,t) reaction rate was determined by vacuum extraction of the accumulated tritium and its activity determination by low-level autocoincidence β-counting in a gas proportional counter filled with methane. Data analysis is ongoing.

★ KFA Jülich.

(1) S. Qaim, R. Wölfle and H. Liskien, PR C25 (1982) 203.

Cu(n,α) and Ni(n,α) cross sections in the 5 to 10 MeV neutron energy range

E. Wattecamps, F. Arnotte, H. Liskien

Copper is foreseen as structural material for future fusion reactors (magnets, limiters, etc.). Its behaviour will be strongly influenced by neutron-induced helium production. However, our knowledge on the Cu(n,α) cross section is poor (Fig. 1.19.a). Best estimates have been obtained by using the $^{63}Cu(n,\alpha)$ activation data of Winkler [1] and theoretical results for $^{65}Cu(n,\alpha)$ from Hetrick [2], which, however, contribute only to a small fraction.

To check these best estimates, measurements were performed at the CBNM Van de Graaff using the multi-angle telescope counter developed earlier.

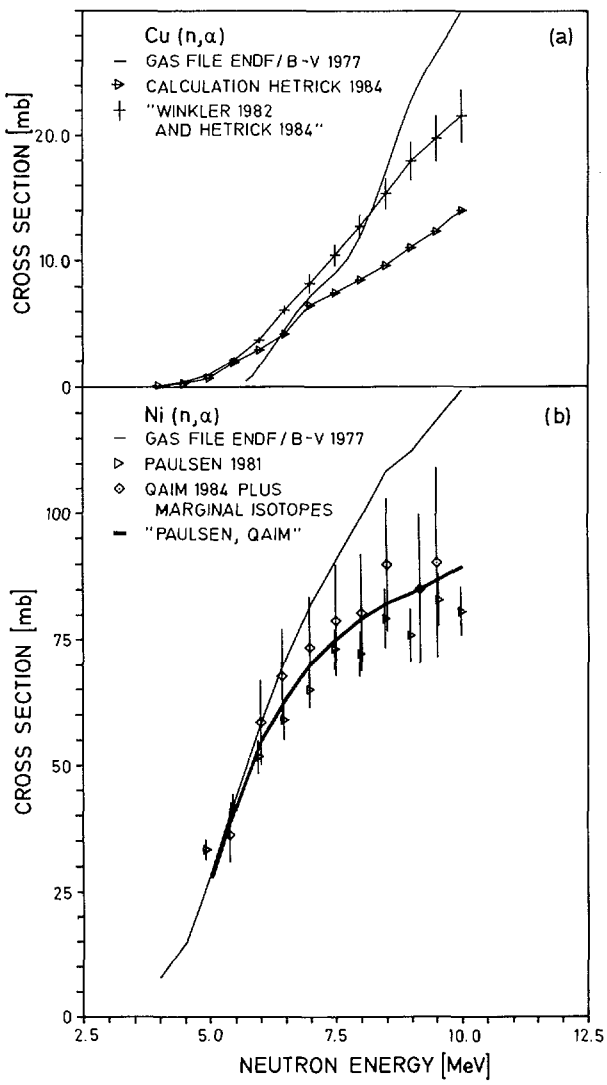

Fig. 1.19. Present knowledge (a) on the Cu(n,α) cross section and (b) on the Ni(n,α) cross section

(1) G. Winkler, Proc. Europhysics Topical Conf. p. 417, Smolenice, 1982.

(2) D.M. Hetrick et al., ORNL-TM-9083, Aug. 1984.

The α-particle yield from a 2.8 mg/cm^2 thick copper layer was determined for five average emission angles (14°, 52°, 80°, 110°, and 141°) in the neutron energy range of 5 to 10 MeV in steps of 0.5 MeV.

The Cu(n,α) cross sections are small, typically 2 to 20 mb, and therefore development work was needed to obtain reasonable counting rates and acceptable signal-to-background conditions.

The necessary small source-sample distance excluded measurements relative to the n-p scattering cross section. Instead measurements were performed relative to the Ni(n,α) cross sections which have recently been determined by two independent measurements (Fig. 1.19.b): the data of Paulsen et al. (1) were obtained with our multi-angle telescope relative to H(n,n) while the data labelled Qaim were derived from his recent activation results for ^{58}Ni, ^{62}Ni, ^{64}Ni (2) and theoretical results for ^{60}Ni and ^{61}Ni, which contribute only marginally. Both sets agree reasonably. The quality of the Cu(n,α) measurement is illustrated in Fig. 1.20 by the various α-particle spectra, Cu-foreground minus Ta-background, observed under 80°. The Coulomb barrier hinders the emission of low-energy α-particles and from measurements with Ni it is known that emitted α-particles have at least 4 MeV energy. The spectra were therefore evaluated down to 3.2 or 3.9 MeV. In the neigbourhood of this bias and below, the background increases rapidly.

Nevertheless, for neutron energies above 7 MeV the statistical uncertainty on the integrated spectra is small and the arbitrariness of the choice of the lower bias is negligible. For neutron energies below 7 MeV the statistical accuracy of the alpha-spectra below 5 MeV is poor. They are slightly but systematically positive, though statistically some negative values are expected.

Cu/Ni(n,α) cross section ratios as obtained after integration over the α-particle energy and over the emission angle are given in Fig. 1.21 together with a best estimate curve as defined above.

Uncertainties of the experimental results vary between $\pm$ 4 and $\pm$ 17 % for neutron energies between 10 and 5 MeV, respectively, while the best estimate curve should be accurate within $\pm$ 16 %. Independently from the neutron energy all measured cross section ratios are higher than the best estimate curve and this difference is not yet understood. It corresponds to 1 mb at 5 MeV and 4 mb at 10 MeV.

---

(1) A. Paulsen et al., Nucl. Sci. Eng. 78, 377-385 (1981).

(2) S.M. Qaim et al., Nucl. Sci. Eng. 88, 143-153 (1984).

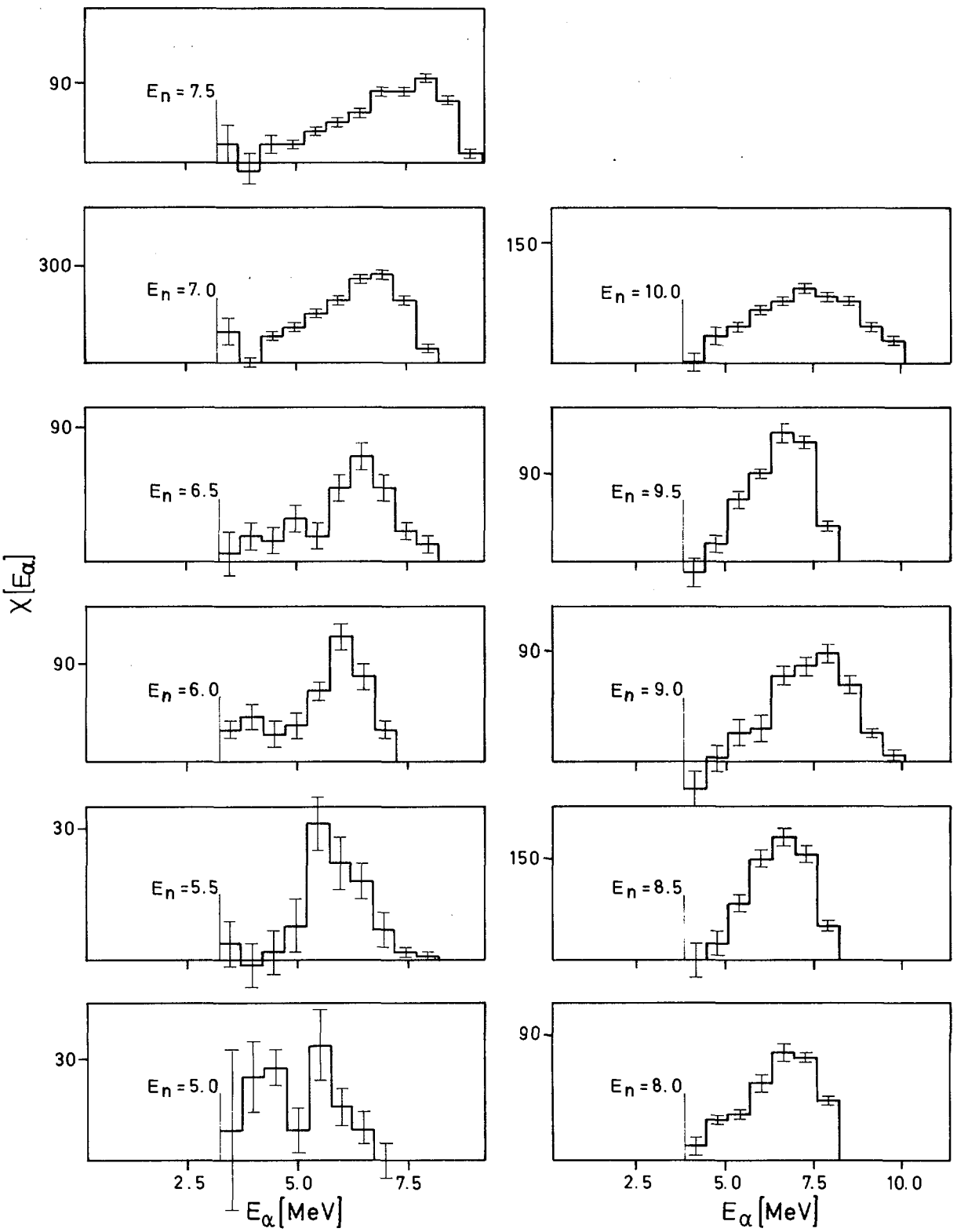

Fig. 1.20. Alpha-particle spectra, Cu-foreground minus Ta-background, for various neutron energies

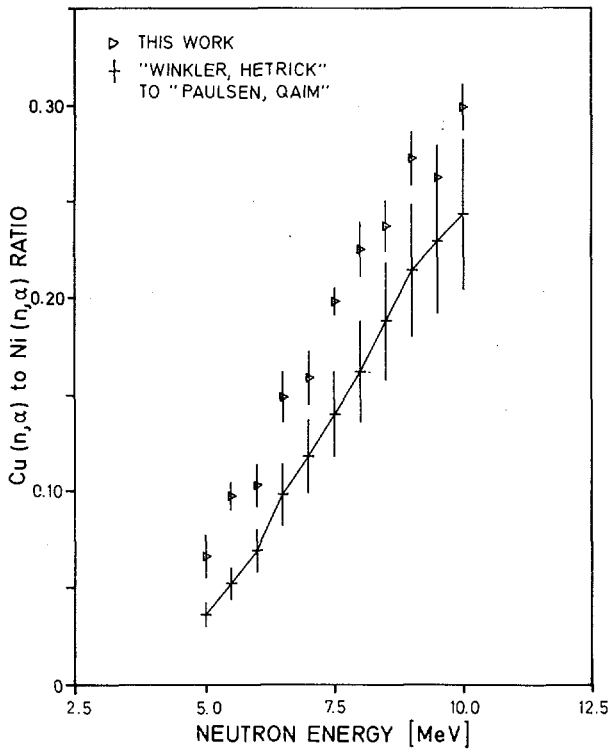

Fig. 1.21. Comparison of measured Cu(n,a) to Ni(n,a)-cross-section ratio with recommended ratio from literature

2. NUCLEAR METROLOGY

2.1. RADIONUCLIDE METROLOGY

The work in radionuclide metrology proceeds along three lines:

- preparation of special standards,
- participation in international comparisons as quality control,
- improvement of measurement techniques to increase the accuracy.

The standardization of Niobium-93m for use as a Reference Material for reactor neutron dosimetry

B.M. Coursey★, R. Vaninbroukx, D. Reher, W. Zehner

The reaction $^{93}Nb(n,n')^{93}Nb^{m}$ is very useful for the determination of fast neutron fluences especially for radiation damage studies of reactor pressure vessels. The $^{93}Nb^{m}$ is assayed almost exclusively by counting the 17-keV KX-rays with Si(Li) or pure Ge semiconductor detectors.

The present work was initiated to develop a benchmark reference material for the European reactor community to provide a consistent basis for the measurement of neutron fluence with niobium dosimeters.

Niobium-93m has been standardized by liquid-scintillation counting with an uncertainty in the radioactivity concentration (N_0) of 0.8 %. Particular attention was paid to systematic uncertainties due to the chemical characteristics of the solution and to the non-detection probability of the liquid-scintillation detector for the low-energy conversion electrons.

Solutions 1 M in HF and 1 M in HNO_3 in teflon vials were found to be stable. Two different types of liquid scintillators were used. The highest efficiencies were obtained with Scinti Verse II and Aqualuma Plus scintillators deaerated with argon gas. In the best cases less than 1.5 % of the events produced two-photoelectron pulses. Extrapolations were developed to find the non-detection probability and the number of one-photoelectron events. Figure 2.1 shows the liquid-scintillation spectra observed for three samples.

★ Visiting Scientist from NBS, Washington, USA.

Figure 2.1.a is for an unquenched sample and demonstrates a near-Gaussian full-energy peak for the 31-keV transition. Figure 2.1.c is for a quenched sample and shows the Poission distribution characteristic of the RCA 8850 phototube. Figure 2.1.b shows the intermediate case.

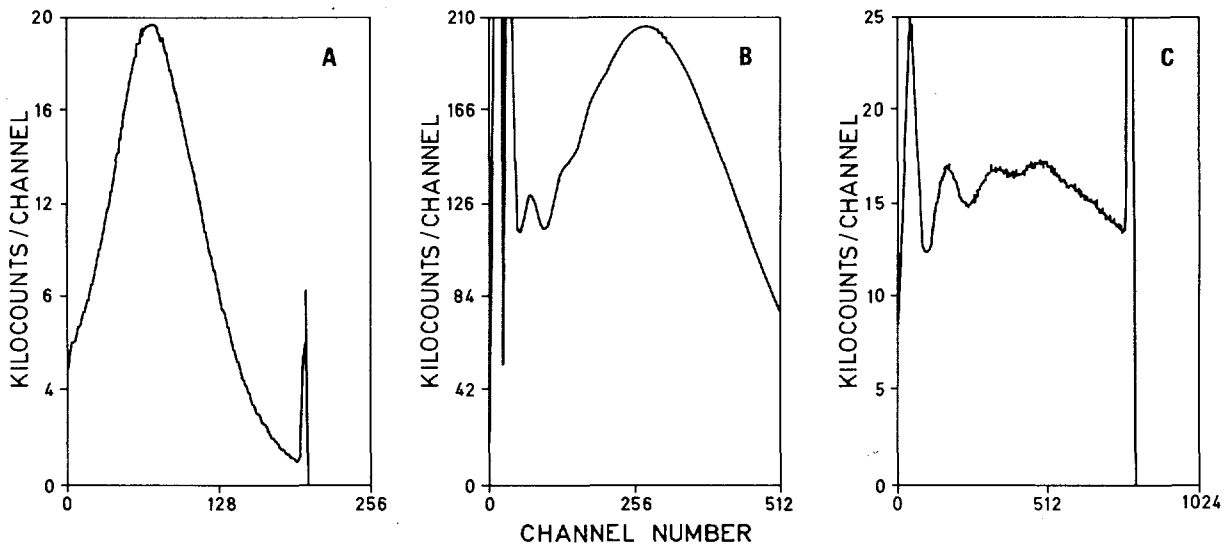

Fig. 2.1. Liquid scintillation spectra of niobium-93m.

Fig. 2.1.a: Unquenced sample in Aqualuma Plus scintillator.

Fig. 2.1.b: Moderately quenched sample in ScintiVerse II scintillator.

Fig. 2.1.c: Severely quenched sample in Lumagel scintillator.

Solution samples of the calibrated material in teflon vials were sent to twelve laboratories (Table 2.1). The six laboratories marked with ★ agreed to measure the X-ray emission rate for the 17-keV KX rays (N_{KX}). The probability for emission of KX rays, P_{KX}, defined as the ratio N_{KX}/N_0, is needed for routine measurements with niobium neutron dosimeters in order to convert KX-ray emission-rate data to neutron fluence. In previous measurements at CBNM and PTB, there was a 7 % discrepancy in this parameter [1,2].

---

(1) R. Vaninbroukx, Int. J. Appl. Radiat. Isot., 34, 1211 (1983).

(2) W.G. Alberts, R. Hollnagel, K. Knauf, M. Matzke and W. Pressara, in Proc. Fourth ASTM-EURATOM Symposium on Reactor Dosimetry, Gaithersburg 1982, Kam, F.B.K. (ed.), NUREG/CP-0029, Vol. I, p. 433.

Table 2.1. Distribution list for niobium-93m radioactivity Reference Material for neutron dosimetry solution 8403

★	Idaho National Engineering Laboratory	(USA)
★	Central Bureau for Nuclear Measurements - Geel	(B)
	Energieonderzoek Centrum - Petten	(NL)
	Kraftwerk Union - Erlangen	(D)
★	Laboratoire de Metrologie des Rayonnements Ionisants - Saclay	(F)
	GKSS Forschungszentrum - Geesthacht	(D)
★	Physikalisch-Technische Bundesanstalt - Braunschweig	(D)
	Atomic Energy Establishment - Winfrith	(UK)
	Studiecentrum voor Kernenergie - Mol	(B)
	Atomic Energy Research Establishment - Harwell	(UK)
★	National Physical Laboratory - Teddington	(UK)
★	National Bureau of Standards - Washington	(USA)

★ KX-ray emission rate measurements.

Preliminary values for P_{KX} measured by CBNM, NBS [1] and PTB [2] are given in Table 2.2. All the CBNM and PTB measurements were done with calibrated semi-conductor detectors and thus depend on systematic uncertainties in the calibrants. The NBS measurements with a defined-solid angle detector do not rely on standards of other radionuclides. Measurements at INEL, LMRI and NPL are in progress. An internal report on these measurements has been prepared [3].

---

(1) J.M.R. Hutchinson and P.A. Mullen, private communication, 1984.

(2) K. Debertin, private communication, 1984.

(3) B.M. Coursey, R. Vaninbroukx, D. Reher and W. Zehner, The Standardization of Niobium-93m for Use as Reference Material for Reactor Dosimetry, CBNM Internal Report GE/R/RN/11/84.

Table 2.2. Probability for KX-ray emission, P_{KX}, for $^{93}Nb^m$ using N_o determined in this work

Laboratory	Detector	P_{KX} a)
CBNM	high purity Ge (ENERTEC)	0.1123 ± 0.0018
	high purity Ge (DSG)	0.1140 ± 0.0019
	Si(Li)-I	0.1129 ± 0.0019
	Si(Li)-II	0.1125 ± 0.0021
NBS	defined solid angle detector	0.1099 ± 0.0018
PTB	high purity Ge	0.1117 ± 0.0020
	Si(Li)	0.1097 ± 0.0020
overall mean of seven measurements		0.1119 ± 0.0018

a) In all instances, the uncertainty is intended to approximate one standard deviation and include the uncertainty in N_o (0.8 %) combined in quadrature with the uncertainty in the N_{KX} measurements.

Low-energy X-ray standards

W. Bambynek, G. Grosse

Quantitative X-ray measurements with Si(Li) detectors below 5 keV are hampered by lack of suitable efficiency calibration sources. Well standardized radioactive sources are available in the energy range down to 4.5 keV. CBNM has developed techniques to produce and standardize calibration sources below 4.5 keV [1].
The principle of these sources is the excitation of fluorescence KX rays from low-Z elemental or chemical compound foil by Mn-KX rays emitted in the ^{55}Fe decay.

(1) A. Kacperek, B. Denecke, D. Reher and W. Bambynek, Nucl. Instr. and Meth. 192, 109 (1982).

The method to characterize sources emitting Al-KX rays of 1.49 keV is investigated in order to improve the accuracy. In particular the reproducibility of the peak-evaluation technique has been tested. Three ^{55}Fe sources, produced by different methods and each covered with an 0.01 mm thick Al foil, were measured in a solid angle of 1.37 % of 4π sr. In total 33 measurements were performed. The reproducibility of the 5.97 keV Mn-KX-ray peak was found to be on the average 0.3 % and that of the 1.49 keV Al-KX-ray peak 0.8 %. However, these figures vary due to changes of the counting-gas density in the flow counter.
To reduce these variations a static pressure regulator has been installed which nominally controls the gas pressure within 50 Pa (about 5 mm H_2O). Measurements are in progress to test the effect of the pressure control on the counting rate of the 1.49 keV peak. In addition, the various corrections to allow for the systematic deviations are investigated.

International comparison of activity measurements of a ^{123}I solution

D. Reher, R. Vaninbroukx

The results of the international comparison of activity concentration measurements of a ^{123}I solution, carried out in 1983, have been evaluated and a joint paper on this subject has been published (1). The nuclide ^{123}I is of importance in nuclear medicine.
The results of the participating laboratories are given in Table 2.3 and Table 2.4, the latter providing data on the ^{125}I impurity measurements. The standard deviation of the weighted mean of the ^{123}I activity measurement is less than 0.3 %, which is a very satisfying result.

(1) D. Reher, R. Vaninbroukx, B. Chauvenet, J. Morel, R. Vatin, M. Woods, S. Lucas, C. Ballaux and R. Jacquemin, Standardization of ^{123}I, Int. J. Appl. Radiat. Isot., 35, 923 (1984).

Table 2.3. Reported ^{123}I activity concentration values at the reference time

Laboratory	Standardization method	Activity concentration (Bq/mg)	Uncertainty * (Bq/mg)
CBNM	4π(PC)A,X-γ coincidence	501.0	± 2.7
	gamma-ray spectrometry	500.4	± 3.8
LMRI	gamma-ray spectrometry	500.0	± 5.7
	ionization chamber	500.4	± 1.4
NPL	ionization chamber	502.3	± 1.2
SCK-CEN	4π gamma-ray counting	495.2	± 1.4
IRE	gamma-ray spectrometry	512.6	± 11.8

* Corresponding to one standard deviation of the mean taking into account class A (random) and class B (systematic) uncertainties (1).

Table 2.4. Impurity measurements at reference time *

Laboratory	Detector	^{125}I Activity concentration (Bq/mg)	Uncertainty ** (Bq/mg)
CBNM	High Purity Ge and Si(Li)	6.4	± 0.4
LMRI	High Purity Ge and Ge(Li)	6.06	± 0.25
NPL	High Purity Ge	6.5	± 0.2
SCK-CEN	4πγ[NaI(Tl)] integral ***	6.16	± 0.06
IRE	Si(Li)	6.0	± 0.2

* The bulk of the activity and impurity measurements were made near the reference time which was one day past the end-of-bombardment (EOB).

** Corresponding to one standard deviation of the mean taking into account class A (random) and class B (systematic) uncertainties (1).

*** After decay of ^{123}I.

(1) P. Giacomo, Metrologia 17, 69 (1981).

Third international comparison of ^{133}Ba activity concentration measurements

D. Reher, E. Celen, R. Vaninbroukx

The third international comparison of ^{133}Ba activity concentration measurements was again organized by the BIPM. The solutions were distributed by the NBS. Although the discrepancies in the previous forerunner comparisons were not explained, this exercise was carried out on a large scale involving less experienced laboratories.

At the occasion of the first exercise in 1981 CBNM found a 1.5 % significant difference between the activity concentrations of two ampoules (1). This discrepancy could not be explained, neither by the producer of the solution, nor by the evaluating BIPM. The spread of the results of the participants - all experienced laboratories - was unusually high.

At CBNM the calibrated NaI(Tl) gamma ray counter, having an efficiency stability of 10^{-4} per year over the past 20 years, was used to measure the relative disintegration rate of the sources prepared from the ^{133}Ba solutions from all comparisons. These measurements were consistent with the results obtained by the $4\pi(AX)$-γ-coincidence method, used in the standardizations.

Each batch of ampoules, i.e. of each comparison, was measured by the BIPM and the distributor using calibrated ionization chambers. Such measurements can only check the total activity per ampoule, but not the repartition of the activity within an ampoule.

CBNM participated in this 3rd large scale comparison using the $4\pi(AX)$-γ-coincidence method. The result was 1163.0 $\pm$ 1.4 Bq/mg at the reference date. This result is consistent with previous results as the calibrated NaI(Tl)-gamma-ray counter measurements have shown.

This third comparison will not explain the large spread of the previous results. Therefore a thorough study of the reasons for the earlier discrepancies should be carried out, especially on possible inhomogeneities of carrier free ^{133}Ba solutions which could be caused by the precipitation of insoluble Ba compounds.

---

(1) D. Reher, E. Celen and R. Vaninbroukx, Determination of the Radioactivity Concentration of Two ^{133}Ba Solutions in the Frame of an International Comparison, CBNM Internal Report CBNM/RN/6/81 (1981).

International comparison of activity-concentration measurements of a ^{109}Cd solution

D. Reher, E. Celen, U. Wätjen, W. Zehner

In the past ten years ^{109}Cd has been recognized as a very useful radionuclide for the efficiency calibration of silicium and germanium detectors in the 10-100 keV energy region. The emission probabilities of the X and γ rays of ^{109}Cd are not known with sufficient accuracy to improve considerably the efficiency calibration of semi-conductor detectors. The main reason for this is the rather large uncertainty on the measurements of the desintegration rate.

On behalf of Section II (Mesures des radionucléides) of the Comité Consultatif pour les Etalons de Mesure des Rayonnements Ionisants (CCEMRI) the Bureau International des Poids et Mesures, Sèvres, is launching an international comparison of activity-concentration measurements of a ^{109}Cd solution. Six experienced laboratories (see Table 2.5) were invited to exercise a trial comparison. The ^{109}Cd solution was distributed by the Hungarian National Office of Measures (OMH) during Mid-December.

Table 2.5. Participants of the ^{109}Cd comparison

1.	Atomic Energy of Canada Ltd. (AECL)
2.	Bureau International des Poids et Mesures (BIPM)
3.	Central Bureau for Nuclear Measurements (CBNM)
4.	Laboratoire de Métrologie des Rayonnements Ionisants (LMRI)
5.	National Physical Laboratory (NPL)
6.	Physikalisch Technische Bundesanstalt (PTB)

The CBNM will participate in this comparison using the 4π-pressurized proportional counter, the 4πCsI-sandwich spectrometer, and calibrated Si(Li)- and Ge-spectrometers. These instruments were tested in standardizing a ^{109}Cd solution (Nr. 109-Cd-8402) which was prepared from a solution bought in 1982 from Amersham International.
A new method to standardize ^{109}Cd is being developed as well: efficiency tracing using the 4π(AX)-γ-coincidence method with ^{65}Zn as a tracer. This method should give more accurate results than any other method because the influence of decay-scheme dependent corrections on the result is extremely small. The nuclide ^{109}Cd itself cannot be standardized by the 4π(AX)-γ-coincidence method due to the long-lived metastable state at 88 keV. Because no suitable cadmium isotopic tracer is available ^{65}Zn was chosen. This method is only applicable if ^{65}Zn and ^{109}Cd can be precipitated in mixed crystals as source deposit. This was verified by analyzing ZnS-CdS deposits on vitreous-carbon backings using the CBNM RBS-PIXE facility. Six targets were scanned with a He^+ beam of 2 MeV having a diameter of about 1 mm. A number of 39 RBS spectra from 4 targets were evaluated and the ratio of the areas of the Cd- and Zn-peaks were determined. In Table 2.6 these results are collected. The small spread of the Cd/Zn ratio indicates that the deposits are formed by (Cd,Zn)S mixed crystals of a constant composition.

Table 2.6. Results of the RBS measurements on the Cd/Zn ratio

Target number	Number of measurements	average Cd/Zn ratio	standard deviation
3	12	2.13	0.10
4	13	2.10	0.15
5	5	2.17	0.03
6	9	2.21	0.09

For the purpose of the efficiency-tracing measurements a solution of ^{65}Zn was standardized to better than 0.3 %. Sources containing accurately known quantities of the ^{65}Zn and ^{109}Cd solutions were prepared by the pycnometer method. The droplets were kept under a H_2S atmosphere for about two hours in order to precipitate the Zn-Cd-sulfide. The solubility products of ZnS and CdS are smaller than 10^{-22} which indicates a rapid and quantitative precipitation even from these very diluted solutions, if H_2S is available in surplus.
Ten sources of different $^{109}Cd/^{65}Zn$-activity ratios were measured by efficiency extrapolation using absorber foils for the variation of the efficiency. The efficiency curves obtained were different from those of pure ^{65}Zn measurements. Furthermore, the efficiencies of open, uncovered sources were much less than those obtained from the pure ^{65}Zn sources. The results of these first measurements show an unusually large spread and several percent deviation from those obtained with calibrated Si(Li) spectrometers.
The investigations are continued.

Properties of a 4π-CsI(Tl)-sandwich spectrometer for the measurement of photons with an energy between 10 and 200 keV

B. Denecke

A 4π-CsI(Tl)-sandwich spectrometer was constructed and installed. An internal report (1) has been written with the following abstract:

> "In the energy region between 10 and 200 keV only a few radionuclides are available to be used as standards for the efficiency calibration of photon detectors. To increase the accuracy and reliability for interpolated values on this curve, calibrations should be performed at as many different energies as possible. The calibration sources should be measured with high accuracy by an absolute method.
> For this purpose a photon spectrometer with almost 100 % efficiency has been developed. It consists of two windowless CsI(Tl)-scintillation crystals sandwiching radioactive sources on thin plastic foils, reaching a solid angle of detection very close to 4π steradians.
> To stop all particles which disturb the photon detection, bowler-hat-shaped absorbers are introduced between source and detectors which fit into semi-spherical cavities machined in the crystals.
> The absorbers are fabricated in various thicknesses by hot pressing of polyethylene.

---

(1) B. Denecke, Properties of a 4π-CsI(Tl)-sandwich spectrometer for the Measurement of Photons with an Energy between 10 and 200 keV, CBNM Internal Report GE/R/RN/19/84 (1984).

The optimal shaped absorbers minimize photon attenuation and improve essentially the response of the spectrometer resulting in a full-energy peak having a minimum of low-energy tailing. The counting efficiency is calculated by a computer programme, using Monte-Carlo simulation of the detection process. The absorption in the backing foil, the gas, the plastic absorbers and the transmission through the detector edges are taken into account.
The sandwich spectrometer will be used to measure the emission rates of the 60-keV γ rays in the decay of ^{241}Am and the 88-keV γ rays in the decay of ^{109}Cd. A preliminary result of the KX-ray emission probability of $^{93}Nb^{m}$ is obtained to be 0.111 ± 0.003. The expected uncertainty of photon-emission rates is estimated to be 0.5 %. Finally, possible improvements of this prototype spectrometer are discussed."

Figure 2.2 shows the mechanical structure of the sandwich spectrometer.

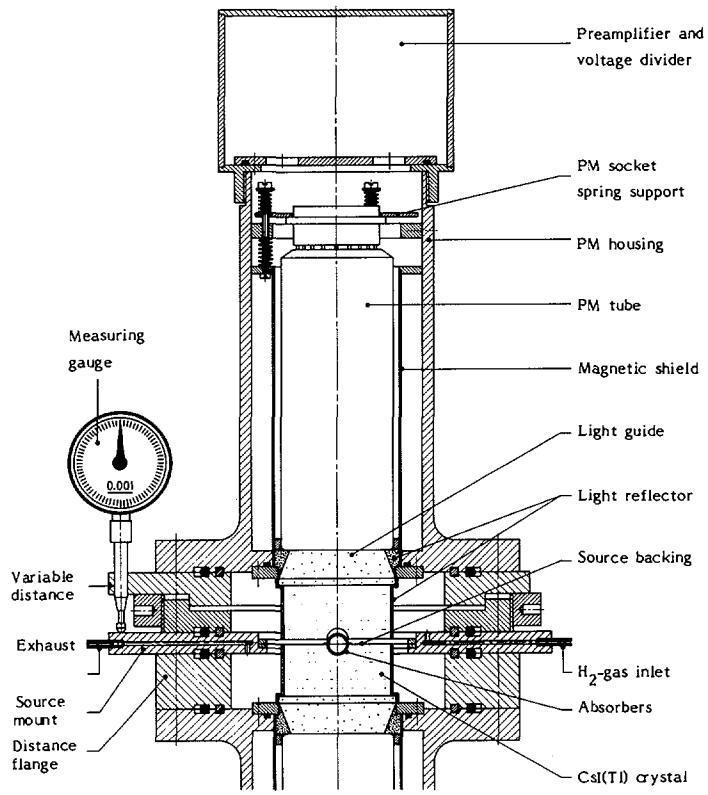

Fig. 2.2. Mechanical structure of the sandwich spectrometer. The source and the absorbers are mounted in their positions. The top detector still has to be moved down

Alpha-particle peak shape

G. Bortels, P. Collaers★

In a number of studies on the asymmetrical response of surface-barrier detectors to ^{4}He and other ions it was shown that the convolution product of a gaussian and an exponential weighting function produced a good approximation for the experimental peak [1-3]. We have examined the performance of this peak fitting model using ^{234}U α-particle spectra. These spectra had been produced at CBNM for the measurements of the α-particle emission probabilities. Care had been taken to improve the long-term peak stability and to reduce the interferences due to conversion electrons. The ^{234}U spectra had been measured using a passivated ion-implanted detector of 20 mm^2 active area without a diaphragm and for a solid angle of about 0.04 sr. It was found that, in this case the model could not describe adequately the too important experimental peak tailing. Taking the sum of an exponential and a constant as the weighting function, the expression for the peak model becomes

$$p(u) = A \exp\left[(u-\bar{u})/\tau + \sigma^2/(2\tau^2)\right]\left[1 - \mathrm{erf}(((u-\bar{u})\tau + \sigma^2)/(\sigma\tau\sqrt{2}))\right]$$

$$+ B\left[1 - \mathrm{erf}((u-\bar{u})/(\sigma\sqrt{2}))\right]$$

where u is the energy, σ and τ are parameters of respectively the gaussian and the exponential, $\bar{u}$ is the mode of the gaussian, A and B are the parameters for respectively the peak height and the tail height. The first term of the expression is simply the convolution product of a gaussian and an exponential; the second term stands for the convolution product of a gaussian and a constant.

★ Stagiaire from the "Industriële Hogeschool Kernenergie", Mol, Belgium.

(1) A. L'Hoir, Thèse 3ème cycle, Université Paris (1975).

(2) G. Amsel, C. Cohen, A. L'Hoir, Experimental Measurements, Mathematical Analysis and Partial Deconvolution of the Asymmetrical Response of Surface Barrier Detectors to MeV/^{4}He, ^{12}C, ^{14}N, ^{16}O Ions, in: Ion Beam Surface Layer Analysis, eds., O. Meyer, G. Linker and K. Käppeler (Plenum Press, New York, 1976) p. 953.

(3) A. L'Hoir, Nucl. Instr. and Meth. 223, 336 (1984).

With some approximation, the second term can be replaced by its convolution with an exponential which allows for some tailing correction to be made over the entire spectrum prior to actually fitting the peaks.
Figure 2.3 shows the result for one of the ^{234}U spectra mentioned above. Work on the use of a different weighting function and spectra which have been measured with a small diaphragm in front of the detector is in progress.

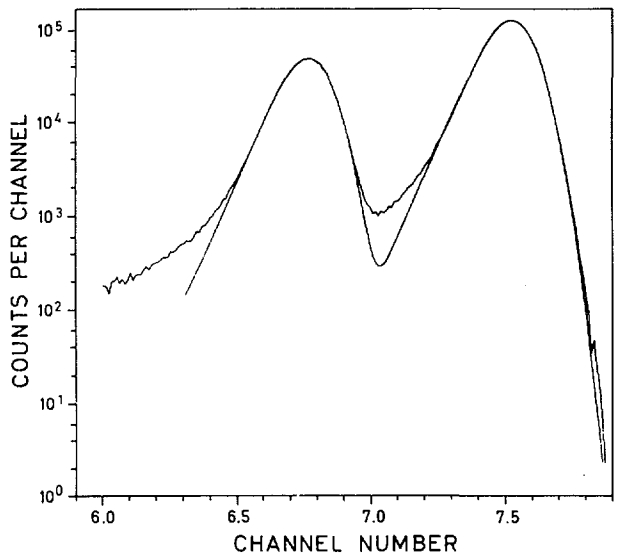

Fig. 2.3. Alpha-particle spectrum of ^{234}U fitted with the convolution product of a Gaussian and the sum of an exponential and a constant

ELEGANT, an electron-, gamma- and alpha peak spectrum evaluation programme

G. Bortels, D. Reher, W. Westmeier*

The peak fitting programme "ELEGANT" formerly named "GEELEE" has been extended for the fitting of alpha-particle spectra, using a long range exponential function for extensive low-energy peak tails. This version has been tested successfully for spectra containing mixed electron and gamma-ray peaks.
Even in cases of multipletts, consisting of electron and γ-ray peaks, these components can be separated, as is shown in Fig. 2.4. After the first tests it can be stated that the programme is (i) simple to use, (ii) numerically very stable, and (iii) flexible in its options.
The programme architecture is very modular which allows changes and expansions rather easily.
We have tested the performance of ELEGANT also for the analysis of alpha-particle spectra using reference spectra of NBS plutonium, SRM 947 and ^{234}U. These spectra have been measured at CBNM.
The spectrum A is one from a measured set of spectra whereas B and C are the sum of several spectra. The number of counts in spectrum B is nine times that in spectrum A. Care has been taken in these spectra to reduce peak drifts and interferences due to conversion electrons. The results are shown in Table 2.7. The results from ELEGANT were obtained by summing the areas of the individual peaks in the spectra. Their uncertainties were obtained from the quadratic summing of the uncertainties on the individual peaks. They represent one standard deviation for a single analysis.
The reference values for B and C were obtained from a larger set of measurements and the quoted overall uncertainties correspond to one standard deviation for the mean. The uncertainty of the reference value for spectrum B corresponds to one standard deviation of the single measurement. It is concluded that the results of ELEGANT in all cases agree with the reference values.

---

* University Marburg, FRG.

```
ITCNT =   83   CONVER. =  1   TIME = 250.45   IBACK =  0   FIT =  0.37

PEAK NR :  1    (E)
POS :  548.20 +-      0.18   HGT :  18062.04 +-      981.06  E : 548.195 +-    0.182  AREA : 244978.73 +-    4026.55
FWHM : 7.253 +-  0.059      CAP :   4.9839E-05 +-    1.6689E-05
EXHGT :   7.8800E-02 +-    6.9574E-03   EXDECAY :   1.1276E-01 +-    6.6506E-03

PEAK NR :  2    (E)
POS :  565.54 +-      0.13   HGT :   4485.97 +-      138.22  E : 565.545 +-    0.129  AREA :  61251.39 +-    1950.09
FWHM : 7.253 +-  0.039      CAP :   4.9839E-05 +-    1.5949E-05
EXHGT :   7.8800E-02 +-    2.1093E-02   EXDECAY :   1.1276E-01 +-    3.9696E-02

PEAK NR :  3    (G)
POS :  572.02 +-      0.05   HGT :   7923.70 +-      176.99  E : 572.024 +-    0.054  AREA :  43959.91 +-     426.14
FWHM : 5.015 +-  0.015      CAP :   2.8231E-04 +-    6.9650E-05
```

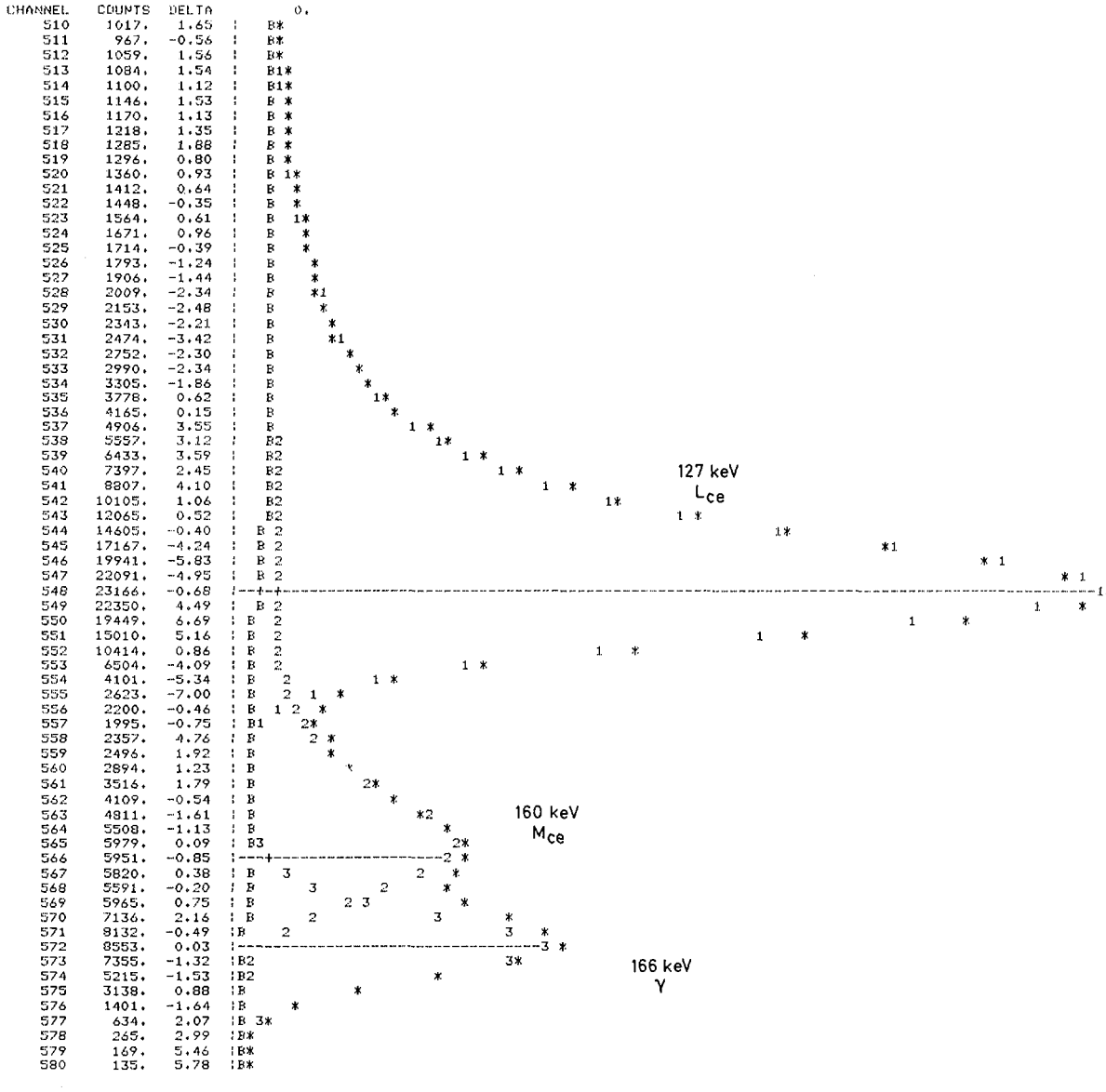


```
139-CE Q#DE305 OFFEN SILI LEXES                                    REHER          23.CE1007

LIST OF PEAKS EVALUATED  :
```

POSITION (CHANNEL)	DELTA ABS	HEIGHT (COUNTS)	DELTA ABS	ENERGY (KEV)	DELTA ABS	AREA (COUNTS)	DELTA PERCENT	FWHM CHNL	TYPE	FIT	TIME
548.20	0.18	18062.0	981.1	548.195	0.182	244978.7	1.644	7.25	(E)	0.37	OVER
565.54	0.13	4486.0	138.2	565.545	0.129	61251.4	3.184	7.25	(E)	0.37	OVER
572.02	0.05	7923.7	177.0	572.024	0.054	43959.9	0.969	5.01	(G)	0.37	OVER

Fig. 2.4. Example of a computer outprint of the programme ELEGANT, shown in the separation of the γ ray, the L- and M-conversion electrons of ^{139}La after ^{139}Ce decay

Table 2.7. Comparison of results from the code ELEGANT with reference values measured at CBNM

Spectrum No.	Material	Ratio measured	Result from Code ELEGANT	Reference value
A	Plutonium SRM 947	$(P_{a43}/P_{a0})_{^{238}Pu}$	0.409 ± 0.010	0.4087 ± 0.0014
		$^{238}Pu/^{239+240}Pu$	0.512 ± 0.016	0.5190 ± 0.0012
B	Plutonium SRM 947	$(P_{a43}/P_{a0})_{^{238}Pu}$	0.411 ± 0.008	
		$^{238}Pu/^{239+240}Pu$	0.522 ± 0.005	0.5185 ± 0.0012
C	^{234}U	P_{a53}/P_{a0}	0.402 ± 0.014	0.3982 ± 0.0007

Construction and characterization of a Pulse-Shape-Discrimination-Liquid-Scintillation System for use in standardization of radionuclides

B.M. Coursey★, E. De Roost, D. Mouchel, W. Zehner

Pulse-shape discrimination based on the full time of a liquid-scintillation pulse is a commonly-used technique for reducing the gamma-ray component in neutron detectors (1), and the beta-particle + gamma-ray component in low-level alpha-particle detectors (2). A pulse-shape-discrimination liquid-scintillation (PSDLS) system has been built at CBNM for use in standardizing mixtures of alpha- and beta-emitting nuclides, such as the pairs ^{243}Am-^{239}Np and ^{237}Np-^{233}Pa. The liquid-scintillation detector is optically coupled to a single, vertically-mounted RCA 8850 phototube. A schematic of the electronic system is shown in Fig. 2.5. The normal pulse-height distribution is obtained from the dynode pulse while the timing information is extracted from the anode pulse.

---

(1) G.J.H. Jacobs, Neutron Energy Spectra Produced by α-Bombardment of Light Elements in Thick Targets, Thesis Technische Hogeschool Eindhoven, 1982, p. 15.

(2) J.W. McKlveen, W.J. McDowell, Nucl. Instr. and Meth. 223, 372 (1984).

★ Visiting Scientist from NBS, Washington, USA.

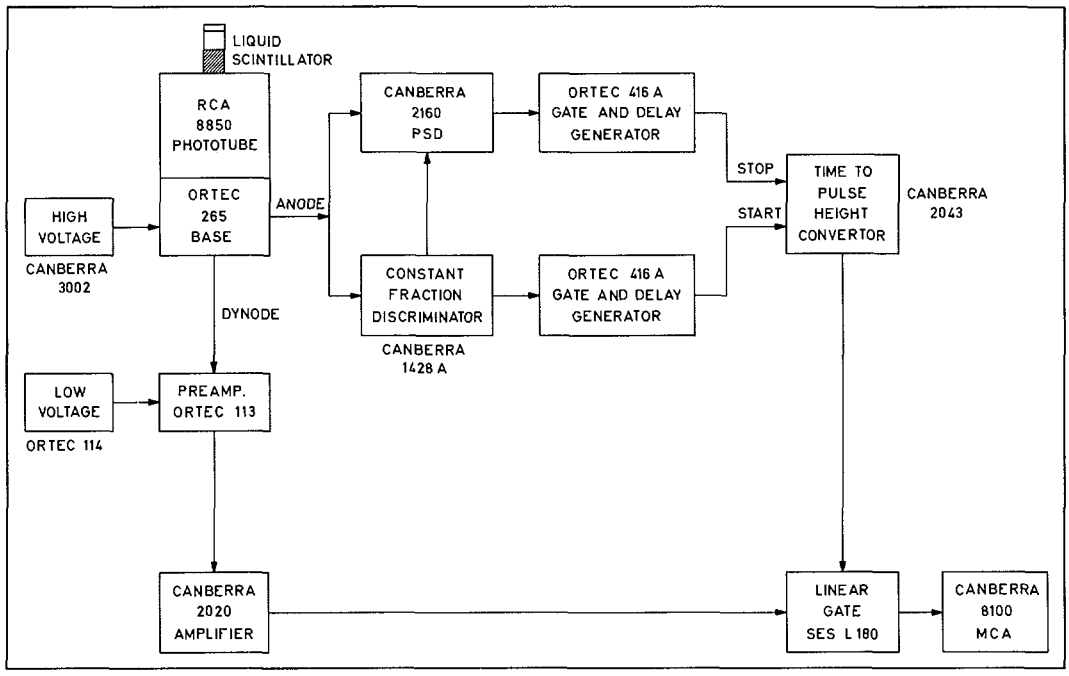

Fig. 2.5. A schematic drawing of the pulse-shape discrimination liquid-scintillation (PSDLS) counting system

The operating characteristics of the new detector were established using sources of the following radionuclides:

$^{93}Nb^{m}$	conversion electrons
^{3}H, ^{36}Cl	low- and high-energy beta particles
^{238}Pu	alpha particles
^{113}Sn, ^{22}Na, ^{137}Cs	gamma rays
^{243}Am-^{239}Np	equilibrium mixture of alpha particles and beta particles.

Some of the more important characteristics are compared in Table 2.8 with those for the EKCO system which has been used for previous liquid-scintillation measurements [1].

---

(1) R. Vaninbroukx, in "Liquid Scintillation Counting: Recent Applications and Development" Vol. 1, Physical Aspects, Academic Press, New York, 1980, p. 143.

Lucite adapters allow the same 2-ml glass vials to be used with both the PSDLS and EKCO systems. The high background for the PSDLS can be reduced by shielding the detector from external gamma radiation. In preliminary pulse-shape-discrimination measurements there is about 10 % overlap of the alpha- and beta-particle peaks in the time mode. The electronic discrimination has been optimized but the resolution of the peaks depends strongly on the oxygen concentration in the scintillator. The sample must be thoroughly deaerated with argon gas. Preliminary measurements of ^{243}Am-^{239}Np indicate that the detector efficiency is also high enough to allow direct $4\pi\beta$(LS) counting. Comparative measurements of ^{3}H and ^{239}Np are underway using also the computations from programme EFFY (1).

Table 2.8. Some characteristics of the PSDL and EKCO Liquid-Scintillation-Counting Systems

	PSDLS	EKCO (a)		
Scintillator volume (ml)	2	2	7	15
Counting Efficiency for ^{3}H (b) (%)	69	37	56	44
Figure of merit (4) (keV/e^{-})	2	7	3.5	5.5
Background Counting Rate (c) ($0.5\ s^{-1}$)	1800	19	35	40
Operating Temperature (°C)	4.5	11.5		
Phototube (2300 V)	RCA 8850	RCA 8850		
Shielding	none	2.5-cm lead minimum		
Pulse Shape Discrimination	Canberra 2160	none		

(a) The "2-ml" vials have a 1.6 cm^2 surface exposed to the phototube while larger volume samples are counted in the Standard EKCO vials which have a 9.1-cm^2 area on the bottom of the cylinder.

(b) Using NBS ^{3}H-H_2O SRM 4927 standardized by gas counting.

(c) Background includes single-photoeletron (mono's) peak.

---

(1) B.M. Coursey and D. Reher, EFFY, A Program to Calculate the Fermi Spectrum and Counting Efficiency of Data Particle in Liquid Scintillators. This report.

EFFV: A programme to calculate the Fermi spectrum and counting efficiency of beta particles in liquid scintillators

B.M. Coursey*, D. Reher

This Fortran IV programme was originally written for the UNIVAC 1100/80 computer at the J.E.N. [1]. The calculations performed provide the basis for a method of standardizing pure beta-particle-emitting radionuclides [2]. In one of the initial subroutines, SPECTR, the theoretical beta-particle spectrum for a radionuclide is computed. The input data required are the shape factor (for allowed and various forbidden transitions), the number Z of the residual nucleus, and the maximum beta-particle energy. The programme, with the addition of some input and output facilities, has been installed on the RNDAS computer [3]. Furthermore, a function subroutine to compute the double-precision hyperbolic sine has been included. The spectra obtained may be written to the RNDAS experiment data file in the same format as 1024 channel MCA spectra. They can then be integrated, printed and plotted using the RNDAS programmes REVINT, PRINTS and PLTSPC, respectively. Typical spectra are shown in Fig. 2.6 for ^{3}H and ^{90}Sr. The average energies for 16 beta-emitting nuclides computed using this programme are compared in Table 2.9 with some literature values [4-6]. The last column in Table 2.9 gives the fraction of decays in the low-energy region below 5 keV. The detection of these events is the principal problem in liquid scintillators which have a threshold of about 2 keV.

---

(1) E. Garcia-Toraño, A. Grau, Comp. Phys. Comm. 23, 385 (1981).

(2) A. Grau, E. Garcia-Toraño, Int. J. Appl. Radiat. Isot. 33, 249 (1982).

(3) D. Reher, A.B. Idzerda, Nucl. Instr. and Meth. 221, 586 (1984).

(4) NCRP Report 58, A Handbook of Radioactivity Measurements Procedures, Appendix A.3, Washington, 1978.

(5) J.A.B. Gibson, AERE-Harwell, private communication to B.M. Coursey, July 1980.

(6) D.C. Kocher, "Radioactive Decay Tables", Doc/TIC-11026, 1981.

* Visiting Scientist from NBS, Washington, USA.

Table 2.9. Maximum and average beta-particle energies and the low-energy component for 16 beta-emitting radionuclides

Radionuclide	E_β max. (keV) INPUT [a]	E_β ave. (keV) EFFY CBNM	E_β ave. (keV) others	Reference	Decay Events Having E < 5 keV (%) EFFY-CBNM
^{3}H	18.6	5.70	5.68 5.69	(1) (2)	49.0
^{241}Pu	20.8	5.87	5.24 5.23	(2) (3)	55.9
^{63}N	65.87	17.34	17.13 17.16	(1) (2)	20.0
^{14}C	156.48	49.51	49.47 49.35	(1) (2)	5.1
^{95}Nb	159.7	43.54	43.37	(2)	8.0
^{35}S	167.47	48.96	48.80 48.82	(1) (2)	6.6
^{135}Cs	205	56.59	56.3	(4)	6.1
^{203}Hg	212.2	57.87	57.7 57.40	(1) (2)	6.0
^{32}Si	213.0	64.77	64.7 64.70	(1) (4)	4.6
^{147}Pm	224.6	62.11	61.96 61.83	(1) (2)	5.5
^{45}Ca	256.9	77.34	77.2 77.22	(1) (2)	4.0
^{99}Tc	293.5	84.72	84.6	(2)	3.9
^{60}Co	317.9	95.89	95.8	(1)	3.3
^{94}Nb	471	145.70	145.6	(1)	2.1
^{90}Sr	546	199.05	195.8 195.8	(1) (4)	1.3
^{36}Cl	709.5	251.24	251.33 230.2	(3) (4)	0.8

(a) Maximum beta-particle energy recommended by the Reference(s) cited for this nuclide.

(1) NCRP Report 58, 1978.

(2) J.A.B. Gibson, AERE-Harwell, private communication, 1980.

(3) D. Kocher, Radioactive Decay Data Tables, DOE/TIC-11026, 1981.

(4) J. Blachot and C. Fich, Ann. Phys. 6(Suppl.), 3 (1981).

When testing EFFY at CBNM it turned out that for high-Z nuclides having a low beta-endpoint energy, e.g. ^{241}Pu, numerical problems arise. For small energy bins and at low energies, floating overflow occurs in routines computing the double-precision hyperbolic sine and the double-precision gamma function. As a consequence, the beta spectrum is computed rather inaccurately. To overcome this problem, the algorithm used to compute the Coulomb factor should be reconsidered and programmed for higher numerical stability.

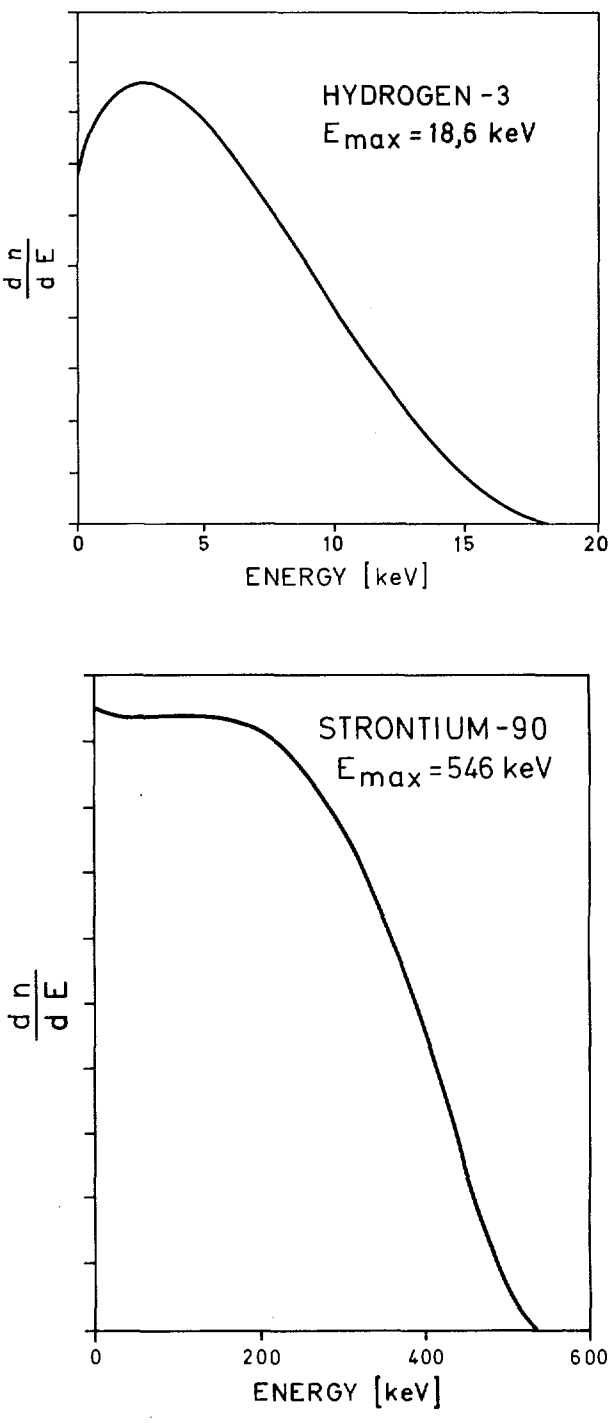

Fig. 2.6. Theoretical beta-particle spectra computed with programme EFFY

A second subroutine EFFIC computes the counting efficiency for liquid-scintillation detectors for a given nuclide as a function of the figure of merit, which is the beta energy required to produce one photoelectron at the first dynode of the phototube. Two versions of EFFY are used at CBNM: EFFYSI and EFFYCO for single phototube and coincidence systems, respectively. Two different single-phototube systems are in use at CBNM; the EKCO and PSDLS★ (1) systems.

Table 2.10 gives the LS counting efficiency for a single tube system as a function of the figure of merit for four pure beta emitters. One can use these data and a radioactivity standard of tritium obtained from other means (e.g. gas counting) to standardize any of the other three radionuclides (2).

Although EFFY is a very useful programme it should be improved in two ways: (i) better numerical stability for extreme cases and (ii) computation of uncertainties of the results as a function of uncertainties of the input parameters.

Table 2.10. Liquid scintillation counting efficiency as a function of the figure of merit for a single phototube system for four pure beta emitters

Figure of Merit (keV/photoelectron)	Counting Efficiency computed with EFFSI (%)			
	^{3}H	^{63}Ni	^{14}C	^{99}Tc
1	82.80	93.50	98.28	98.76
2	70.11	88.15	96.84	97.68
5	46.66	75.62	92.81	94.83
8	34.58	66.09	88.94	92.24
10	29.44	60.87	86.42	90.60
20	16.82	43.22	74.87	83.05
25	13.84	37.64	69.83	79.62
30	11.76	33.30	65.28	76.38

(1) B.M. Coursey, D. Mouchel and W. Zehner, This report.

(2) B.M. Coursey, J.A.B. Gibson, M.W. Heitzman, J.C. Leak, Int. J. Appl. Radiat. Isot., 35, 1103 (1984).

★ Pulse Shape Discrimination Liquid Scintillation (PSDLS) counting system.

2.2. METROLOGY OF NEUTRON FLUX AND DOSE

Neutron dosimetry via calorimetry

A. Paulsen, H. Nerb, R. Widera

It is intended to extend CBNM's experience in absolute neutron fluence rate measurements towards neutron dose rate measurements. The indicated instrument for this purpose would be a tissue-equivalent calorimeter. Based on the experience with the RUG graphite calorimeter the construction of a graphite calorimeter as an intermediate step is planned.
All materials, components and equipment required for the construction of an NBS-type graphite calorimeter have been produced. The assembling of this calorimeter will be carried out in 1985.
The design of the tissue-equivalent calorimeter is not yet finished. The dimensions of the components are roughly fixed, however, up to now it could not be clarified in what way jacket and shield can be heated homogeneously and what type of thermoregulation should be applied. The large difference in the thermal parameters between TE-plastic and graphite prohibits a simple copy of the graphite calorimeter.
For use with this TE-calorimeter a high intensity neutron field is planned making use of the Be(d,n) neutron source reaction at E_d = 7 MeV and I_d = 20 μA. Preparatory work was carried out for the required accelerator beam extension and the experimental area. A neutron collimator was designed and ordered. This collimator will make available collimated beams as used in neutron therapy but reduces the dose rate outside the beam to values requested by radioprotection.

Study of a graphite calorimeter

A. Paulsen, E. Cottens[+], A. Janssens[★], H. Nerb, L. van Rhee, R. Widera

At the University of Gent (RUG[★]) a graphite calorimeter of the NBS type has been constructed for gamma and electron dosimetry. The calorimeter has been used in an electron beam of high intensity. A contract has been placed with RUG to transfer the experience and know-how gained at Gent to a working group

---

[+] Ministerie van Volksgezondheid, Brussel.

[★] Rijksuniversiteit Gent.

at CBNM. The graphite calorimeter is built up by four thermally isolated graphite bodies (from inside to outside): core (i = 1), jacket (i = 2), shield (i = 3) and medium (i = 4). The medium is kept on a fixed reference temperature (~ 30°) by an electronic temperature controller. The temperature differences to this reference temperature, T_i, of the three inner bodies are assumed to be determined by a system of linear first order differential equations:

$$P_1 dt = C_1 dT_1 + K_{13}(T_1 - T_3)dt + K_{12}(T_1 - T_2)dt$$

$$P_2 dt = C_2 dT_2 - K_{12}(T_1 - T_2)dt + K_{23}(T_2 - T_3)dt$$

$$P_3 dt = C_3 dT_3 - K_{13}(T_1 - T_3)dt - K_{23}(T_2 - T_3)dt + K_{34} T_3 dt$$

The symbols P_i, C_i and K_{ij} represent the dissipated constant powers, the heat capacities and the heat transfer coefficients, respectively. The contract work focussed on the performance of the calorimeter in the calibration mode, because the problems of a proper heat loss correction arise only in the electrical calibration, whereas the calorimeter experiences nearly ideal adiabatic conditions under irradiation.

Equilibration of the absorbed dose calorimeter

The operation of the absorbed dose calorimeter both in irradiation and in calibration mode requires the achievement of nearly perfect thermal equilibrium of all the bodies with the thermo-regulated medium.
It is a common practice to search for equilibrium by observation of the temperature of the different bodies on a recorder, and to dissipate amounts of electrical energy in the bodies in a trial-and-error procedure. This works as long as the drift rates are positive. For an experienced operator it takes nearly one hour to reduce this way the drifts below 10^{-7} K s^{-1}. For short calibration or irradiation runs with a temperature rise of the order of 0.01 K this is sufficient. However if one wishes to use the calorimeter near its limits of sensitivity, the signal is one order of magnitude smaller and correspondingly a drift rate of $1 \cdot 10^{-8}$ K s^{-1} should be pursued. This can hardly be achieved by the above-mentioned trial-and-error procedure.

A faster equilibrium procedure has been set up by measuring drift rates of all bodies to determine their departure from the equilibrium and then to calculate the energy amounts required to achieve equilibrium using the set of transfer equations. The problem reduces to a matrix multiplication between a vector containing the drifts and a matrix which depends on the heat capacities, the heat transfer coefficients and the dissipation period. This latter dependence is however small and one can use a fixed matrix as long as the dissipation period is small compared to the time constants of the bodies. At present data from a digital voltmeter are read directly by a microcomputer that also calculates the drift from a linear fit to the data and determines the required dissipation powers and the corresponding voltages (programme DRICOR in BASIC). In general it is not possible to reach perfect equilibrium through only one dissipation run because of the imperfections of the method. However, very often a second run is already sufficient to reach drifts of a few times 10^{-8} K s^{-1}. Such further runs are only possible when the temperatures of the bodies (at least of the shields) are still rising. The time required to achieve equilibrium is of the order of 15-30 min.

New measurement of the calorimeter heat transfer coefficients

These coefficients can be determined by measuring the equilibrium temperatures achieved by constant power dissipation in one of the three bodies. However, for the corresponding measurements the influence of temperature changes of the medium has to be reduced either by reducing the measuring time, by improving the temperature stability, or by reducing the calorimeter sensitivity.
Since the achievement of equilibrium takes a too long time (1-2 days) the procedure was accelerated by the same technique already described in the section above. For that purpose the code DRICOR was adapted and extended (code TRACO). The new thermal equilibrium is attained by iterative application of electrical energy to all three bodies during certain short time intervals and a continuous application of an equilibrium power to one of the bodies as calculated by the code TRACO.
However, with the normal sensitivity of the calorimeter these improvements alone were insufficient. In practice it still took 2 to 8 hours until the equilibrium was sufficiently approximated. This is due to the fact that thermal drift rates of core, jacket and shield have to be measured successively with sufficient accuracy during each iteration cycle. Furthermore, there does not exist a reasonable theoretical solution for all possible situations.

Since a water bath can be controlled to better than ± 50 mK a series of measurements was carried out with the calorimeter immersed in an externally controlled water bath. However, the results were disappointing. The calorimeter drift rates due to room temperature changes were somewhat reduced but not at all to that extent one would expect according to the water temperature stabilization. Obviously there exists another heat path from the inner components of the calorimeter to the outside (electrical connection leads?) which makes the temperature of those components still sensitive to the room temperature although with a delay of a few hours. This approach was finally discarded.
A successful method was to reduce the calorimeter sensitivity (by use of a switchable lock-in amplifier) and to dissipate an accordingly higher power in core, jacket or shield so that the room temperature dependent drifts became negligible. This method turned out to be very successful and delivered the most reproducible results.
The final results for the heat transfer coefficients K_{ij} are summarized in Table 2.11 with the calculated standard error of the mean and number of measurements.

Table 2.11. Heat transfer coefficients

	K_{12} (mW/K)	K_{23} (mW/K)	K_{34} (mW/K)	K_{13} (μW/K)
Mean value	0.705	0.954	5.01	17.8
Standard error (%)	0.14	0.10	0.60	1.2
Number of measurements	8	11	10	7

These results clearly demonstrate the existence of a direct heat link between core and shield as it was already supposed by Cottens et al. [1]. This heat leak path is constituted by the core leads which are not thermally attached to the jacket. The effect is in good agreement with expectations [1].

---

(1) E. Cottens, A. Janssens, G. Eggermont and R. Jacobs, Proc. Biomedical Dosimetry, Paris 1980, IAEA-SM-249/32.

Electrical calibration of the calorimeter

The calorimeter was recalibrated by dissipation of an accurately known amount of electrical energy in the core. The amount of electrical energy was varied from about 100 mJ (high level) over 10-20 mJ (medium level) to about 1 mJ (low level) to study the range of applicability of the instrument. Furthermore the dissipation time of these energies was changed between 50 and 1600 s to study the correctness of the applied heat loss corrections. Most of the calibration runs (115) were carried out with heat loss compensation and only a few (12) were done under non-adiabatic condition.
There is a natural grouping of all calibration measurements by the amount of injected electrical energy and measuring period. This leads to 15 data groups containing 3 to 22 measurements each. The resulting experimental calibration factor is given as

$$8.452 \pm 0.012 \ (\pm 0.14\ \%)\ \text{Gy/V}$$

with 14 degrees of freedom. This calibration factor is valid for the whole range of executed calibrations.

Neutron dosimetry via ionometry

A. Paulsen, H. Nerb, R. Widera

CBNM is going to put at the disposal of interested EC institutions standardized neutron fields and irradiation facilities for radiobiological and radioprotection studies. For this purpose also equipment for ionometric neutron dosimetry must be set up. During 1984 several instruments were procured. Total dose determinations will be carried out by means of the T2 (XRADIN) 0.5 cm^3 and IC-18 (FWT) 0.1 cm^3 ion chambers, both tissue-equivalent. For these chambers a remotely controlled electrometer was developed. It employs an operational amplifier 1702 (TELEDYNE-PHILBRICK) with leak currents of 2-6 fA and will be operated with an external digital voltmeter.
The gamma dose contribution will be measured by means of a MG2 (XRADIN) 0.5 cm^3 magnesium/argon chamber using the same electrometer system or by means of GM counters. Of the latter two types will be available: Winfrith probes (ZP 1300, ALRAD) and GM-2 (18509, FWT), both energy compensated.

As a neutron beam monitor a flat chamber of 30 cm^3 (type 233612, PTW) with $C_5H_8O_2$ as wall material will be used. This chamber will be connected to a commercially available electrometer (type IQ4, PTW) with a leak current of 10 fA.
The ion chambers (with the exception of the monitor chamber which is an open air chamber) will be operated with a gas flow system for tissue-equivalent gas (64.4 % CH_4, 32.4 % CO_2, 3.2 % N_2) or argon with flow rates between 10 and 100 ml/min. Gas temperature and pressure are measured and digitally displayed. At a later stage the whole ionometric dose determination will be computerized. A gamma-irradiation device was ordered for testing ionization chambers and calorimeters. It will contain a ^{137}Cs source of 250 Ci activity giving a dose rate of 0.1 Gy/min at 35 cm distance from the source. The safety container reduces the dose rate to 0.1 μGy/min at 10 cm distance from the container surface. The device will be integrated into the accelerator safety interlock system.
In 1985 this equipment will be used to determine the neutron absorbed dose in a series of neutron irradiations to be carried out at the CBNM 7 MV Van de Graaff accelerator for radiobiological investigations of the radiobiology department of the SCK/CEN at Mol. The neutron energy will be 2.5 MeV using the $T(p,n)^3He$ neutron source reaction and the dose rate at sample position (16 cm from the target) will be about 3 mGy/min. The neutron beam size at the sample was fixed to 60 x 70 mm. A corresponding neutron collimator screening outside the beam to less than 0.05 of the beam dose was designed and ordered.

Proton recoil detector

H.-H. Knitter, C. Budtz-Jørgensen, H. Bax, R. Vogt

A feasibility study for a neutron fluence detector working on the basis of the neutron proton scattering process was started. This detector is intended to be used as an absolute neutron fluence detector in measurements of neutron standard cross sections. The study should finally reveal with what accuracy the neutron fluence can be measured with this detector. An ionization chamber with Frisch grid is used to measure the recoil proton emitted from a radiator foil positioned coplanar in the centre of the ionization chamber cathode.

The neutron beam enters vertical with respect to the chamber electrodes. The gas pressure in the chamber is adjusted such that the recoil protons emitted vertical with respect to the cathode have a range just a little shorter than the distance between cathode and Frisch grid. Then the pulse height obtained from the anode is proportional to the energy of the proton whereas the cathode pulse height depends on the proton energy and on the emission angle with respect to the normal of the cathode. Both signals together allow in a biparametric representation an effective discrimination against background events, since the recoil protons form a ridge within a well defined area as shown in Fig. 2.7.

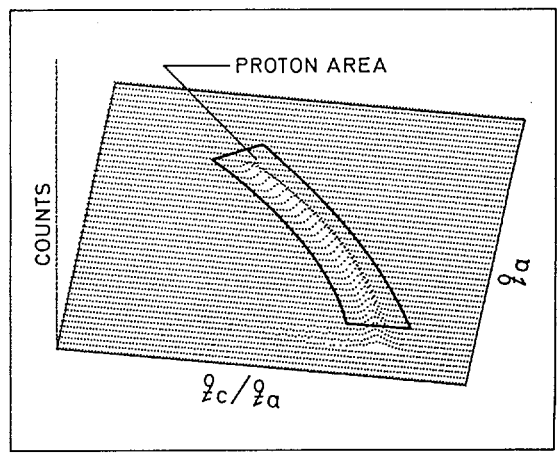

Fig. 2.7. Biparametric spectrum of recoil protons measured at 1.885 MeV incident neutron energy with signals from the anode q_a and cathode q_c of a gridded ionization chamber

This spectrum is measured at an incident neutron energy of 1.885 MeV. The events from this area are used to obtain proton recoil energy spectra, which have to be analyzed to determine the total number of recoils which were induced in the radiator foil. In order to understand more closely the operation of the detector, measurements with tristearin radiator foils of different thicknesses were made at the incident neutron energies of 0.297 MeV, 0.597 MeV, 1.096 MeV, 1.496 MeV and 1.895 MeV. These measurements gave an absolute energy calibration for the detector of better than 0.5 % above 0.5 MeV and demonstrated the linearity of the response.

To understand the proton recoil spectrum shapes and to obtain the total number of proton recoil events which took place in the radiator foil, the experiment was simulated by Monte Carlo calculations. Here the problem of radiator foil inhomogeneities became evident and has to be resolved for the next test measurements. Also the problem of the hydrogen content determination of the radiator foil needs further attention.
The spectrum measurements and the Monte Carlo calculations done so far are described in a paper presented at the IAEA-Advisory Group Meeting on Nuclear Standard Reference Data, held at CBNM Geel, 12-16 November 1984, with the title: "Investigation for a precise and efficient neutron fluence detector based on the n-p scattering process" and following abstract:

> "An ionization chamber with Frisch grid is used to detect the recoil protons induced by fast neutrons in an advantageous 2π-geometry. The working principles of the detector are explained. Recoil proton spectrum measurements are made at several incident neutron energies below 2 MeV using four radiator foils of different thicknesses. These measurements permit a proton energy calibration of the detector and the determination of proton stopping powers for the radiator foil material. Proton recoil spectra are interpreted by Monte Carlo calculations with the aim of understanding closely the spectrum shape and to obtain the total number of proton recoils."

International fast neutron fluence intercomparison

R. Widera, A. Paulsen, H. Liskien

Neutron cross-section determination demands the determination of a reaction rate and a fluence rate. The only exceptions are total and total absorption cross-sections. This makes neutron fluence rate determination a key issue in neutron metrology. Hidden systematic uncertainties may be found by comparing results between laboratories.
CBNM participated in a fast neutron fluence intercomparison running under the auspices of BIPM (Sèvres) which was coordinated by NPL (Teddington) and is based on the $^{115}In(n,\gamma)^{116}In^{m}$ ($T_{1/2} \approx 54$ min) activation reaction. NPL provides us with a 4π-β counter, 6 thin Indium foils and a ^{60}Co check source (transfer instruments). The quantity to be compared is the activity at the end of irradiation per unit neutron flux density at the sample position and per mass unit of the In foil and will consequently be given in units of $cm^2.g^{-1}.s$. The intercomparison covers the neutron energies 144 and 565 keV. CBNM participated only at 565 keV.

After some test runs a series of three measurements with different In foils and neutron counter distances was carried out during the months April and May. Neutrons were produced via the $^{7}Li(p,n)$ reaction at E_p = 2.292 MeV. A LiF target of 241 $\mu g/cm^2$ thickness was used. The average proton beam current was 13.6 μA. The wobbled target was cooled by a jet of pressurized air hitting the target backing. The In foil was irradiated at 0° relative to the proton beam at 8 cm for about 2.5 half-lives. The convolution of neutron energy spread due to target thickness and sample solid angle results in a mean neutron energy of 561 keV and an energy distribution between 545 and 578 keV. The neutron fluence rate was determined by means of our proton recoil proportional counter CP2. The standard gas filling was 1.6 bar methane at 23°C. The counter was positioned at 0° relative to the proton beam on the target and at distances to the target of 80 or 180 cm.

Figure 2.8 shows experimental and theoretical proton recoil spectra from this counter. The measured neutron fluence rate was corrected for air attenuation, counter in- and out-scattering, attenuation by the In foils and in-scattering by the target backing. The uncertainty of the neutron fluence rate is mainly determined by systematic uncertainties and was estimated to be about $\pm$ 1.6 %. With the NPL ^{60}Co check source the plateau of the counting system was determined to have a slope of 0.3 % between 2010 and 2220 V. An operating voltage of 2100 V was chosen. The ^{60}Co check source was measured 30 times during the period 13.03 to 29.05.1984 and the counting system was stable within the statistical accuracy of $\pm$ 0.3 %. The ^{60}Co activity was calculated to be 2790 $\pm$ 1.4 dps on January 1st 1984. The background with different inactive In foils was determined to be 0.79 $\pm$ 0.01 cps. The $^{116}In^{m}$-activity at the end of the irradiation was determined by following the first 1.5 half-lives. An own $^{116}In^{m}$ half-life determination taking into account activities up to five half-lives resulted in $T_{1/2}$ = (54.1 $\pm$ 0.2) min.

At each irradiation a second In-foil was positioned at 15 cm distance from the target. Its activity was used to determine a correction for a deviation from the inverse square law of distance dependence. NPL proposed to interprete such a deviation in terms of a constant room-scattered neutron field. A contribution of 0.8 to 2.5 % of this constant neutron field to the activity of the In-foil at 8 cm distance was found. The statistical uncertainty of these figures is large (about 25 %). Another correction for a contribution of the $^{115}In(n,n')$ reaction to the activity was determined from a remeasurement of the foil activities 10 hours after the end of irradiation. This correction amounts to 0.76 $\pm$ 0.10 % at the end of irradiation.

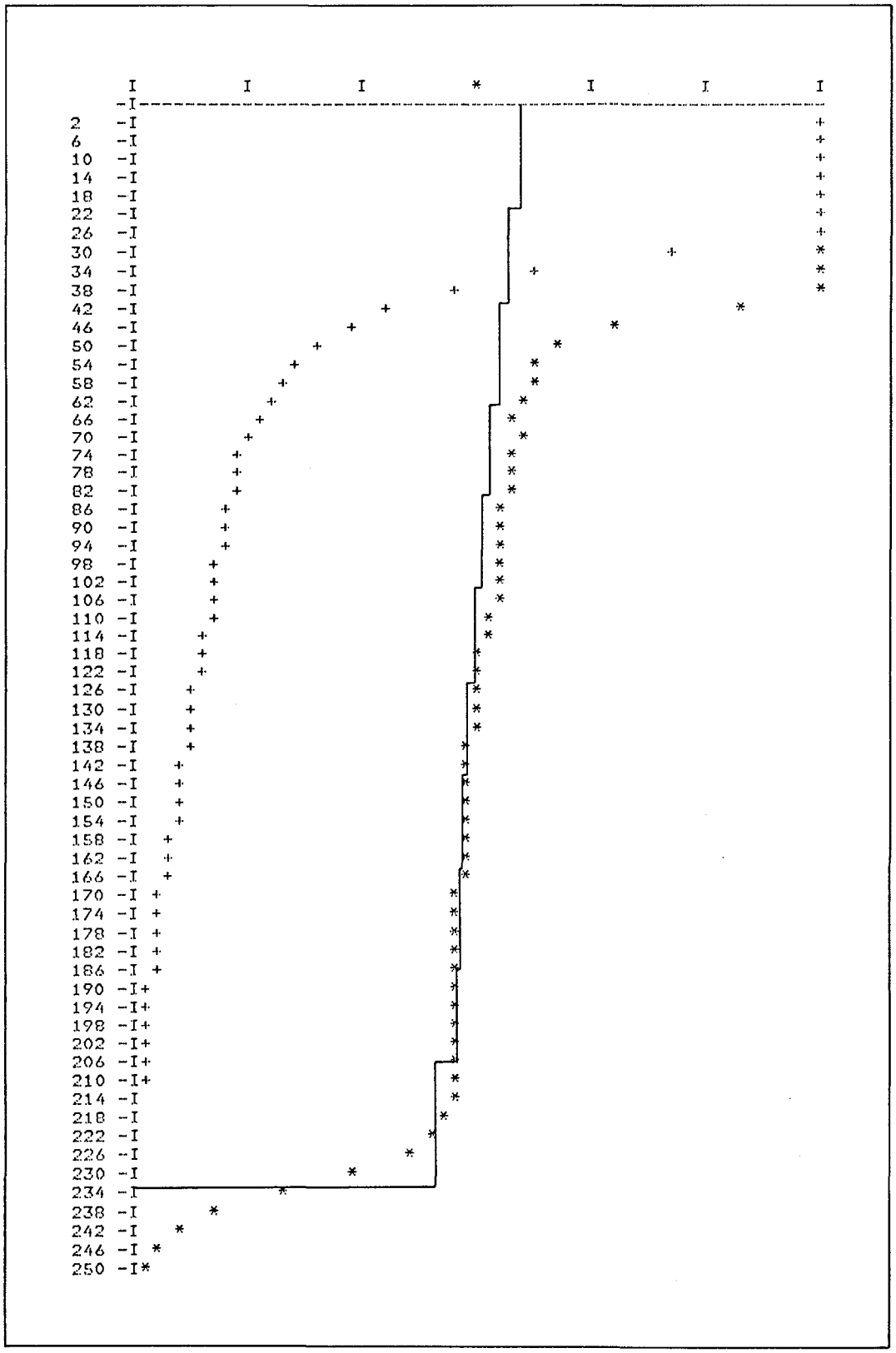

Fig. 2.8. The proton recoil spectrum (★) after subtraction of the background (+) which was determined with a polyethylene shadow cone. The given histrogramme is the result of Monte Carlo calculations

The calculated intercomparison values for the three measuring runs reproduce within $\pm$ 1 %.

Hidden systematic uncertainties in neutron fluence determinations may be found by comparing results between laboratories. Under the auspices of BIPM four branches of such international intercomparisons were organized. Two of these branches are ended. They were coordinated by NPL and CBNM, respectively. Results were presented in a common paper at the 5th Symposium on Neutron Dosimetry (München, September 1984) and at the IAEA Advisory Group Meeting on Nuclear Standard Reference Data (Geel, November 1984). The abstract reads as follows:

> "Fluence determinations for 2.5, 5.0 and 14 MeV neutrons as performed in standard laboratories have been compared. Two methods of intercomparison were used: One is based on the determination of a γ-rate ratio between ^{115m}In as induced by fast neutrons in an indium sample on one hand and ^{51}Cr from a calibrated source on the other hand and is used at all energies. The second method is restricted to 14-15 MeV neutrons and is based on measuring the ^{93m}Nb γ-activity induced in a niobium sample.
> Results show that the uncertainty contribution from the transfer methods does not essentially increase the overall uncertainty and that there is generally consistency".

An extensive report (GE/R/VG/44/84) on our participation in the third branch has been written and sent to the coordinator. The transfer instruments belonging to the fourth branch are expected to arrive in Geel in 1985.

TECHNICAL APPENDIX

Van de Graaff Accelerator

Post-acceleration bunching system

A. Crametz, S. de Jonge, H. Liskien, F. Arnotte, P. Falque, J. Leonard, W. Schubert

In order to improve the energy resolution in fast neutron time-of-flight experiments, the 1.5 ns FWHM pulses delivered with 400 ns pulse distance by the vertical, single ended, klystron bunched CN-7.0 MV Van de Graaff accelerator have been further compressed. The time compression is based on a two-gap buncher.

Principle of post-acceleration bunching in a two-gap system

From the relation

$$\frac{\Delta E}{E} = 2 \cdot \frac{\Delta t}{t} \qquad (1)$$

one deduces that the necessary energy modulation ΔE should be a linear function of the time. Therefore, in an ideal bunching system, the applied RF voltage should have the form of a sawtooth. This can be approximated by a sinusoïdal voltage if only a phase range of $\pm$ 30° is used. The general principle of bunching is given in Fig. 1: during the flight time up to the target, the pulse is compressed in time due to the imposed energy modulation. The buncher in a two-gap system consists of a drift tube of length ℓ inductively excited by a RF power. This tube is located between two end tubes at ground potential, such that two gaps of length ℓ_1 remain. The axis of the tube has to coincide with the flight direction of the positive ion pulses. In such a system, the wanted phase change of 180° between the two gaps can only be realized for one relative design velocity $\beta_\circ = \frac{v_\circ}{c}$:

$$\ell + \ell_1 = \beta_\circ \cdot \frac{\lambda}{2} \qquad (2)$$

where λ is the wavelength of the RF power.

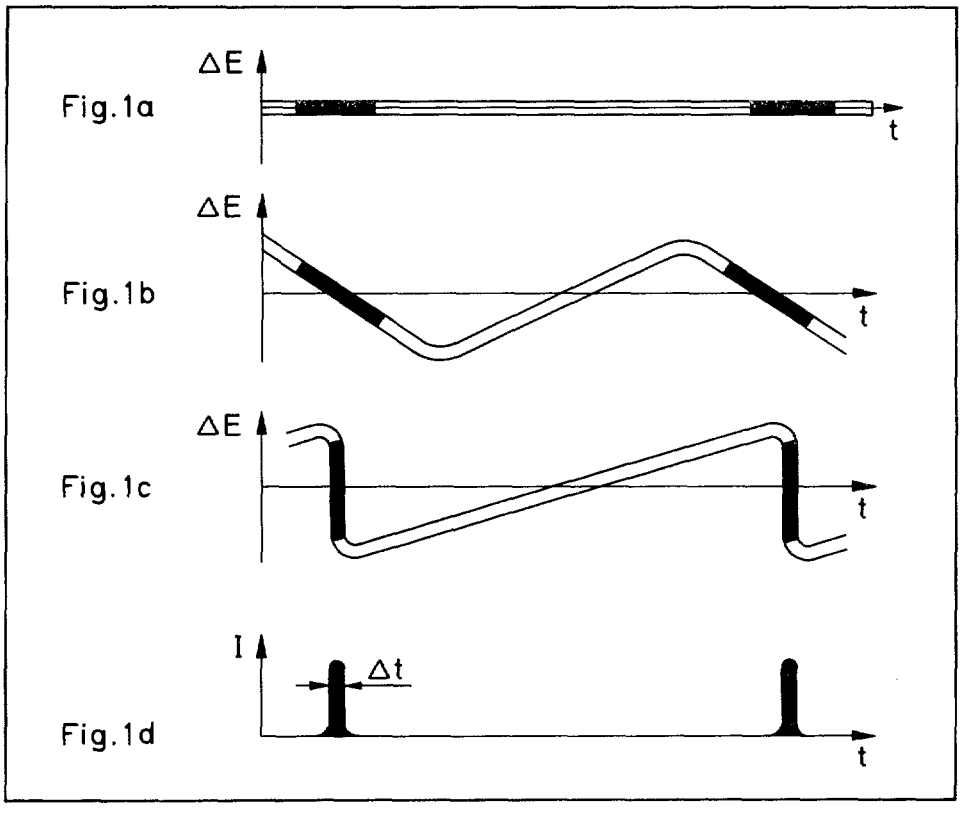

Fig. 1. Representation of the energy modulation versus time
- *at entrance (a) and exit (b) of the buncher,*
- *at the target (c),*
- *intensity distribution at the target is given in (d).*

It can be shown [1] that for a two-gap buncher the optimum bunching amplitude for singly charged ions is given approximately by the relation:

$$U_{op} = \frac{\beta^3 \cdot \lambda \cdot E_o}{4\pi \cdot e \cdot L \cdot \sin\Delta} = (2 \cdot N \cdot R_p)^{1/2} \qquad (3)$$

where β = relative velocity of the ions

E_o = rest energy of the ions

L = distance between buncher and target

$\Delta = \frac{\pi}{2} \cdot \frac{\beta_o}{\beta}$

---

(1) A. Crametz, Internal Report CBNM/VG/33/79.

The amplitude of the buncher voltage U_{o_p} is in turn fixed by the RF power N and the parallel resistance R_p of the buncher. The internal energy spread ΔE of the beam will result in a lower limit for the obtainable pulse width given by:

$$\Delta \tau = \frac{L}{c \beta^3 E_o} \cdot \Delta E \qquad (4)$$

The energy is modulated following the relation

$$E(\varphi) = U_{o_p} \cdot e \cdot [\cos \varphi - \cos (\varphi + 2\Delta)] \qquad (5)$$

and extreme values are given by

$$E_{\pm} = \pm 2\, U_{o_p} \cdot e \cdot \sin \Delta \qquad (6)$$

If all phases are allowed (DC beam), this energy modulation results in a spectrum given by

$$N(E) = (E_+^2 - E^2)^{-1/2} \qquad \text{if} \quad E_- \leqslant E \leqslant E_+ \qquad (7)$$

Description of the spiral resonator

This type of resonator has been developed at the Max-Planck Institut für Kernphysik at Heidelberg for their heavy ion post-accelerator [1] and is used here as post-acceleration buncher. As schematically represented in Fig. 2. it consists of an Archimedean spiral ① in the cross section plane of a circular tube. The spiral is grounded by a leg on the tank, a cylinder of inner diameter 35 cm and length 25 cm. The spiral is formed from two square 0.93 x 0.93 cm^2 Cu-profiles with a 0.7 cm diameter cooling channel silver soldered together in the radial plane which is coiled up with a pitch of around 4.3 cm. The drift tube ② is fixed at the free end of the spiral. The buncher is closed by two metallic end plates parallel to the spiral plane. The 105 MHz (λ = 286 cm) RF power is inductively coupled by a tunable loop ③ near the leg of the spiral and thermal frequency shifts are compensated by a servo-operated turning plate ④ . Spiral, coupling loop, tuning plate

---

(1) B. Kolb, H. Ingwersen, G. Ihmels, E. Jaeschke, R. Repnow and Th. Walcher, Rev. Phys. App. 12 (1977) 1571.

and inner diameter tank are water cooled. The buncher is vacuum pumped to about 10^{-7} Torr, using a cryogenic pump connected directly on it. The length of the spiral is 1/4 of the wavelength associated to the RF power. The length of the drift tube is calculated for a relative design velocity $\beta_o = 0.08$ which corresponds to 3 MeV protons or 6 MeV deuterons. One obtains from equation (2) $\ell = 9.4$ cm for a gap of $\ell_1 = 2$ cm.

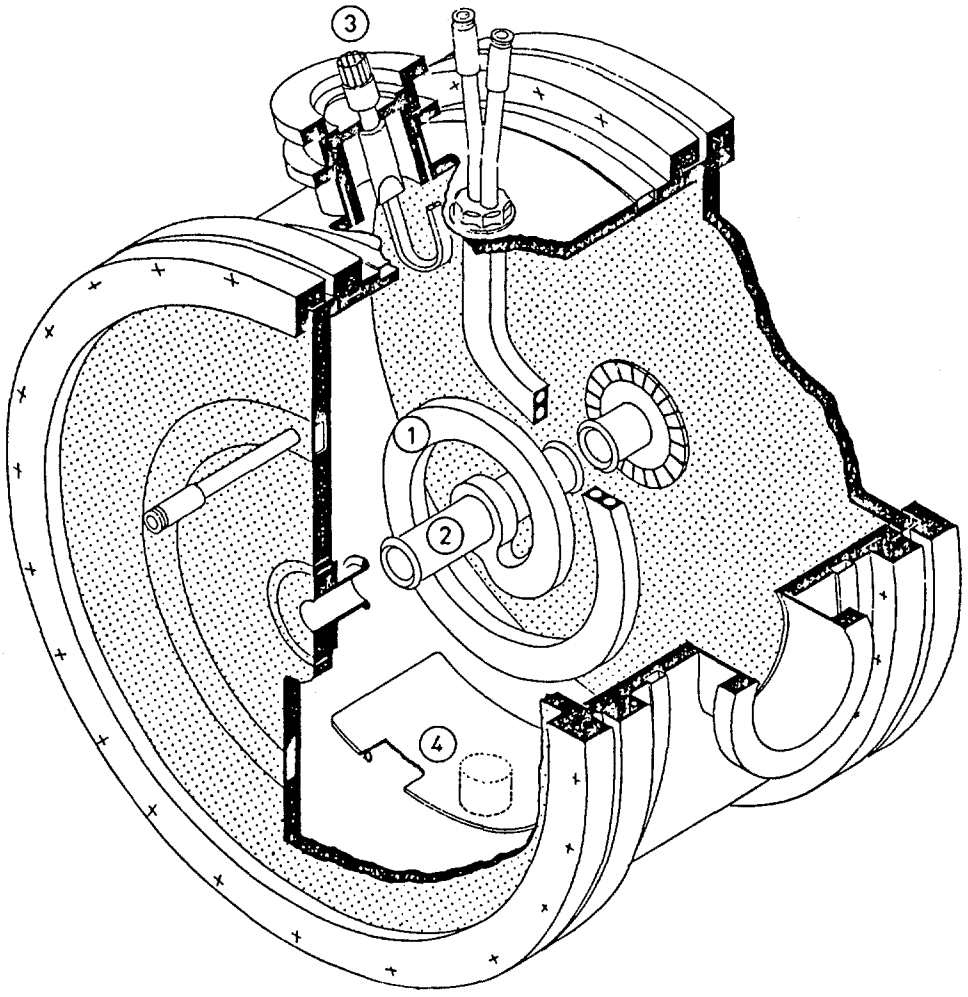

Fig. 2. Sectional drawing of a spiral resonator showing spiral ① , drift tube ② , coupling loop ③ and tuning plate ④ . Tank inner diameter: 35 cm, drift tube length: 9.4 cm for $\beta_o = 0.08$, aperture diameter: 2 cm, gap width: 2 cm.

Synchronization and regulation

To synchronize and drive the post acceleration buncher, the control units are triggered by a pick-up electrode signal of 2.5 MHz frequency which is the repetition rate of the ion pulses. The correct synchronization between this frequency and the RF power of 105 MHz is realized by a gated phase lock device (GPL). The block diagram in Fig. 3 represents this GPL.

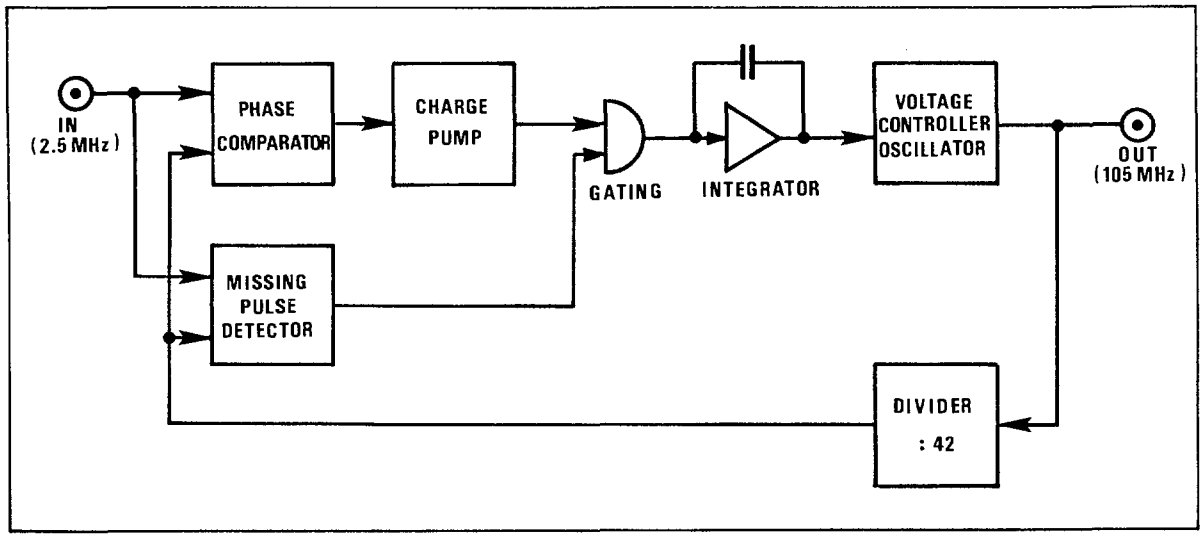

Fig. 3. Block diagram of the gated phase lock device (GPL)

To a standard phase lock oscillator [1] two devices are added: a missing pulse detector and a gate between the charge pump and the integrator. If at the reference input, one or several pulses are missing, the missing pulse detector is activated and inhibits the correction signal from the charge pump to the integrator. During this time, the integrator acts as a phase memory, keeping the phase at the output constant. If all pulses are present the circuit acts as a normal phase lock oscillator. The corresponding electronic circuit is drawn in Fig. 4 and is such that the input signals are shaped by a leading edge trigger, composed of circuits 1A, 2A and 2B, which delivers 200 ns wide negative pulses to the reference input of the phase detector. The gate input is used for test purpose only to suppress reference signals in simulation.

---

(1) MTTL Complex functions, Phase frequency detector MC 4344, Motorola Inc. 1972.

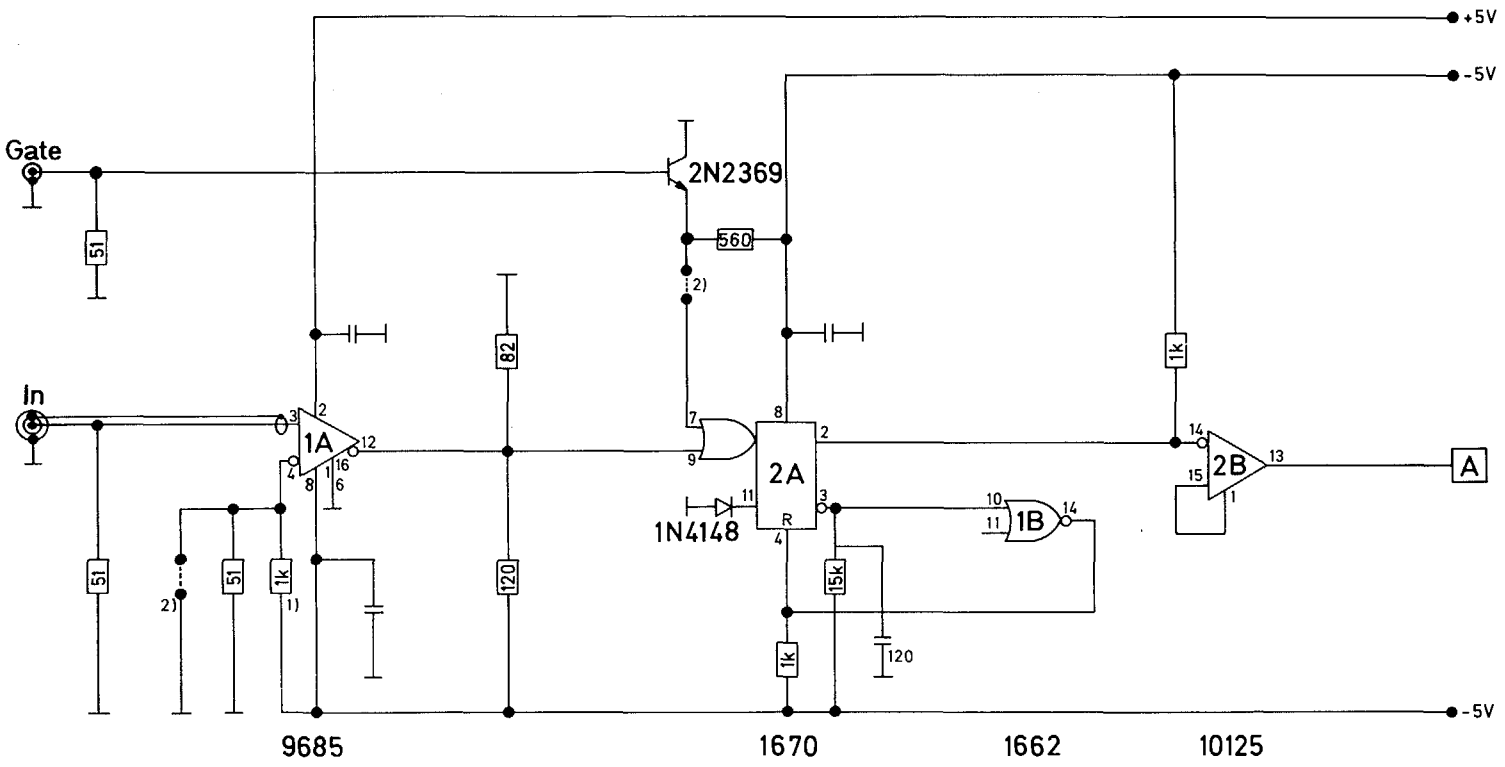

All ⊣⊢ cond. 10 nF ceram	L1	4 turns	8 mm x	5 mm ø
All ⊣⊢ cond. 10 µF tantalum	L2	3	10	9
1) for 250 mV threshold	L3	2	6	9
2) straps for testing	L4	2	6	9
3) R selected for Vs = Vg	wire dia: 1 mm			

Fig. 4.a. Electronic circuit of the gated phase lock oscillator

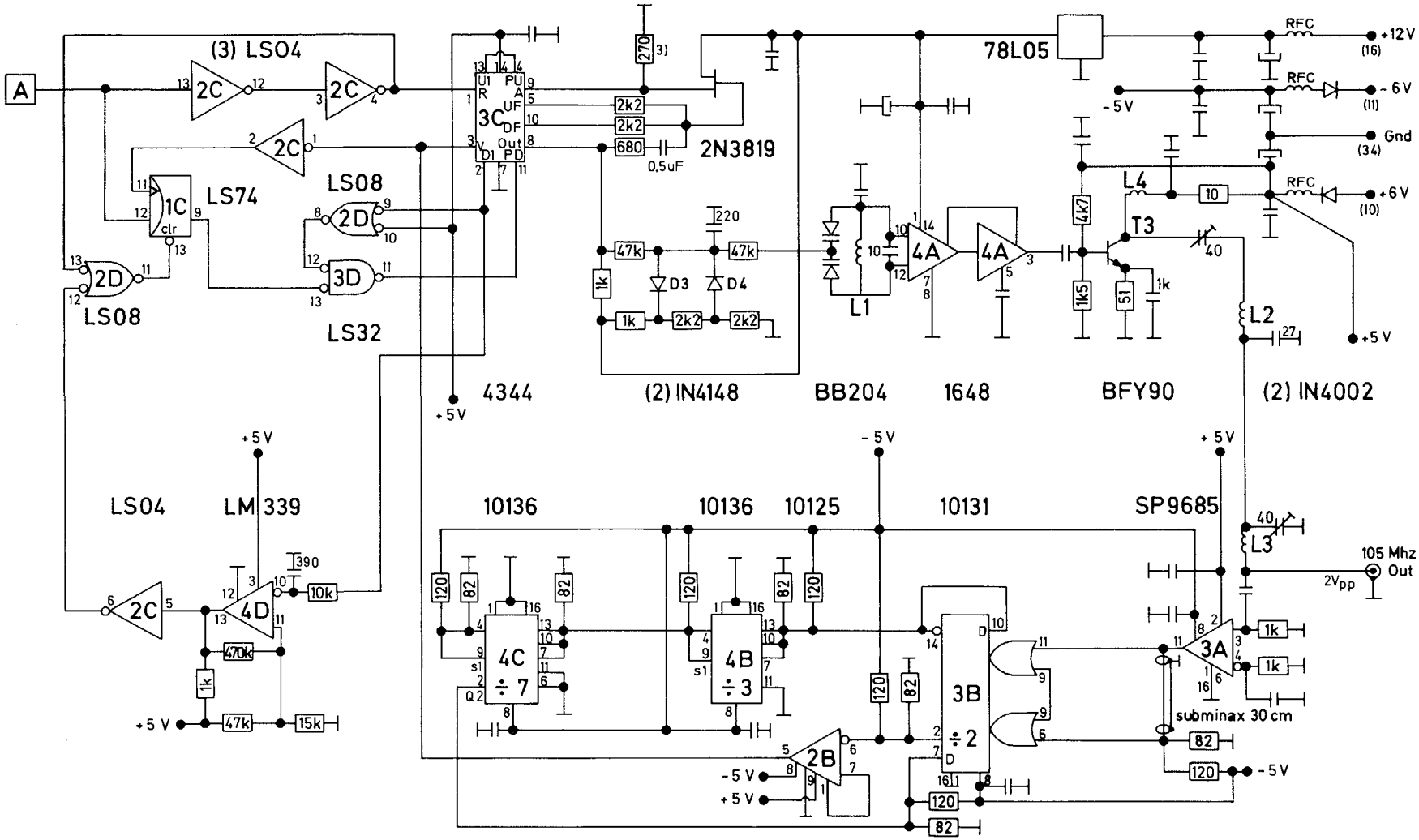

Fig. 4.b. Electronic circuit of the gated phase lock oscillator

The phase detector 3C is switched for the mode zero frequency f_o and phase difference at lock. As long as there is no lock condition, the D flip-flop 1C is cleared by the reference signal and by the fact that the output D1 of the phase detector is negative. In this way gate 3D is kept open so that the lock condition can be established i.e. the negative edges of the input $f_o/42$ and the reference input are coïncident, while outputs U_1 and D_1 of the phase detector are positive.
The presence of reference input pulses is now detected by D flip-flop 1C, while the propagation delay of inverters 2C ensures proper set up conditions for this flip-flop. The presence of input reference pulses will keep the flip-flop in the set condition while the absence of reference input pulses will clear the flip-flop. During the period in which a reference input pulse is missing the output D_1 of the phase detector goes negative. This signal which is an input to the charge pump is gated off. Gate 2D matches for differences in propagation delays.
The output U_1 of the phase detector is not gated as U_1 stays positive during the absence of reference input pulses. The tuning voltage of the VCO voltage controlled oscillator 4A is limited by diodes D_3 and D_4 to keep its range within the bandwidth of the output tank circuit of T_3.
The clamping point is decoupled with a small capacitor to remove the spurious 2.5 MHz signal originating from the integrator and having an amplitude of a few millivolts. The divider determining the frequency ratio (3B, 4B, 4C) and driven by a fast zero crossing detector (3A) is of the synchronous type in order to maintain a phase stability as high as possible.
As the servo loop is in fact open during the absence of reference input pulses, the phase stability of the 105 MHz output signal during this time depends on short term stability of the voltage controlled oscillator. Precautions taken to ensure this are:

- separately stabilized supply voltage and decoupling to one point;
- mechanical stability of the tuned circuit and screening of this circuit.

As a result no phase drift can be observed even if ten succeeding reference input pulses are missing.
This output signal is sent towards the radiofrequency divider for the experimental measurement of the pulse width and the regulation device of the post-acceleration buncher as represented in Fig. 5.

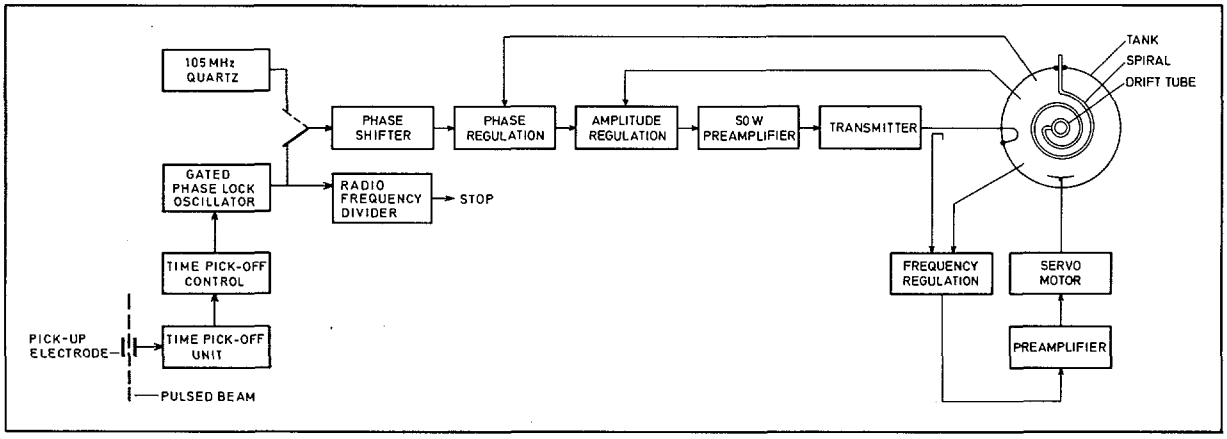

Fig. 5. Block diagram of the regulation device for the post-acceleration buncher

The phase-shifted RF signal is fed through a phase and amplitude regulation unit and compared with the RF feedback signal. It is then preamplified by a ENI type 550 L and amplified by a Herfurth type HV 20-80 K 108 unit. A decoupled forward power signal is utilized for the frequency control of the buncher. It is also phase compared with the RF pick-up signal and a signal proportional to the phase difference drives the tuning plate through a servo motor.

Experimental set up

In Fig. 6 are represented the position of the pick-up electrode 36 cm ahead the entrance of the analyzing magnet, of the post-acceleration buncher just after the exit slits of this magnet and L = 751 cm upstream of the target on the 0° exit of the switching magnet, and of the detector.
To determine the pulse width obtainable with the post-acceleration buncher, the block diagram of the electronics used is represented in Fig. 7.
A stop signal at 2.5 MHz is derived from the 105 MHz GPL signal and is divided by 42 in the radio frequency divider.
For the start signal, the following set up has been adopted: Coulomb scattered ions from a 0.6 mg·cm^{-2} gold foil installed 68 cm before the target, are observed in the 45° direction at 17 cm from the foil. They are detected by a totally depleted ORTEC surface barrier detector of 390 μm thickness, 25 mm^2 active area, 7.2 kΩ · cm nominal resistivity, operated with an overbias of 150 Volts. Timing and energy signals are sent through ADC's towards an ND 6660 analyzer.

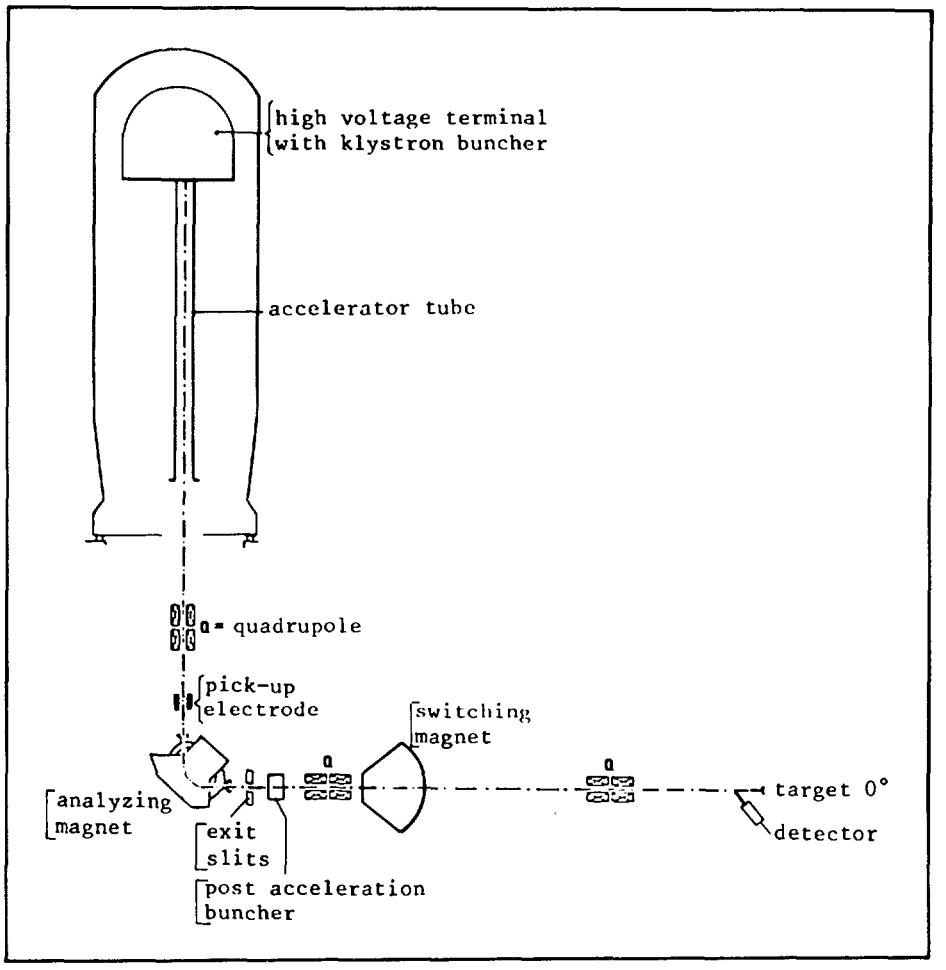

Fig. 6. Schematic representation of the experimental set up

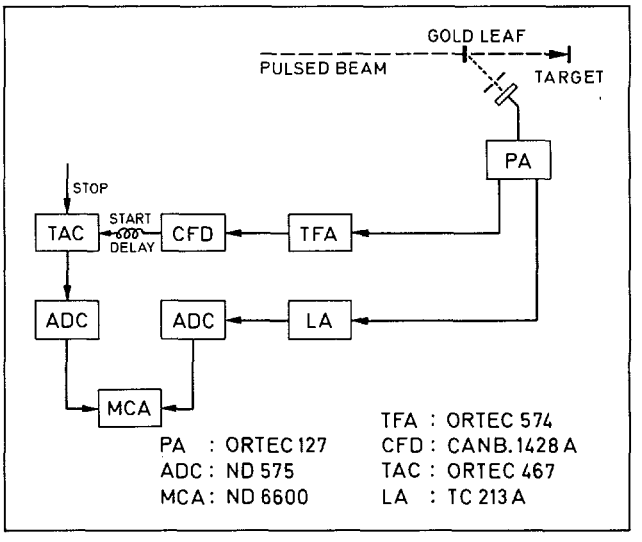

Fig. 7. Electronics used to perform time resolution measurements

Results

Determination of the pulse width with a DC beam.

Measurements were performed with a 2 μA DC 5.4 MeV proton beam (β = 0.107) [1]. With the post-acceleration buncher switched off, an energy resolution of 23 keV FWHM was obtained for the pulse-height spectrum (Fig. 9.a). When varying the RF power N between 0.9 and 1.9 kW by steps of 0.1 kW, the maximum energy spread $E_+ - E_-$ proportional to U_{o_p} has been determined following eq. (6) taking into account the resolution. From these data a value of R_p = (0.55 $\pm$ 0.04) MΩ has been deduced using eq. (3). Optimum bunching conditions were found for 1.6 kW in perfect agreement with expectations from eq. (3) and are represented in Fig. 8.

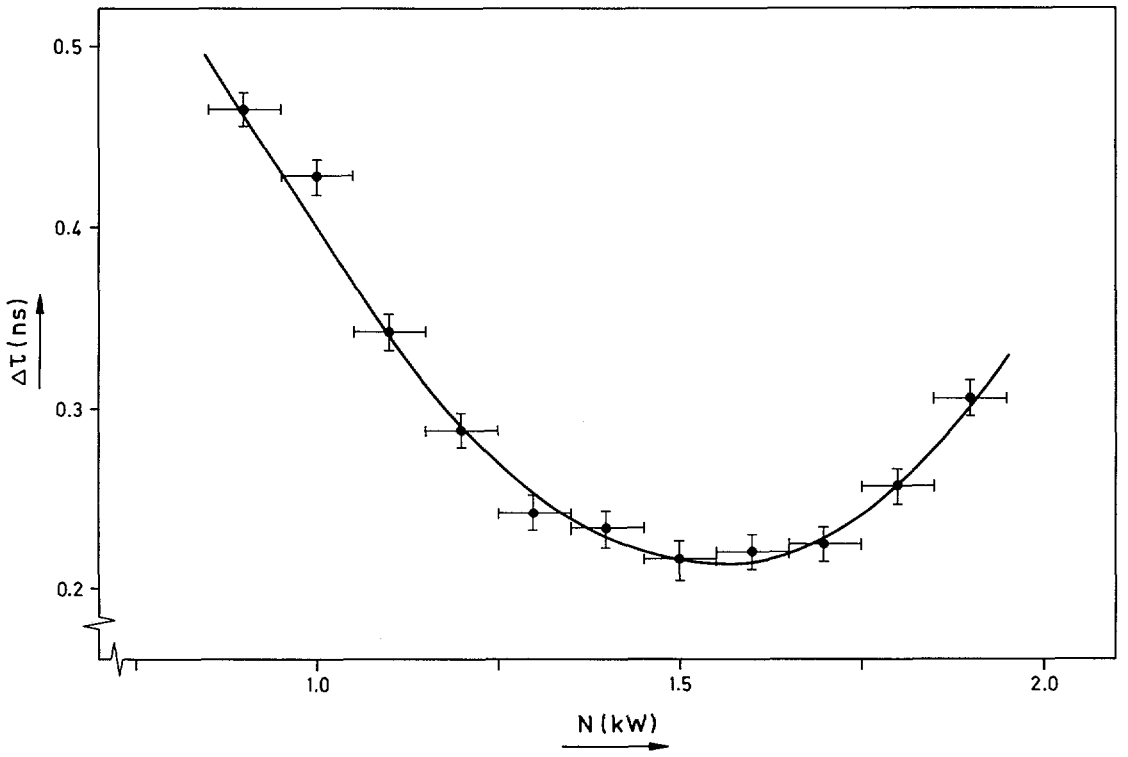

Fig. 8. Optimum bunching conditions at 1.6 kW

(1) A. Crametz and H. Liskien, Internal Report GE/R/VG/40/83.

The energy modulation for optimal bunching is shown in Fig. 9.b together with the pulse height spectrum to be expected theoretically (dashed curve). This curve corresponds to eq. (7) when folded with the resolution function of Fig. 9.a. The corresponding TOF spectrum is shown in Fig. 9.c. Knowing that in pulsed mode only the cross-over region of the buncher voltage is used, a window as indicated in Fig. 9.d has been set in the pulse height spectrum and the corresponding TOF spectrum is shown in Fig. 9.e. For every cross-over the beam bunches are clearly seen, alternatively time-focussed and time-defocussed, the integrals over these bunches being equal. The time-focussed bunches have a FWHM of 0.15 ns.

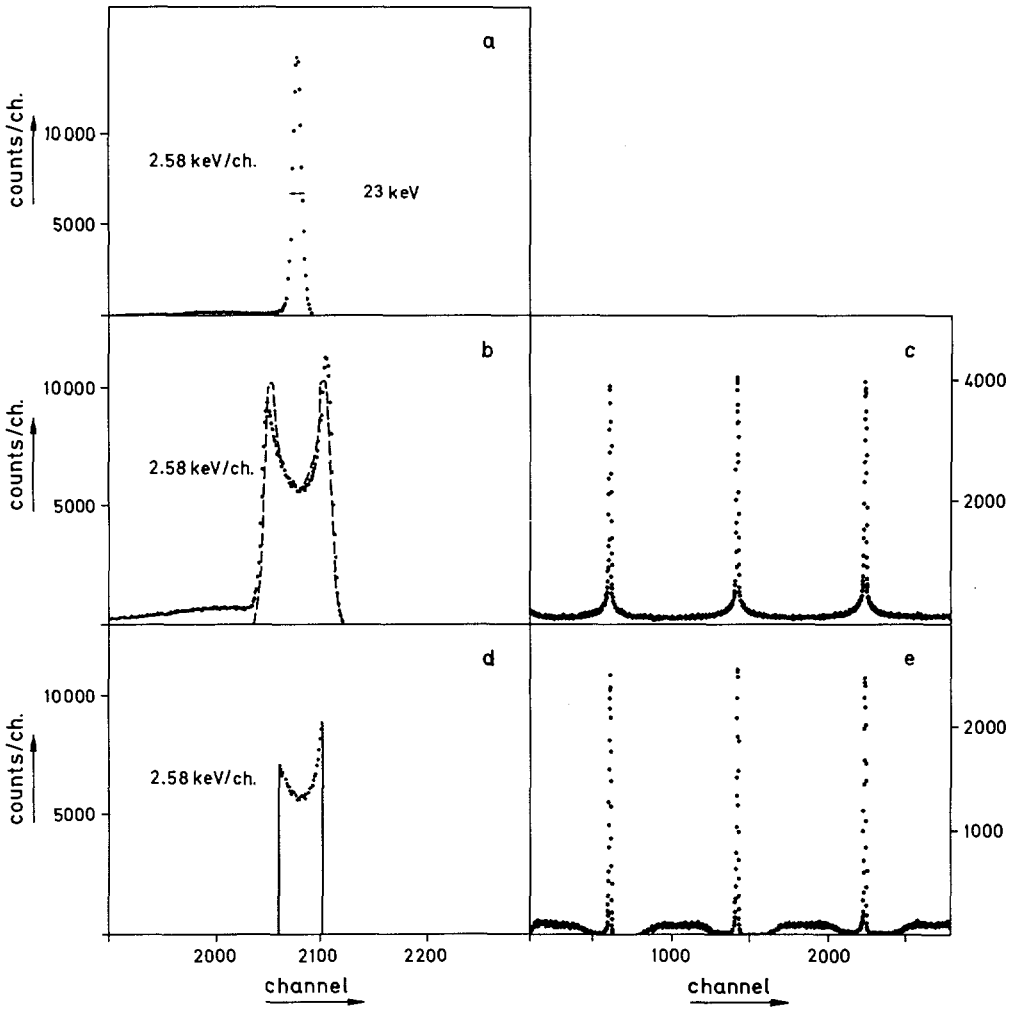

Fig. 9. Energy distribution of Coulomb-scattered protons (a) without and (b) with the optimum bunching switched on. (c) is the corresponding TOF spectrum. Setting an energy window as indicated in (d) results in the TOF spectrum (e)

Determination of the pulse width with a pulsed beam.

In this mode, a 2 μA pulsed 7.0 MeV deuteron beam (β = 0.086) with pulses of FWHM = 1.4 ns at the output of the klystron buncher (prebunched beam) has been used as input for the post-acceleration buncher.
Using the same technique a postbunched beam with pulse widths of FWHM = 0.20 ns has been obtained and results are shown in Fig. 10. The needed power delivered by the transmitter was 1.2 kW as expected from eq. (3). The obtained pulse width of 0.20 ns must be regarded as an upper limit. This number contains the intrinsic time resolution of the electronics used. From the $\pm$ 2 kV ripple of the accelerator voltage one may calculate a 0.08 ns theoretical lower limit following eq. (4).

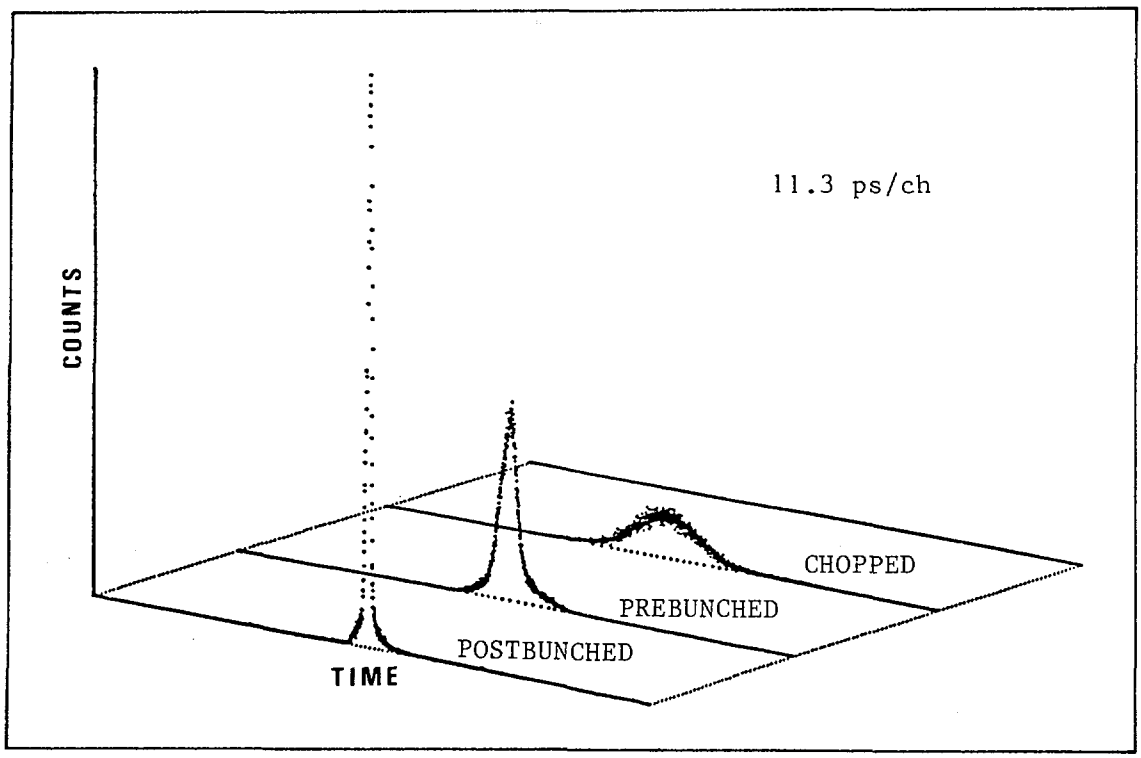

Fig. 10. Obtained results for the time resolution measurements of:
- *the post-acceleration bunched pulse : FWHM = 0.20 ns*
- *the pre-acceleration bunched pulse : FWHM = 1.4 ns*
- *the chopped pulse : FWHM = 8.6 ns*

Conclusion

A spiral resonator as developed at the Max-Planck Institut für Kernphysik at Heidelberg for their heavy ion post-accelerator has been installed at the 7 MV Geel Van de Graaff accelerator as post-acceleration buncher. Synchronization between the pre- and post-acceleration buncher has been obtained by pick-up signals from the accelerated ion pulses and a phase lock oscillator to which a missing pulse detector and a gate between the charge pump and the integrator were added. Pulses of 0.15 ns FWHM in DC mode and 0.20 ns FWHM in pulsed mode have been obtained. These numbers are upper limits only as they contain unknown contributions from the measuring electronics. A theoretical lower limit determined by the ion energy spread before post-acceleration bunching is 0.08 ns. The needed RF power for minimum pulse widths and the observed energy modulation are in perfect agreement with theoretical expectations. Depending on the needs of future neutron experiments, this new feature can be used to increase either the TOF resolution at a fixed intensity or the intensity without losing TOF resolution.

L I S T O F P U B L I C A T I O N S 1 9 8 4

TOPICAL REPORTS

BATCHELOR, R. - Multiannual Programme of the Joint Research Centre 1980-1983, 1983 Annual Status Report on Nuclear Measurements - EUR 9032 EN (1984)

VERLINDEN, J.*, GIJBELS, R.*, SILVESTER, H., DE BIEVRE, P. - Rhenium filaments: Investigation of their purity by spark source and secondary ion mass spectrometry - Their purification by thermal treatment - EUR 9653 EN (1984)

VANSANT, E.F.*, THIJS, A.*, PEETERS, G.*, VERHAERT, I.*, DE BIEVRE, P. - Occlusion and storage of krypton in solids - EUR 9353 EN (1984)

CONTRIBUTIONS TO CONFERENCES

SALOME, J.M., BOCKHOFF, K.H. - The new pulse compression system at GELINA - International Neutron Interlab Seminar 6-8 June 1984, Braunschweig

BASTIAN, C. - ANGELA: A comprehensive analysis system for nuclear spectra and their uncertainties - Ibid.

LISKIEN, H. - International fluence rate intercomparison based on $^{115}In(n,n')$ - Ibid.

DEKEMPENEER, E.*, LISKIEN, H., MEWISSEN, C.*, POORTMANS, F.* - Experimental calibration of a NE 213 liquid scintillator - Ibid.

BASTIAN, C., BRUSEGAN, A., CORVI, F. - Flux detector intercomparison II: high efficiency detectors - Ibid.

BASTIAN, C., RIEMENSCHNEIDER, H. - Comparison of (n,X) reactions in a Xenon scintillator - Ibid.

SCHILLEBEECKX, P.*, WAGEMANS, C.*, DERUYTTER, A. - Fission fragment mass and energy distribution for spontaneous and thermal neutron induced fission of several plutonium isotopes - Ibid.

---

* Collaborators not belonging to JRC.

WEIGMANN, H., WARTENA, J.A., BÜRKHOLZ, C. - Neutron induced fission cross section of ^{242}Pu - Ibid.

WAGEMANS, C.*, DERUYTTER, A. - Preliminary results of fission cross section measurements with subthermal neutrons - Ibid.

DERUYTTER, A. - High priority European nuclear data measurements requirements for the fission reactor programme and fusion technology - Ibid.

WATTECAMPS, E., ARNOTTE, F., LISKIEN, H. - On the measurements of (n,α) cross-sections for natural copper - Ibid.

CORNELIS, E.*, ROHR, G., VANPRAET, G.* - Neutron capture measurements on ^{241}Am - Ibid.

ROHR, G. - Comments relevant to the 1.15 MeV resonance ^{56}Fe task force - Ibid.

CORVI, F., BRUSEGAN, A., BASTIAN, C., WISSHAK, K.* - Measurements relevant to the 1.15 keV task force - Ibid.

STRAEDE, C.*, BUDTZ-JØRGENSEN, C., KNITTER, H.-H. - Fission fragment mass, kinetic energy and angular distributions for ^{235}U(n,f) in the neutron energy range from thermal to 6 MeV. Verhandlungen der DPG, Vol. 3 (1984). Frühjahrstagung DPG, 26-30 März 1984, Innsbruck (Austria) - ORA 31342

WINKLER, G.*, PAVLIK, A.*, UHL, M.*, PAULSEN, A., LISKIEN, H. - Neutronen-induzierte Reaktionen an ^{58}Ni - Ibid.

ESCHBACH, H.L. - Untersuchungen an Oberflächen und dünnen Schichten mit energiereichen (MeV) Protonen und He-Ionen, Seminarvortrag Max Planck Institut Göttingen - ORA 31386

DE BIEVRE, P., BAUMANN, S.*, GÖRGENYI, T.*, DERON, S.*, KUHN, E.*, DE REGGE, P.* - 1983 target values for uncertainty components in fissile element and isotope assay - Achievable uncertainties in destructive assay of nuclear material - 5th ESARDA Symposium Venezia, May 14-18, 1984 - ORA 31412

VERDINGH, V., ZIJP, W.L.* - Repeatability and reproducibility of gravimetric uranium determinations in UO_2 pellets - ESARDA Symposium Venice, May 14-18, 1984 - ORA 31413

KNITTER, H.-H., BUDTZ-JØRGENSEN, C. - Two measurement techniques and experimental results obtained with them on transactinium isotopes - Third IAEA Advisory Group Meeting on Transactinium Isotope Nuclear Data, May 21-25, 1984, Uppsala (Sweden) - ORA 31565

DE BIEVRE, P. - Isotopic characterization of targets for nuclear measurements at CBNM - 12th World Conference of the International Nuclear Target Development Society (INTDS) - Antwerpen, September 25-28, 1984 - ORA 31633

GEERTS, K., VAN GESTEL, J., PAUWELS, J. - Thin ^{33}S layers for $^{33}S(n,\alpha)$ cross-section measurements - Ibid. - ORA 31417

PAUWELS, J., VAN GESTEL, J., VANDECASTEELE, C.*, STRIJCKMANS, K.* - Irradiation tests of thin substrate materials for nuclear targets - Ibid. - ORA 31493

PAUWELS, J. - The development of a method for the preparation of large amounts of ^{234}Th purified ^{238}U-oxide - Ibid.

VAN DEN BERG, M., PAULSEN, A., BERTHELOT, C., BABELIOWSKY, T. - The feasibility of electromagnetic actinide isotope separation in the European Community - Ibid. - ORA 31634

EYKENS, R., PAUWELS, J., VAN AUDENHOVE, J. - The hydrofluorination of uranium and plutonium - Ibid. - ORA 31736

VAN AUDENHOVE, J., PAUWELS, J., FUDGE, A.J.* - EC source of reference materials for neutron metrology requirements - Ibid. - ORA 31741

BUDTZ-JØRGENSEN, C., KNITTER, H.-H., BORTELS, G. - Assaying of targets for nuclear measurements with a gridded ionization chamber - Ibid. - ORA 31814

DE BIEVRE, P., BAUMANN, S.*, GÖRGENYI, T.*, KUHN, E.*, DERON, S.*, DE REGGE, P.* - 1983 target values for uncertainty components in fissile element and isotope assay - Institute of Nuclear Material Management 25th Annual Meeting, July, 15-18, 1984 - Columbus, Ohio, USA - ORA 31636

KÖHLER, R.*, MEWISSEN, L.*, POORTMANS, F.*, VAN PARIJS, I.*, WEIGMANN, H. - High resolution neutron resonance spectrometry - Conference on Neutron-Nucleus Collisions - ORA 31745

LISKIEN, H., LEWIS, V.E.* - International fluence rate intercomparison for 2.5, 5.0 and 14 MeV neutrons - Fifth Symposium on Neutron Dosimetry, September 17-21, 1984, Neuherberg (FRG) - ORA 31769

VANINBROUKX, R., BAMBYNEK, W. - Evaluation of selected decay data for some actinides - Presented at the Third IAEA Advisory Group Meeting on Transactinium Isotope Nuclear Data, Uppsala, 21-25 May, 1984, in press - ORA 31893

VANINBROUKX, R. - Status report 1984, JRC-CBNM participation in the IAEA coordinated research programme on the measurement and evaluation of transactinium nuclear decay data - Presented at the seventh Research Coordination Meeting on the Measurement and Evaluation of Transactinium Isotope Nuclear Data, Vienna, 5-9 November 1984, in press - ORA 31892

VANINBROUKX, R. - Emission probabilities of selected gamma rays for radionuclides used as detector-calibration standards - Presented at the IAEA Advisory Group Meeting on Nuclear Standard Reference Data, Geel, 12-16 November, 1984 - ORA 31864

AXTON, E.J. - Evaluation of the thermal neutron constants of ^{233}U, ^{235}U, ^{239}Pu and ^{241}Pu and the fission neutron yield of ^{252}Cf - Ibid. - ORA 31885

WAGEMANS, C.*, DERUYTTER, A.J. - Sub-thermal fission cross-section measurements - Ibid. - ORA 31886

WAGEMANS, C.*, DERUYTTER, A.J. - New results on the $^{235}U(n,f)$ fission integrals - Ibid. - ORA 31881

LISKIEN, H., LEWIS, V.E.* - International fluence rate intercomparison for 2.5, 5.0 and 14 MeV neutrons - Ibid. - ORA 31884

DERUYTTER, A.J. - Requirements for nuclear standard reference data from the users' point of view - Ibid. - ORA 31883

WARTENA, J.A., KNITTER, H.-H., BUDTZ-JØRGENSEN, C., BAX, H. BURKHOLZ, C., PIJPSTRA, R., VOGT, R. - Flux detector intercomparison. Part 1: Low efficiency detectors - Ibid. - ORA 31910

CORVI, F., RIEMENSCHNEIDER, H., VAN DER VEEN, T. - Flux detector intercomparisons: High efficiency detectors - Part II - Ibid. - ORA 31894

BASTIAN, C., RIEMENSCHNEIDER, H. - Measurement of the $^{6}Li(n,\alpha)/^{10}B(n,\alpha)$ ratio - Ibid. - ORA 31895

BAMBYNEK, W. - Emission probabilities of selected X rays for radionuclides used as detector-calibration standards - Ibid. - ORA 31888

BUDTZ-JØRGENSEN, C., KNITTER, H.-H. - Assaying of ^{235}U fission layers for nuclear measurements with a gridded ionization chamber - Ibid. - ORA 31889

BUDTZ-JØRGENSEN, C., KNITTER, H.-H., VOGT, R. - Neutron emission from the spontaneous fission of ^{252}Cf - Ibid. - ORA 31890

STRAEDE, C.*, BUDTZ-JØRGENSEN, C., KNITTER, H.-H. - Fission fragment mass, kinetic energy and angular distribution for $^{235}U(n,f)$ in the neutron energy range from thermal to 6 MeV - Ibid. - ORA 31891

KNITTER, H.-H., BUDTZ-JØRGENSEN, C., BAX, H. - Investigation for a precise and efficient neutron fluence detector based on the n-p scattering process - Ibid. - ORA 31907

DERUYTTER, A.J. - Summary report of the IAEA Advisory Group Meeting on Nuclear Standards Reference Data held at CBNM 12-16 November 1984 - Nuclear Data Forum AEE-Winfrith 18.12.1984 - ORA 31909

BASTIAN, C., CERVINI, C. - Representing and Handling Spectra in APL - Proc. SEAS Spring Meeting 1984, April 09-13,1984, Knokke Belgium, p. 416-429

BAMBYNEK, W. - New evaluation of K-shell fluorescence yields - in: A. Meisel (ed.) X84, X-ray and inner shell processes in atoms, molecules and solids, Leipzig, August 20-24, 1984 (VEB Druckerei, Thomas Münzer, Langensalza, 1984), p. 1

SCIENTIFIC OR TECHNICAL ARTICLES

BLONS, J.*, MAZUR, C.*, PAYA, D.*, RIBRAG, M.*, WEIGMANN, H. - On the existence of triple-humped fission barriers in physics ^{231,233}Th - Nucl. Phys. A414, 1 (1984) - ART 25403

BORTELS, G., VERBRUGGEN, A. - Accurate measurement of the ^{238}Pu alpha-activity fraction in the NBS plutonium SRM 946 and 947 - in: L. Stanchi (ed.) Proceedings of the 6th ESARDA Symposium on Safeguards and Nuclear Material Management, Venice, Italy, 14-18 May 1984, (ESARDA Symposium Secretariat, JRC Ispra, 1984) p. 431 - ART/ORA 31387

MICHIELS, E., DE BIEVRE, P. - Determination of cadmium in whole blood by isotope dilution mass spectrometry (IDMS) manual series "Environmental Carcinogens" - Selected Methods of Analysis Vol. 7 (Metals) - ART 25740

AVALDI, L., MITCHELL, I.V., ESCHBACH, H.L., DOBMA, W. - L-shell X-ray production cross sections of $_{55}$Cs, $_{56}$Ba, $_{57}$La and $_{64}$Gd for protons of energy from 1-2 MeV - J. Phys. B At. Mol. Phys. 17, 2851 (1984) - ART 25741

AVALDI, L., MITCHELL, I.V., ESCHBACH, H.L., Precise X-ray production cross-section measurements of medium Z elements by protons - Nucl. Instr. Meth. B3, 21 (1984)

BORTELS, G., REHER, D., VANINBROUKX, R. - Emission probabilities for the 4.449 MeV alpha particles in the decay of ^{224}Ra-^{220}Rn - Int. J. Appl. Radiat. Isot., 35, 305 (1984) - ART 95746

TRONC, D.*, SALOME, J.M., BOCKHOFF, K.H. - A new pulse compression system for intense relativistic electron beams - Nucl. Instr. Meth. 228,No.2/3, 217 (1985) - ART 25827

REICH, C.W.*, VANINBROUKX, R. - Current status of nuclear decay data and report on the IAEA Coordinated Research Programme in the Measurement and Evaluation of Transactinium Isotope Nuclear Decay Data - Presented at the seventh IAEA Research Coordination Meeting on the Measurement and Evaluation of Transactinium Isotope Nuclear Data, Vienna, 6-9 November, 1984, in press - ART/ORA 31553

PAUWELS, J., GALLET, M., VERBRUGGEN, A. - Preparation and characterization of a set of $^{234}UF_4$ reference fission foils - Newsletter of the INTDS 11,No.1, 15 (1984) - ART 25852

REHER, D., VANINBROUKX, R., CHAUVENET, B.* , MOREL, J.*, VATIN, R.*, WOODS, M.*, LUCAS, S.*, BALLAUX, C.*, JACQUEMIN, R.* - Standardization of ^{123}I - Int. J. Appl. Radiat. Isot. 35, 923 (1984) - ART 25283

ROHR, G. - New perspectives on the level density of compound resonances - Zeitschrift für Physik A 318, 299 (1984) - ART 25860

WAGEMANS, C.*, ALLAERT, E.*, DERUYTTER, A., BARTHELEMY, R., SCHILLEBEECKX, P.* - Comparison of the energy and mass characteristics of the $^{239}Pu(n_{th},f)$ and the $^{240}Pu(sf)$ fragments - Phys. Rev. C30, 218 (1984)

VERLINDEN, J.*, GIJBELS, R.*, SILVESTER, H., DE BIEVRE, P. - Bulk and surface trace analysis of rhenium filaments by spark source and secondary ion mass spectrometry, J. Microprobe and Trace Anal., in press - ART 25945

BARFOOT, K.M., MITCHELL, I.V., AVALDI, L., ESCHBACH, H.L., GILBOY, W.*, Si(Li) detector photopeak efficiency below 10 keV - Nucl. Instr. Meth. B5, 534 (1984) - ART 25966

WEIGMANN, H., WARTENA, J.A., BÜRKHOLZ, C. - Neutron induced fission cross section of ^{242}Pu - Nucl. Phys., in press - ART 25983

REHER, D., IDZERDA, A.B. - A data acquisition system for a radionuclide laboratory - Nucl. Instr. Meth. 221, 586 (1984) - ART 25473

BASTIAN, C., CERVINI, C. - Polygon shading with a pen plotter - APL quod quad - 14,No.3, 14 (1984) - ART 25472

KLOPF, P., STÜBER, W. - A dedicated CAMAC crate controller for Z80-microcomputers - Nucl. Instr. Meth. 223,No.1, 107 (1984) - ART 25486

MOUCHEL, D., HANSEN, H.H. - Half lives of the 482.2 keV and 615.3 keV levels in ^{181}Ta - Z. Phys. A315, 113 (1984) - ART 25471

BUDTZ-JØRGENSEN, C., KNITTER, H.-H. - Investigation of fission layers for precise fission cross-section measurements with a gridded ionization chamber - Nucl. Sc. and Eng. 86, 10 (1984)

HANSEN, H.H. - MOUCHEL, D. - Determination of the K-shell internal conversion coefficient for the 37.2 keV transition in the decay of $^{121}Sn^{m}$ - Z. Phys. A315, 239 (1984)

NYLANSTED LARSEN, A., BORTELS, G. - DENECKE, B. - Satellite peaks in high-resolution alpha-particle spectra of decay-chain members measured with silicon surface-barrier detectors - Nucl. Instr. Meth. 219, 339 (1984)

VANINBROUKX, R., BORTELS, G., DENECKE, B. - Alpha-particle-emission probabilities in the decay of ^{234}U and photon-emission probabilities in the decays of ^{234}U, ^{239}Np and ^{243}Am - Int. J. Appl. Radiat. Isot. 35, 1081 (1984)

MOORE, M.S.*, CALABRETTA, L.*, CORVI, F., WEIGMANN, H. - Analysis of intermediate structure in the fission and capture cross sections of (^{235}U+n) - Phys. Rev. C30, 214 (1984)

BORTELS, G. - BRINKMAN, G.A.*, MANN, W.B.* - Preface - Int. J. Appl. Radiat. Isot. 35, V (1984)

BORTELS, G. - Introduction - Int. J. Appl. Radiat. Isot. 35, 237 (1984)

BORTELS, G., DENECKE, B., VANINBROUKX, R. - Alpha-particle and photon emission probabilities in the ^{238}Pu-^{234}U decay - Nucl. Instr. Meth. 223, 329 (1984)

BORTELS, G., HUTCHINSON, J.M.R.* - Concluding ICRM session - Nucl. Instr. Meth. 223, 617 (1984)

VANINBROUKX, R., BORTELS, G., DENECKE, B. - Determination of photon-emission probabilities in the decay of ^{237}Np and its daughter ^{233}Pa - Int. J. Appl. Radiat. Isot. 35, 905 (1984)

HANSEN, H.H. - Compilation of experimental values of internal conversion coefficients and ratios for nuclei with $Z > 6\sigma$ - Physik Daten - Physics Data 17-2 (Fachinformationszentrum Energie, Physik, Mathematik, Karlsruhe), in press

BAMBYNEK, W. - International committee for radionuclide metrology - Int. J. Appl. Radiat. Isot. 36, 171 (1985)

COPPIETERS, L.*, VAN CAMPENHOUT, J.*, TRIFFAUX, J., VAN AUDENHOVE, J. - Development of a piezoelectric pulsed drop jet device for the preparation of nuclear targets - Nucl. Instr. and Meth. in Phys. Res. 224, 41 (1984) - North Holland, Amsterdam

PEISER, H.S.*, HOLDEN, N.E.*, DE BIEVRE, P., and SAIC Committee - Element by element review of their atomic weights, Pure & Appl. Chem. 56,No.6, 695 (1984) - ART 25151

DE BIEVRE, P., GALLET, M., HOLDEN, N.E.*, BARNES, I.L.* - Isotopic abundances and atomic weights of the elements - Journal of Physical and Chemical Reference Data 13,No.3, 809 (1984) - ART 25150

DE BIEVRE, P. - Activities of ESARDA Working Group destructive techniques and standards - ESARDA Bulletin 6 (1984) - ART 25766

BUDTZ-JØRGENSEN, C., KNITTER, H.-H. - A precise method for charged particle counting employing energy and angle information from gridded ion chambers - Nucl. Instr. and Meth. 223, 295 (1984) - ART/ORA 30959

LISKIEN, H. - International fluence rate intercomparison for 2.5 and 5.0 MeV neutrons - Metrologia 20, 55 (1984) - ART 25483

SPIRLET, J.C., MÜLLER, W., VAN AUDENHOVE, J. - Single crystal growth of actinide metal and compounds - Proceedings of the 12th World Conference of the International Nuclear Target Development Society (INTDS) - (Antwerp 1984) - Nucl. Instr. Meth., in print

SPIRLET, J.C., MÜLLER, W., VAN AUDENHOVE, J., FUGER, J.* - Direct reduction of actinide oxide and carbide to metals application to the preparation of plutonium metal - Ibid., in print

Updated List

AVALDI, L., MILAZZO, M.*, TRIVIA, G.*, MITCHELL, I.V. - Recent results on K-shell ionization by ion collisions - IEEE Trans. Nucl. Sci 30, 961 (1983)

MITCHELL, I.V., REHER, D. - Assay of radionuclide sources by energetic ion beams - Int. J. Appl. Radiat. Isot. 34, 1277 (1983)

BERTHELOT, Ch., ESCHBACH, H.L., VERDINGH, V., VERHEYEN, F. - The homogeneity control of reference materials by photon activation - Intern. Environ. Anal. Chem. 16, 227 (1983)

THIJS, A.*, PEETERS, G.*, VANSANT, E.F.*, VERHAERT, I.*, DE BIEVRE, P. - Purification of gases in H-mordenite modified with silane and diborane - J. Chem. Soc., Faraday Trans. 1, 79, 2821 (1983)

THIJS, A.*, PEETERS, G.*, VANSANT, E.F.*, VERHAERT, I.*, DE BIEVRE, P. - Encapsulation of gases in H-mordenite modified with silane and diborane - J. Chem. Soc., Faraday Trans. 1, 79, 2835 (1983)

BASTIN, J.*, BOMANS, M.*, DUGAIN, F.*, MICHAUT, C.*, PUJADE-RENAUD, J.-M.*, VAN AUDENHOVE, J. - Utilisation de matériaux de référence pour analyse commerciale de grande précision - Exemple de minerais concentrés de zinc - III. - Sélection de trois méthodes de référence pour le dosage du zinc - Analusis 11,N°1, 2 (1983)

TECHNICAL NOTES

WERZ, R., DE BIEVRE, P. - Orthodox uncertainty assessment of single collector isotope mass spectrometry - An intermediate approach, March 1983 - CBNM-MS-R-26-83

WERZ, R., DE BIEVRE, P. - Orthodox evaluation of uncertainties of synthetic isotope mixtures, March 1983 - CBNM-MS-R-30-83

DE BOLLE, W. - Conversion of uranium oxide to UF_6 for isotopic measurements by UF_6 gas mass spectrometry, April 1983 - CBNM-MS-R-44-83

LENAERS, G. - Atomic weight determinations of silicon by isotope mass spectrometry - Contribution to a redetermination of the avogadro constant, June 1983 - CBNM-MS-R-57-83

MÜSCHENBORN, G.†, DE BOLLE, W. - $^{235}U/^{238}U$ isotope ratio measurements on double collector UF_6 mass spectrometers, August 1983 - CBNM-MS-R-74-83

TRAAS, L.J. - Interfacing a MAT TH5 mass spectrometer to a personal computer using the IEEE-488 interface bus system, August 1983 - CBNM-MS-R-75-83

DE BOLLE, W. - Preparation of $^{235}U_3O_8$ and $^{235}UF_6$ as IRM batches, September 1983 - CBNM-MS-R-81-83

DE BOLLE, W., LYCKE, W. - Measuring small differences in $^{235}U/^{238}U$ ratios in natural uranium, November 1983 - CBNM-MS-R-112-83

DUCHATEAU, N., DE BIEVRE, P. - The assay of boron in zirconium at the < 1 ppm level by isotope dilution mass spectrometry, March 1984 - CBNM-MS-R-28-84

LENAERS, G., WERZ, R., DE BIEVRE, P. - Atomic weight determinations of silicon by isotope mass spectrometry - An introductory study to prepare a contribution to a redetermination of the avogadro constant, April 1984 - CBNM-MS-R-31-84

WERZ, R., DE BIEVRE, P. - Reliable uncertainty statements on atomic weights by orthodox data reduction of mass spectrometric measurements, July 1984, CBNM-MS-R-66-84

DE BOLLE, W. - Investigation of observed discrepancies between the $^{235}U/^{238}U$ ratios determined by UF_6 mass spectrometry and $^{235}U/^{238}U$ ratios of synthetic isotope mixtures, August 1984 - CBNM-MS-R-67-84

WIDERA, R., PAULSEN, A., LISKIEN, H. - CBNM participation in an international fast neutron fluence intercomparison based on indium (n,γ)-activation - GE.R.VG.44.84

BASTIAN, C., CERVINI, C. - Multiparameter event list analysis in APL, February 1984 - GE.TN.DE.102.84

DE ROOST, E. - Photon activation analysis measurement facility III, November 1984 - GE.TN.DE.102.84

HORSTMANN, H. - Personal and professional computers, November 1984 - GE.R.DE.207.84

HORSTMANN, H. - Data processing at the Central Bureau for Nuclear Measurements, December 1984 - GE.R.DE.208.84

HORSTMANN, H. - Connection of data acquisition stations to the IBM 4381 computer, October 1984 - GE.NI.DE.202.84

FALOT, W.*, VERDINGH, V. - Studie van wateropname door uranium oxides - Internal Report GE/R/AS/03/84

VERDINGH, V., SLOWIKOWSKI, B. - Water pick-up of uranium oxides - Internal Report GE/R/AS/06/84

LE DUIGOU, Y. - Proposal for the production of a lot of plutonium sulphate tetrahydrate to serve as an EC certified material for the elemental analysis of plutonium - Internal Report GE/R/AS/01/84

LE DUIGOU, Y., VERDINGH, V. - Certification of a uranium dioxide reference material for in-plant uranium determinations - Internal Report GE/R/AS/02/84

REHER, D. - The experiment data file structure of RNDAS - Internal Report GE/R/RN/02/84

REHER, D. - An auxiliary subroutine package for the Radionuclides Group Data Acquisition System - Internal Report GE/R/RN/09/84

COURSEY, B.M.*, VANINBROUKX, R., REHER, D., ZEHNER, W. - The standardization of niobium-93m for use as reference material for reactor neutron dosimetry - Internal Report GE/R/RN/11/84

REHER, D., HANSEN, H.H., VANINBROUKX, R. - The decay of ^{47}Sc - Internal Report GE/R/RN/12/84

REHER, D. - A new version of the RN data acquisition program - Internal Report GE/R/RN/13/84

COURSEY, B.M.*, GRAU MALONDA, A.*, GARCIA-TORAÑO, E.*, GIBSON, J.A.B.*, REHER, D. - Intercomparison of beta-particle-emitting standards of radioactivity by scintillation counting - Internal Report GE/R/RN/14/84

DENECKE, B. - Properties of a 4π-CsI(Tl)-sandwich spectrometer for the measurement of photons with an energy between 10 and 200 keV - Internal Report GE/R/RN/19/84

COMMUNICATIONS

DEBUS, G.H. (editor) - PPR Nuclear Measurements - July/December 1983 - COM 4126

DEBUS, G.H. (editor) - PPR Nuclear Measurements and Reference Materials - January-June 1984 - COM 4167

PAULSEN, A., BERTHELOT, Ch., VAN DEN BERG, M., BABELIOWSKY, T. - The feasibility of electromagnetic actinide isotope separation in the European Community - COM 4139

LE DUIGOU, Y., VERDINGH, V. - Certification of a uranium dioxide reference material for in-plant uranium determination - COM 4146

DE BIEVRE, P., ESCHBACH, H.L., LESSER, R., MEYER, H., VAN AUDENHOVE, J. - Certification report - ^{235}U isotope abundance certified reference material (U_3O_8) for gamma-spectrometry - COM 4153

SPECIAL PUBLICATIONS

DEBUS, G.H. (Ed.) - Annual Progress Report on Nuclear Data 1983

VAN AUDENHOVE, J. (Ed.) - Newsletter of the International Nuclear Target Development Society (INTDS): 11,No.1 (1984)

VAN AUDENHOVE, J. (Ed.) - Newsletter of the International Nuclear Target Development Society (INTDS): 11,No.2 (1984)

C I N D A E N T R I E S L I S T

ELEMENT		QUANTITY	TYPE	ENERGY		DOCUMENTATION				LAB	COMMENTS
S	A			MIN	MAX	REF	VOL	PAGE	DATE		
LI	006	N,ALPHA	EXPT-PROG	10+0	40+5	INDC(EUR)	19	5	085	GEL	BASTIAN+REL TO 10B(N,A)
LI	007	NEM	EXPT-PROG	16+6	16+7	INDC(EUR)	19	55	085	GEL	DEKEMPENEER+DOUBLE DIFF XSECT
LI	007	INELASTIC G	EXPT-PROG	80+6		INDC(EUR)	19	55	085	GEL	LISKIEN+NEUTR ANG DISTR
BE	009	N,TRITON	EXPT-PROG	13+7	20+7	INDC(EUR)	19	58	085	GEL	LISKIEN+TRITIUM DETERM
BE	009	N,TRITON	EXPT-PROG	16+7	20+7	INDC(EUR)	19	58	085	GEL	QAIM+TRITIUM DETERM
SI	028	SNG	EXPT-PROG	+3	18+6	INDC(EUR)	19	52	085	GEL	MARTIN+
S	033	N,ALPHA	EXPT-PROG	+3	+6	INDC(EUR)	19	53	085	GEL	WAGEMANS+
CA	041	N,ALPHA	EXPT-PROG	40+3	10+6	INDC(EUR)	19	53	085	GEL	WAGEMANS+
V	051	N,TRITON	EXPT-PROG	16+7	20+7	INDC(EUR)	19	58	085	GEL	QAIM+TRITIUM DETERM
CR	050	RESON PARAMS	EXPT-PROG	28+1	80+5	INDC(EUR)	19	43	085	GEL	VAN MARCKE+NEUTRON RES PARAMS
CR	050	RESON PARAMS	EXPT-PROG	10+3	30+5	INDC(EUR)	19	42	085	GEL	CORVI+HIGH RESOL CAPT GAMMA
CR	052	RESON PARAMS	EXPT-PROG	10+3	40+5	INDC(EUR)	19	43	085	GEL	ROHR+TOF CAPTURE+TRANSM
CR	053	RESON PARAMS	EXPT-PROG	10+3	20+5	INDC(EUR)	19	44	085	GEL	BRUSEGAN+TOF CAPTURE+TRANSM
FE	054	RESON PARAMS	EXPT-PROG	30+4	10+6	INDC(EUR)	19	44	085	GEL	CORNELIS+NEUTRON RES PARAMS
FE	056	RESON PARAMS	EXPT-PROG	11+3	12+3	INDC(EUR)	19	45	085	GEL	BRUSEGAN+HIGH RESOL TRANSM
FE	056	RESON PARAMS	EXPT-PROG	11+3	12+3	INDC(EUR)	19	45	085	GEL	CORVI+HIGH RESOL CAPT
NI		N,ALPHA	EXPT-PROG	50+6	10+7	INDC(EUR)	19	59	085	GEL	WATTECAMPS+
NI	058	TOT	EXPT-PROG	30+4	20+7	INDC(EUR)	19	48	085	GEL	MEWISSEN+TOF TRANSM TBD
NI	060	TOT	EXPT-PROG	30+4	20+7	INDC(EUR)	19	48	085	GEL	MEWISSEN+TOF TRANSM TBD
NI	061	TOT	EXPT-PROG	30+4	20+7	INDC(EUR)	19	48	085	GEL	MEWISSEN+TOF TRANSM TBD
CU		N,ALPHA	EXPT-PROG	50+6	10+7	INDC(EUR)	19	59	085	GEL	WATTECAMPS+
IN		N,TRITON	EXPT-PROG	16+7	20+7	INDC(EUR)	19	58	085	GEL	QAIM+TRITIUM DETERM
SM	149	NG	EXPT-PROG	10+3	10+6	INDC(EUR)	19	49	085	GEL	CORVI+AVERAGE CAPT XSECT
PB	207	TOT	EXPT-PROG	20+5	20+7	INDC(EUR)	19	51	085	GEL	KOEHLER+HIGH RESOL TOT XSECT
U	235	N,FISSION	EXPT-PROG	25-2	30+4	INDC(EUR)	19	6	085	GEL	WAGEMANS+REL TO 10B(N,A)
U	235	N,FISSION	EXPT-PROG	10-3	25-2	INDC(EUR)	19	34	085	GEL	WAGEMANS+TBD COLD NEUTRONS
U	235	FISS YIELD	EXPT-PROG	25-2	60+6	INDC(EUR)	19	7	085	GEL	STRAEDE+PROMPT MASS SPECTRUM
U	235	FRAG SPECTRA	EXPT-PROG	25-2	60+6	INDC(EUR)	19	7	085	GEL	STRAEDE+ENERGY AND ANG DISTR
U	235	ETA	EXPT-PROG	10-3	10-1	INDC(EUR)	19	34	085	GEL	WARTENA+TBD COLD NEUTRONS
PU	238	FISS YIELD	EXPT-PROG	SPON		INDC(EUR)	19	39	085	GEL	WAGEMANS+PRENEUTRON FRAGM MASS
PU	238	FRAG SPECTRA	EXPT-PROG	SPON		INDC(EUR)	19	39	085	GEL	WAGEMANS+ENERGY DISTR
PU	242	FISS YIELD	EXPT-PROG	SPON		INDC(EUR)	19	40	085	GEL	SCHILLEBEECKX+PRENEUTRON FRAGM MASS
PU	242	FRAG SPECTRA	EXPT-PROG	SPON		INDC(EUR)	19	40	085	GEL	SCHILLEBEECKX+ENERGY DISTR
AM	243	N,FISSION	EXPT-PROG	08+0	10+5	INDC(EUR)	19	37	085	GEL	KNITTER+
AM	241	ABSORPTION	EXPT-PROG	25-2	60+5	INDC(EUR)	19	35	085	GEL	VANPRAET+C6D6 TOF SCINT
CF	252	SPECT FISS N	EXPT-PROG	SPON		INDC(EUR)	19	9	085	GEL	BUDTZ-JORGENSEN+TOF

Edited by G.H. DEBUS